

BIOCHEMICAL CHARACTERIZATION OF THE *YERSINIA*
EFFECTOR PROTEIN, YOPJ

APPROVED BY SUPERVISORY COMMITTEE

Kim Orth, Ph.D. _____

George DeMartino, Ph.D. _____

Elizabeth Goldsmith, Ph.D. _____

Hongtao Yu, Ph.D. _____

Dedicated to

Maa and Babata

for their

love, support and inspiration

BIOCHEMICAL CHARACTERIZATION OF THE *YERSINIA* EFFECTOR
PROTEIN, YOPJ

by

SOHINI MUKHERJEE

DISSERTATION

Presented to the Faculty of Graduate School of Biomedical Sciences

The University of Texas Southwestern Medical Center at Dallas

In Partial Fulfillment of the Requirements

For the Degree of

DOCTOR OF PHILOSOPHY

The University of Texas Southwestern Medical Center at Dallas

Dallas, Texas

May, 2007

Copyright

by

SOHINI MUKHERJEE, 2007

All Rights Reserved

ACKNOWLEDGEMENTS

I have been really fortunate to work under the supervision of my mentor, Kim Orth. She has been an outstanding source of inspiration for hard work and dedication. Her passion for science is worth emulating and that greatly added to my molding as a scientist. Her constructive criticism and scientific outlook helped me to learn the analytical and scientific approach to a problem. I take this opportunity to thank Kim for all the help and guidance that she has provided to me. I also owe sincere thanks to my dissertation committee members, George DeMartino, Hongtao Yu and Betsy Goldsmith for their advice, support and suggestions during the course of my graduate career. I would also like to thank the chair of our department, Dr. Eric Olson for his guidance and encouragement.

It has indeed been a joy to be a part of the Orth lab, for their kind help and friendly advice. I have been greeted by Renee's cheerful smile each morning as I walked into the lab. She has been of immense help to me at crucial times and has always been ready with a solution to any scientific problem. I have had fun times with Jen and Dara and I thank them for bearing with my occasional tantrums. Amy, with whom I have shared my lab space, has been very supportive and cooperative towards my work. Jebs (Gladys) and I, together, formed a perfect team and she played a major role in the completion of my project. I would like to thank her for her generous help and sincere interest during various stages of our YopJ project. The warm friendship of Mel made the lab a very pleasant place and I thank her for her selfless help as and when required. I thank Yi-Heng, Olivia and Veera for their cordial friendship and assistance during the fag end of my research

work. Thanks to our newest Orth lab member, Michelle, for providing last-minute tips with my writing. I also wish to thank the former Orth lab members- Yong, Jona, Huaqun, Sara and Yvonne for their generous help and support. I would be failing in my duty if I do not acknowledge the ready help rendered by Steven and Amy Haughey from time to time.

I would like to thank my friends Indranee, Salil, Pallavi, Deepti and Lakshmanan, who do not live close-by but have always been very close to me. My friends in Dallas- Rashu, Savitha, Shalini di, Kiran, Neeta, Kirthi, Debjani di, Swati, Sumana di, Anirban, Sanjay, Barma da, George, Devanjan and Arvind bhaiya have made my stay very enjoyable and full of fun-filled activities. It was a most fortunate coincidence during my stay at Dallas that I found some true and sincere friends who are very close to my heart- Sonali di and Amit da. Sonali di has been most affectionate and dependable in times of need. As for Amit da, he has been with me in tough times when things had not been working and I am grateful to him for constant encouragement and optimism. His inspiration, persistence and guidance have helped me throughout in every aspect of life.

My husband, Hemanta, has always been a constant source of joy and happiness in my life. He has always been by my side with his wholehearted love and support to boost my morale in times of need. Finally, I am beholden to my parents whose understanding and forbearance enabled me to accomplish my work. It could not have been possible without their support and affection. I seek their blessings for my further endeavors.

BIOCHEMICAL CHARACTERIZATION OF THE *YERSINIA*
EFFECTOR PROTEIN, YOPJ

SOHINI MUKHERJEE, Ph.D.

The University of Texas Southwestern Medical Center at Dallas, 2007

Supervising Professor: KIM ORTH, Ph.D.

Yersinia species, the causal agent of plague and gastroenteritis, uses a variety of type III effector proteins to target eukaryotic signaling systems. The effector YopJ disrupts the mitogen-activated protein kinase and the nuclear factor κ B signaling pathways used in innate immune response by preventing activation of the family of mitogen-activated protein kinase kinases. The catalytic domain of YopJ is similar to Clan CE of cysteine proteases, and mutating the putative catalytic cysteine disrupts YopJ's inhibitory activity. YopJ binds mitogen-activated protein kinase kinases, including MKK1 through MKK6, and the related kinase, I κ B kinase β , however, the mechanism by which this binding leads to

inactivation of these kinases is unknown.

An *in vitro* cell-free signaling system was developed to recapitulate the inhibition of eukaryotic signaling by YopJ. Mass spectrometric studies were undertaken to determine the biochemical nature of modification of the mitogen-activated protein kinase kinases in the presence of YopJ. Based on the observations, a simple, molecular mechanism utilized by YopJ to block the signaling pathways was discovered. YopJ acted as an acetyltransferase, using acetyl coenzyme A, to modify the critical serine and threonine residues in the activation loop of mitogen-activated protein kinase kinases and thereby blocking phosphorylation. The acetylation on the kinase directly competed with phosphorylation, preventing activation of the modified protein.

An essential characteristic feature of bacterial effector proteins is that they usurp or mimic a eukaryotic activity and refine this activity to produce an extremely efficient mechanism to combat eukaryotic signaling. Therefore, modification of amino acids, other than lysine, by acetylation could be a commonly used eukaryotic mechanism that has been undetected previously. The acetylation of these amino acids may compete with various other types of posttranslational modifications, such as ubiquitination, SUMOylation and glycosylation. Several questions that still need to be addressed are: Is this modification reversible? What are the eukaryotic proteins that add and remove this type of posttranslational modification? How do bacterial effectors use this activity? The characterization of a bacterial effector as a serine or threonine acetyltransferase presents a previously unknown paradigm to be considered for other biological signaling pathways.

TABLE OF CONTENTS

ACKNOWLEDGEMENTS.....	v
ABSTRACT.....	vii
TABLE OF CONTENTS.....	ix
LIST OF PUBLICATIONS.....	xii
LIST OF FIGURES AND TABLES.....	xiii
LIST OF ABBREVIATIONS.....	xvii
CHAPTER 1:	
INTRODUCTION.....	20
CHAPTER 2: REVIEW OF LITERATURE	
<i>Yersinia</i> and the Type III Secretion System.....	25
The <i>Yersinia</i> effector, YopJ.....	28
YopJ inhibits the essential signaling pathways at a common point.....	29
Review of the MAPK pathway.....	31
Review of the NFκB pathway.....	34
A single point mutation abrogates YopJ's inhibitory activity.....	38
Review of SUMOylation.....	39
YopJ: a DeSUMOylating enzyme or DUB?.....	42
Goal of this dissertation.....	44

CHAPTER 3: RESULTS

Study of the Inhibitory Effects of YopJ on the MAPK and NFκB Pathways.....	46
Introduction.....	46
Materials and Methods.....	47
Results.....	53
Discussions.....	74

CHAPTER 4: RESULTS

Development of an <i>In Vitro</i> Biochemical Assay to Study YopJ's Mechanism of Action.....	77
Introduction.....	77
Materials and Methods.....	78
Results.....	82
Discussions.....	102

CHAPTER 5: RESULTS

<i>In Vitro</i> Activation of the IKK Complex by HTLV-1 Tax.....	105
Introduction.....	105
Materials and Methods.....	106
Results.....	109
Discussions.....	124

CHAPTER 6: RESULTS

Characterization of the <i>In Vitro</i> Activity of YopJ.....	126
---	-----

Introduction.....	126
Materials and Methods.....	128
Results.....	133
Discussions.....	153
CHAPTER 7: DISCUSSION AND CONCLUSIONS	
YopJ: What is known?.....	156
Discussion of Research Findings.....	157
Summary of Main Contributions: YopJ's Mechanism.....	165
Future Directions.....	168
APPENDIX: TABLES OF PRIMERS.....	171
BIBLIOGRAPHY.....	173
VITAE.....	178

LIST OF PUBLICATIONS

Mukherjee, S., Negi, V.S., and Orth, K. (2007) Biochemical Mechanism of YopJ Acetyltransferase Activity. In preparation

Hao, Y-H., Wang, Y., Burdette, D.L., **Mukherjee, S.**, Keitany, G., Goldsmith, E.J., and Orth, K. (2007) Uncovering Steps of MAPKK Activation by Analyzing an Inhibitor of Activation, *Yersinia* YopJ. *Molecular Cell* (In Review)

Nejmeddine, M., Negi, V.S., **Mukherjee, S.**, Tanaka, Y., Orth, K., Taylor, G.P. and Bangham, C.R.M. (2007) HTLV-1 Tax Protein And ICAM-1 Act Synergistically On The T-Cell Signalling Pathways To Trigger The MTOC Polarization. *Journal of Biological Chemistry* (Submitted)

Mukherjee, S., Hao, Y-H., and Orth, K. (2007) A Newly Discovered Post-translational Modification- the Acetylation of Serine and Threonine Residues. *Trends in Biochemical Sciences* (Epub ahead of print)

Chosed, R., Tomchick, D.R., Brautigam, C.A., **Mukherjee, S.**, Negi, V.S., Machius, M., and Orth, K. (2007) Structural Analysis of *Xanthomonas* XopD Provides Insights into Substrate Specificity of ubiquitin-like protein proteases *Journal of Biological Chemistry* **282**, 6773-6782

Chosed, R., **Mukherjee, S.**, Lois, M.L., and Orth, K. (2006) Evolution of a Signaling System that Incorporates both Redundancy and Diversity: *Arabidopsis* SUMOylation. *Biochemical Journal* **398**: 521-529

Mukherjee, S., Keitany, G., Li, Y., Wang, Y., Ball, H.L., Goldsmith, E.J., and Orth, K. (2006) *Yersinia* YopJ acetylates and inhibits kinase activation by blocking phosphorylation. *Science* **312**: 1211-1214

Trosky, J.E., **Mukherjee, S.**, Burdette, D.L., Roberts, M., McCarter, L., Siegel, R.M., and Orth, K. (2004) Inhibition of MAPK signaling pathways by VopA from *Vibrio parahaemolyticus*. *Journal of Biological Chemistry* **279**: 51953-51957

LIST OF FIGURES

FIGURE 1 (Type III Secretion System).....	26
FIGURE 2 (Effect of Yops on host signaling pathways).....	27
FIGURE 3 (Common point of inhibition of the MAPK and NFκB pathways by YopJ).....	31
FIGURE 4 (The MAPK pathways in higher organisms and yeast).....	33
FIGURE 5 (The NFκB pathway).....	36
FIGURE 6 (YopJ is grouped under Clan CE of cysteine proteases).....	39
FIGURE 7 (Mechanism of SUMOylation).....	41
FIGURE 8 (Phosphorylation vs. SUMOylation).....	42
FIGURE 9 (Inhibition of SUMO conjugation of proteins by YopJ).....	43
FIGURE 10 (<i>In vitro</i> SUMOylation of MKK is sensitive to Ulp1 hydrolase activity).....	54
FIGURE 11 (Assays to test different candidate MKK1 lysine mutants for SUMOylation and activation).....	56
FIGURE 12 (YopJ does not function as a deSUMOylating enzyme).....	58
FIGURE 13 (YopJ does not function as a deubiquitinating enzyme).....	59
FIGURE 14 (Inhibition of the NFκB pathway by YopJ occurs regardless of the upstream stimuli).....	62
FIGURE 15 (YopJ specifically inhibits the IKKβ-dependent pathway).....	65
FIGURE 16 (Study of inhibition of MAPK pathway by YopJ in the presence of the scaffold protein, KSR).....	67

FIGURE 17 (Sub-cellular fractionation studies of the MKK-KSR complex in the presence of YopJ).....	70
FIGURE 18 (MKK forms a high molecular weight complex in the presence of KSR).....	72
FIGURE 19 (Effect of YopJ on the localization and stability of the IKK signalosome)	73
FIGURE 20 (<i>In vitro</i> activation of the MAPK pathway by EGF-treated membranes).....	84
FIGURE 21 (YopJ inhibits MAPK activation <i>in vitro</i>).....	86
FIGURE 22 (YopJ does not inhibit the active membrane complex that activates downstream MKK-ERK signaling).....	88
FIGURE 23 (YopJ inhibits NFκB activation <i>in vitro</i>).....	89
FIGURE 24 (YopJ inhibits <i>in vitro</i> activation of the NFκB pathway by NIK and MEKK1).....	91
FIGURE 25 (YopJ inhibits phosphorylation of exogenous IκB in the <i>in vitro</i> signaling assay).....	93
FIGURE 26 (Inhibition of the signaling pathways by YopJ is independent of phosphatase or DUB activities).....	95
FIGURE 27 (Recombinant YopJ might be requiring some activator or inhibitory factor to exert its inhibitory effect on the MAPK and NFκB pathways).....	98
FIGURE 28 (Purification of recombinant 6xHis-Tax).....	110
FIGURE 29 (<i>In vitro</i> activation of the IKK complex by recombinant HTLV-1 Tax).....	111

FIGURE 30 (Study of the effect of Tax mutants on the NFκB pathway).....	113
FIGURE 31 (<i>In vitro</i> activation of the IKK complex by recombinant Tax mutant proteins).....	115
FIGURE 32 (Effect of okadaic acid on Tax-dependent activation of IKK).....	117
FIGURE 33 (Effect of Geldanamycin on Tax-dependent activation of IKK)....	120
FIGURE 34 (Effect of YopJ on Tax-mediated activation of the NFκB pathway).....	122
FIGURE 35 (YopJ inhibits <i>in vitro</i> activation of the NFκB pathway by recombinant Tax)	123
FIGURE 36 (Model to explain YopJ's inhibitory activity).....	127
FIGURE 37 (Purification and biochemical analyses of rMKK6, rMKK6-J and rMKK6-C/A).....	134
FIGURE 38 (Expression of YopJ prevents the activation of MKK6 by phosphorylation)	137
FIGURE 39 (rMKK6-J is acetylated on Ser 207 and Thr 211 residues in its activation loop).....	139
FIGURE 40 (Alignment of the members of the superfamily of MAPK kinases).....	143
FIGURE 41 (<i>In vitro</i> acetylation of rMKK6 by YopJ).....	144
FIGURE 42 (Ser 207 and Thr 211 are the critical residues for rMKK6 acetylation by YopJ).....	147
FIGURE 43 (<i>In vitro</i> acetylation by YopJ prevents phosphorylation of rMKK6).....	149
FIGURE 44 (Inhibition of NFκB pathway by YopJ in an acetyl CoA-dependent	

manner).....	150
FIGURE 45 (IKK β purified from bacteria is constitutively phosphorylated)....	153
FIGURE 46 (<i>Yersinia</i> YopJ acetylates and inhibits kinase activation by blocking phosphorylation).....	164
FIGURE 47 (Comparison of the catalytic mechanism of a cysteine protease and YopJ)	167
TABLE 1 (Comparison of the activity of three Tax mutants).....	114

LIST OF ABBREVIATIONS

2x YT	Two times yeast extract and tryptone
a.m.u	Atomic mass units
AopP	<i>Aeromonas</i> outer protein P
ARS	ATP regenerating system
ATP	Adenosine triphosphate
AVP	Adenoviral protease
βME	Beta-mercaptoethanol
cdc37	Cell division cycle 37
CoA	Coenzyme A
DMEM	Dulbecco's modified Eagle's medium
DTT	Dithiothreitol
DUB	Deubiquitinating enzyme
<i>E. coli</i>	<i>Escherichia coli</i>
EDTA	ethylenediaminetetraacetic acid
EGTA	ethylene glycol tetraacetic acid
EGF	Epidermal growth factor
ERK	Extracellular-signal related kinase
ESI	Electro-spray ionization
FPLC	Fast protein liquid chromatography
GA	Geldanamycin
GST	Glutathione S-transferase
GTP	Guanosine triphosphate

HA	Influenza A virus hemagglutinin
HEK	Human embryonic kidney
HNT	Hepes-NaCl-Triton X-100 buffer
HOG	High osmolarity growth
Hsp90	Heat shock protein 90
HTLV-1	Human T-cell leukemia virus-1
HTX	HEPES Triton X-100 buffer
IKK	I kappa B kinase
IPTG	Isopropyl-beta-D-thiogalactopyranoside
JNK	c-Jun N-terminal kinase
KSR	Kinase suppressor of Ras
LC	Liquid chromatography
MAPK	Mitogen-activated protein kinase
MEK	MAPK/ERK kinase
MEKK1	MAPK/ERK kinase kinase 1
MKK	MAPK kinase
MKKK	MAPK kinase kinase
MS/MS	Tandem mass spectrometry
NFκB	Nuclear factor kappa B
NIK	NFκB inducing kinase
Ni-NTA	Nickel-nitriloacetic acid matrix (QIAGEN)
O.A.	Okadaic acid
O.D.	Optical density
PBS	Phosphate-buffered saline

PMSF	Phenylmethylsulfonylfluoride
PP2A	Protein phosphatase 2A
PVDF	Polyvinylidene fluoride
RRL	Rabbit reticulocyte lysate
SB	Sample buffer
SDS-PAGE	Sodium dodecyl sulfate-polyacrylamide gel electrophoresis
SUMO	Small-ubiquitin related modifier
TAB1/2	TAK1 binding proteins 1/2
TAK1	TGF β activating kinase 1
TCA	Trichloroacetic acid
TGF β	Transforming growth factor β
TNT	Transcription and translation
TNF α	Tumor necrosis factor α
TRAF6	TNF α receptor associated factor 6
TTSS	Type three secretion system
ULP1	Ubiquitin-like protein protease-1
VopA	<i>Vibrio</i> outer protein A
VS	Vinylsulfone
Ub	Ubiquitin
XopD	<i>Xanthomonas</i> outer protein D
Yop	<i>Yersinia</i> outer protein

CHAPTER ONE

INTRODUCTION

Straley and Bowmer first identified YopJ in 1986 as one of the virulence factors from *Yersinia pestis*, the causal agent for bubonic plague and the Black Death in the middle ages [1]. YopJ is also secreted by the other two closely related species, *Yersinia pseudotuberculosis* and *Yersinia enterocolitica*, that are commonly associated with gastrointestinal disorders [2]. Five other *Yersinia* effectors include YopH, YpkA, YopM, YopE and YopT. The YopJ homolog from *Y. enterocolitica* is also known as YopP. During infection, YopJ as well as all the other effector proteins are secreted into the host cell via the type III secretion system (TTSS) whereupon they disrupt the eukaryotic signaling machinery by blocking phagocytosis and inducing apoptosis [2]. The TTSS is a characteristic feature of the gram-negative bacteria and is initiated when the bacteria comes in contact with the host cell. It functions to transport effector proteins from the bacteria across the inner and outer bacterial membranes and the host cell membrane to reach the host cell cytosol via a syringe-like structure that is made up of 20-25 different proteins [3]. The effector proteins can be considered as viral oncogenes because they mimic or capture an endogenous eukaryotic activity. Supporting this model are previous observations that discovered the mechanism of effectors such as YopH, YopE and YpkA [4-6]. Type III effectors target and manipulate the eukaryotic signaling machinery and are always quiescent inside the pathogen [7].

Studies with YopJ revealed that it blocks both the mitogen activated protein kinase (MAPK) and nuclear factor κ B (NF κ B) signaling pathways at a common point and that is, at or above the level of the superfamily of MAPK kinases (MKKs) [8]. A single point mutation in YopJ (C172A) completely abolishes the inhibitory activity of YopJ and based on structure prediction programs from X-ray crystallographic data, the hydrolase activity of YopJ was predicted to be similar to that of adenoviral protease (AVP) and ubiquitin like protein protease 1 (Ulp1) [9]. YopJ is a unique, 32kD effector protein that has no homology to any known eukaryotic proteins but does have homologues in both animal and plant bacterial pathogens such as AvrA, VopA, AopP and AvrRxv [7, 10-12]. Based on this knowledge, the objective of this dissertation is to discover and characterize YopJ's mechanism of inhibition of the MAPK and NF κ B pathways.

Chapter three focuses on the characterization of the inhibitory effect of YopJ on the MAPK and NF κ B pathway using transfection-based *in vivo* assays. This study shows that YopJ inhibits the activation of I κ B kinase β (IKK β), the MKK analog in the NF κ B pathway, regardless of the upstream stimuli and that YopJ only inhibits the molecule to which it binds, such as MKK1 and IKK β , but not IKK α [8]. Sub-cellular localization studies and glycerol density gradients demonstrate that YopJ does not affect the localization of any of the signaling components or disrupt the signaling complexes in order to block these pathways. Lastly, *in vitro* assays with small ubiquitin-related modifier (SUMO) are unable to demonstrate YopJ's role as a deSUMOylating enzyme and thus refutes the

proposed model that YopJ maybe functioning like Ulp1.

Chapter four takes an unbiased approach and demonstrates the development of an *in vitro* cell-free signaling assay system to study YopJ's inhibition of the MAPK and NF κ B pathways. This assay system shows inhibition by YopJ of these pathways using different upstream stimuli such as epidermal growth factor (EGF), Ras or Raf for the MAPK pathway and (TNF α receptor associated factor 6) TRAF6, NF κ B inducing kinase (NIK) or MAPK/ERK kinase kinase (MEKK1) for the NF κ B pathway. The inhibitory effect of YopJ in these assays requires the maintenance of its catalytic site. Assay with recombinant YopJ, purified from different sources, fails to inhibit the signaling pathways and thus speculates the requirement of an additional factor or activator for YopJ to mediate its inhibitory effect. The study proposes at the end that in the presence of YopJ, the IKK or MKK signaling complexes are changed or modified and as such that they can no longer be activated by the upstream signaling machinery. The observation from this study is consistent with previous genetic, microbial and cellular studies and provides a method for analyzing inhibition of signaling by YopJ *in vitro*.

Chapter five mainly focuses on the protein, called Tax, from human T-cell leukemia virus-1 (HTLV-1). Tax is known to constitutively activate the NF κ B signaling pathway [13] and is also known to bind to the IKK γ component of the IKK complex [14]. Different studies have linked the activity of the serine threonine phosphatase 2A (PP2A) to Tax-mediated activation of the IKK complex [15, 16]. This study presents an *in vitro* system for analyzing Tax/IKK signaling

using purified, recombinant Tax, and reveals that Tax activates the IKK complex independent of any phosphatase activity, contradicting previous observations [15, 16]. This study, infact, supports the proposed model that binding of Tax to the IKK complex causes a conformational change that induces autoactivation of the complex [17]. Although this study does not provide the exact mechanism utilized by Tax, the development of this assay will provide an important tool that can be further used to dissect the molecular mechanism of Tax-mediated IKK activation. The study concludes by demonstrating YopJ-dependent inhibition of Tax-induced IKK activation, in accordance with previous studies [18]. Since YopJ is able to inhibit the proposed Tax-induced conformational change in IKK β , this indicates that IKK β itself is the target for YopJ. The observations from this study, thus supports the model predicted in Chapter four that YopJ is modifying the MAPK kinases such that they can no longer be activated.

Lastly, in chapter six, the mechanism utilized by YopJ to inhibit the MAPK and NF κ B signaling pathways is presented. YopJ acts as an acetyltransferase to modify the critical serine and threonine residues in the activation loop of MAPK kinases, thereby blocking their phosphorylation by the upstream signaling machinery [19]. Mass spectrometric studies reveals that in the presence of YopJ, the molecular weight of a representative MAPK kinase member, MKK6, is altered by the addition of single, double or triple post-translational modifications equal to a mass of 42 amu. Liquid chromatography followed by tandem mass spectrometry (LC-MS/MS) reveals that the highly conserved serine and threonine residues in the activation loop region of MKK6, Ser²⁰⁷ and Thr²¹¹, are acetylated in a YopJ-dependent manner. This offers a

straightforward mechanism that acetylation by YopJ prevents phosphorylation. These findings present the first-time demonstration of acetylation of residues other than lysine and leads to the appealing hypothesis that the modification of phosphorylatable residues by acetylation might be commonly used to regulate eukaryotic signaling machineries.

CHAPTER TWO

REVIEW OF LITERATURE

***Yersinia* and the Type III Secretion System**

Yersinia pestis is the bacterial pathogen that was the causal agent for Black Death in the middle ages. Two closely related species, *Yersinia pseudotuberculosis* and *Yersinia enterocolitica*, are associated with gastrointestinal disorders [2]. *Yersinia* is a gram negative bacterium that uses a type III secretion system (TTSS) to deliver its effector proteins into the host cell during infection. All the *Yersinia* species harbor a 70kb plasmid that encodes these effector proteins, known as *Yersinia* outer proteins (Yops), and the TTSS [2]. The TTSS is a proteinaceous structure used as a transport vehicle by the microbial pathogen to deliver effectors from the bacterial cytosol into the cytosol of the target host cell (Figure 1) [3]. The effectors unfold, get translocated through a syringe-like channel in an ATP-dependent manner and, upon entry into the host cell, they refold and destroy the target cell by crippling the host defense system, blocking phagocytosis and inducing apoptosis. These are the characteristic features of the TTSS. The other secretion systems include the Type I (*E. coli*), Type II (*Pseudomonas*), Type IV (*H. pylori*) and Type V (*H. influenzae*) that are also well studied and characterized [20].

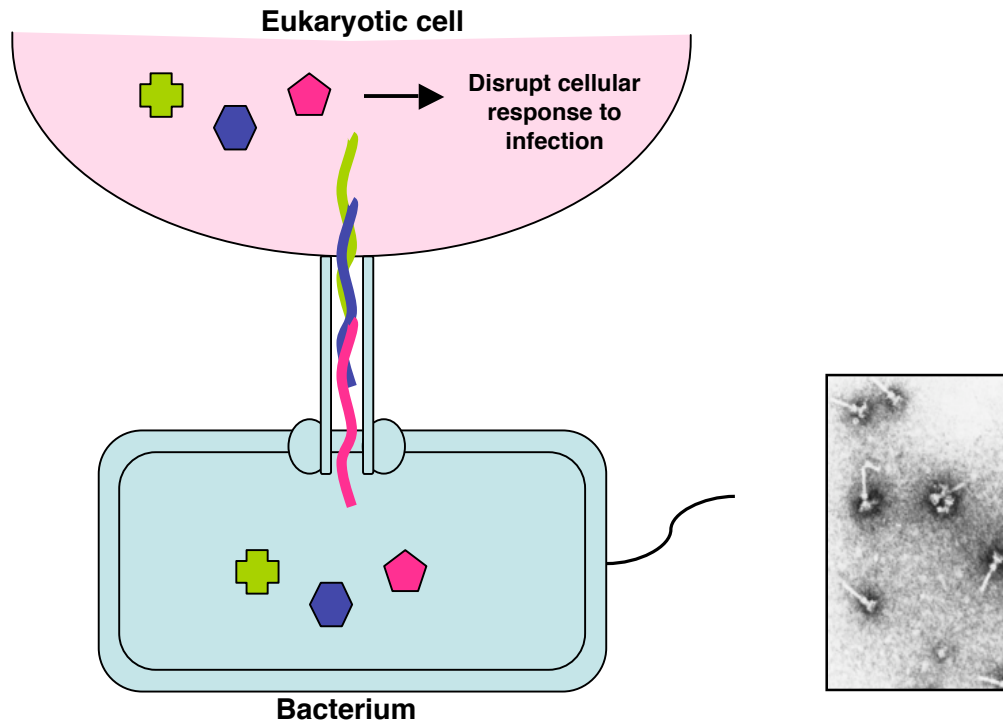


Figure 1: Type III Secretion System. The effector proteins are present in a quiescent state inside the bacterial pathogen. Upon infection, the effectors unfold and get injected into the host eukaryotic cell through a syringe-like channel in an ATP-dependent manner. The needle like structure at the junction of the bacterium and host cell is shown in an electron micrograph picture (right panel; taken from *Science*, 1998, 280: 602). After gaining entry into the host cell, these effectors refold and then disrupt the host cellular signaling machinery.

The TTSS effectors are synthesized inside the bacterial pathogen and are kept in a quiescent state so as not to be detrimental to the pathogen itself. The effectors are quiescent due to the lack of a substrate or an activator or due to the presence of a chaperone [7]. Interestingly, each *Yersinia* effector appears to have usurped or mimicked the activities of eukaryotic proteins that are essential for

maintaining normal signaling in the target cell, thereby allowing the pathogen to gain advantage during infection (Figure 2). For example, YopH is a very potent tyrosine phosphatase that disrupts focal adhesions by dephosphorylating the focal adhesion kinase (FAK) and p130cas [6]; however, it remains quiescent inside the pathogen since tyrosine phosphorylation does not occur in bacteria. Similarly, YopE, a GTP-ase activating protein that depolymerizes actin stress fibres, is also harmless to the bacteria because of the lack of G-proteins [5]. Furthermore, YpkA/YopO, a serine kinase that also leads to actin depolymerization, is quiescent in the bacteria because it requires binding to its activator, actin, upon entry into the host cell and then transforming into a highly active kinase [4]. These observations demonstrate that the *Yersinia* effectors have evolved to capture and seize control over the signaling machinery in the target cell.

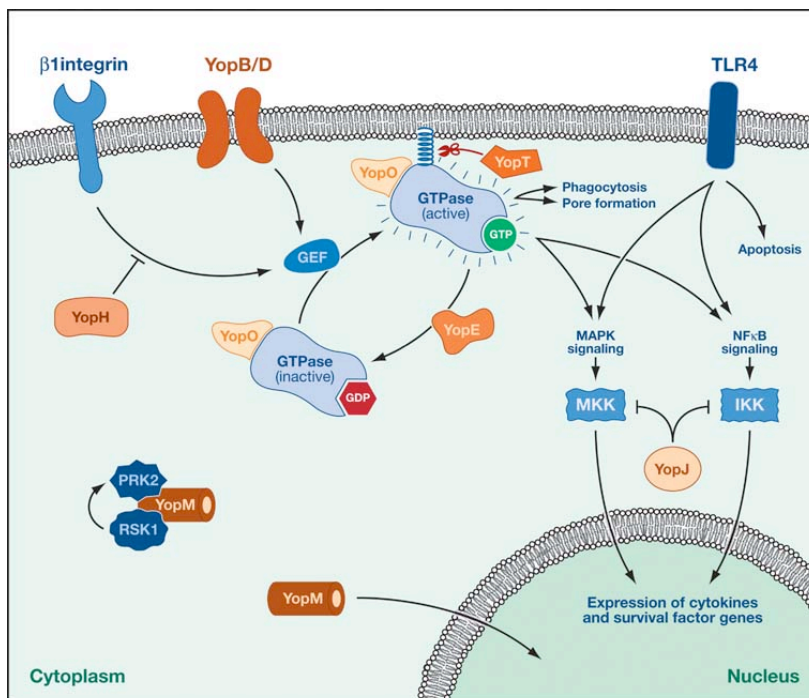


Figure 2: Effect of Yops on host signaling pathways. This schematic diagram depicts how the six different *Yersinia* effector proteins usurp the eukaryotic signaling machinery and thereby gain advantage over the host cell during infection. [Taken from *Annual Review of Microbiology* 2005: 59, 69]

The *Yersinia* effector, YopJ

Straley and Bowmer first identified YopJ in 1986 as a virulence factor from *Y. pestis*, using genetic screens [21]. Compared to other Yops, YopJ is secreted into the infected cell in much smaller amounts [22]. Several studies demonstrated that infection by *Yersinia* induced apoptosis in macrophages and downregulated the inflammatory response. Screening of a library of *yop* mutants by two independent groups identified YopJ (also YopP, *Y. enterocolitica* homolog of YopJ) as the virulence factor responsible for inhibiting cytokine production and inducing apoptosis in target cells during infection [23, 24]. Soon after, Ruckdeschel and colleagues demonstrated that upon infection by *Yersinia* there is profound inhibition of not only the different mitogen activated protein kinase (MAPK) pathways (ERK, p38 and JNK) but also the nuclear factor kappa B (NFκB) pathway [25]. Inhibition of these signaling pathways blocked expression of tumor necrosis factor-α (TNFα) in macrophages and of interleukin-8 (IL-8) in epithelial and endothelial cells of the infected host [22]. Since activation of the NFκB pathway leads to the induction of the anti-apoptosis machinery, these results suggested that *Yersinia* triggered apoptosis by inhibiting the NFκB pathway. Several different groups, using a series of infection and transfection assays, revealed that YopJ was the essential virulence factor that was solely

responsible for inhibiting the MAPK and the NF κ B pathways [26, 27].

This 32kD unique effector protein had no obvious homology to any known eukaryotic protein but was potent enough to inhibit the innate and the adaptive immune response pathways. YopJ-like proteins are found in other animal and plant pathogens such as AvrA of *Salmonella typhimurium* and AvrRxv, VopA of *Vibrio parahaemolyticus*, AopP of *Aeromonas salmonicida* and AvrBst of *Xanthomonas Campestris* pv *vesicatori* [7] [10, 12]. Although YopJ shares 87% similarity with AvrA, *in vivo*, these effectors cannot phenocopy each other [28]. Another YopJ homologue was found to be expressed by *Rhizobium* NGR234, a plant symbiont, thereby suggesting that these effectors not only played a role in blocking signaling pathways but also in modulating them. In total, the YopJ family of effectors is only present in animal and plant bacterial pathogens and thus indicated that they fundamentally functioned in host-pathogen interactions.

YopJ inhibits the essential signaling pathways at a common point

To explore further as to how YopJ was bringing about this global negative effect inside the host cell that resulted in the inhibition of multiple signaling pathways, Orth and colleagues discovered in 1999 that YopJ blocked these pathways at a common point [8]. Inhibition by YopJ was demonstrated at the level of the superfamily of MAPK kinases that includes MEK (MAPK/ERK kinase) for the MAPK pathway and the I κ B kinase β (IKK β) for the NF κ B pathway (Figure 3). The initial clue came from yeast-two hybrid screens that

identified MEKs (MKK1, MKK2 and MKK4) as the binding partners for YopJ [8]. The interaction of YopJ with these kinases was very specific and it did not bind to upstream MAPK kinase kinases (MKKKs) such as B-Raf or even downstream MAPKs such as extracellular signal-regulated kinase (ERK), c-Jun N-terminal kinase (JNK) and p38. Epistasis experiments and phosphorylation studies showed that YopJ inhibited MKK activation by epidermal growth factor (EGF), Ras and Raf [8]. Glutathione S-transferase (GST)-pull down assays further showed that besides MKK, YopJ could also bind IKK β , the MKK equivalent in the NF κ B pathway. *In vivo* YopJ blocked the NF κ B pathway downstream of MEK kinase 1 (MEKK1), one of the kinases known to phosphorylate IKK β [8]. This indicated that YopJ inhibits both the pathways at a common point (Figure 3). By blocking the MAPK pathways as well as the NF κ B pathway, YopJ blocked cytokine production and the innate immune response. Delivery of YopJ led to target cell apoptosis by preventing the production of anti-apoptotic factors. Thus, a common critical point in the MAPK and NF κ B pathways was identified as the target of this single *Yersinia* effector, YopJ. Although the affected pathways, MAPK and NF κ B, do not share any obvious common intermediates, how YopJ prevented the activation of MKK and IKK β and thereby completely shut down these signaling systems, was the major question that needed to be answered. However, before proceeding further into the mechanism that YopJ might be utilizing to inhibit the MAPK and NF κ B pathways, it is important to understand these signaling pathways and all the different signaling components associated with them.

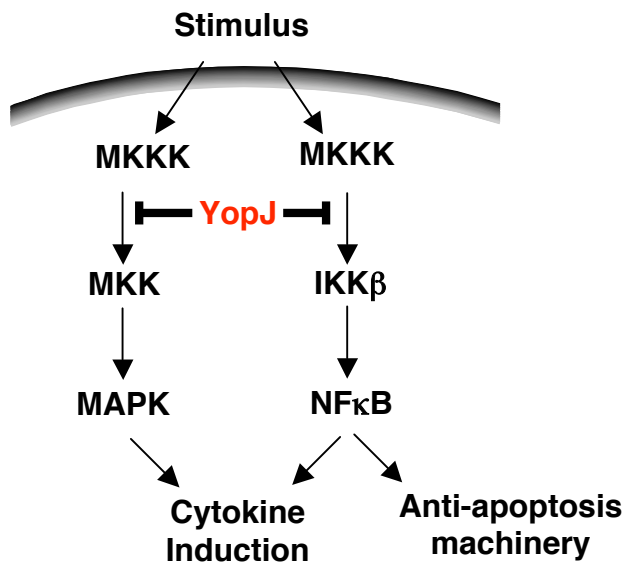


Figure 3: Common point of inhibition of the MAPK and NFκB pathways by YopJ. YopJ inhibits the MAPK pathways and the NFκB pathway by blocking the activation of MKKs and IKKβ, respectively. The inhibition by YopJ results in the block of proinflammatory responses and the anti-apoptosis machinery, thereby promoting cell death. [Adapted from: *Science* 1999, 285: 1920]

Review of the MAPK pathway

The MAPK signal transduction pathway is highly conserved from yeast to mammals and consists of a cascade of protein kinases that operate in a sequential fashion [29]. There are three major types of MAPK cascades that respond to different upstream signals such as growth factors, mitogens or stress (Figure 4A). The most studied MAPK pathway involves activation of Ras, a GTPase protein, by the binding of a ligand, such as EGF, to receptor tyrosine kinases (RTK) at the membrane. Activated Ras binds to Raf, a serine/threonine kinase that

phosphorylates MKK, a dual specific protein kinase, for activation. MKK then phosphorylates and activates a MAPK, ERK that is a serine/threonine kinase, which phosphorylates different proteins involved in transcriptional activity such as c-fos, c-myc and ribosomal S6 kinase (RSK) [30].

A 112kD protein, called kinase suppressor of Ras (KSR) facilitates the activation of this MAPK cascade by acting as a scaffold [31]. KSR binds together Raf, MKK and ERK, providing a platform for the activation of ERK in a sequential fashion. The KSR:MKK complex is known to undergo nucleocytoplasmic shuttling and in the presence of a growth stimulus, the KSR-MKK-ERK signaling complex is recruited to the membrane for activation by Ras and Raf [32]. KSR, like any other scaffold protein, provides specificity to the pathway and prevents crosstalks between the different MAPK pathways. The other two well-studied MAPK cascades are the JNK and the p38 kinases (Figure 4A).

The architecture of the MAPK pathways in yeast is similar to that in mammals and consists of a series of kinases that can be activated by different extracellular stimuli. The p38 equivalent pathway is the high osmolarity glycerol (HOG) pathway in yeast. Yoon and colleagues demonstrated that not only the HOG pathway, but also the pheromone-sensing MAPK pathway was susceptible to YopJ's inhibition (Figure 4B) [33]. This implied that YopJ's mechanism of inhibition of the MAPK pathways is evolutionarily conserved.

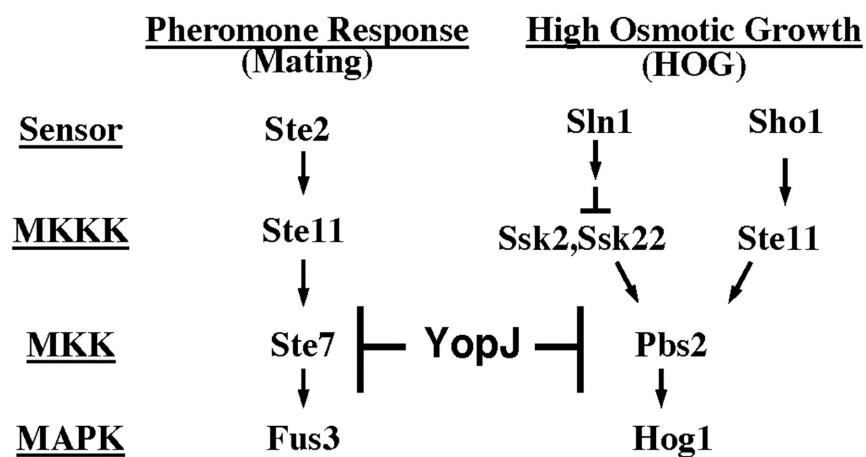
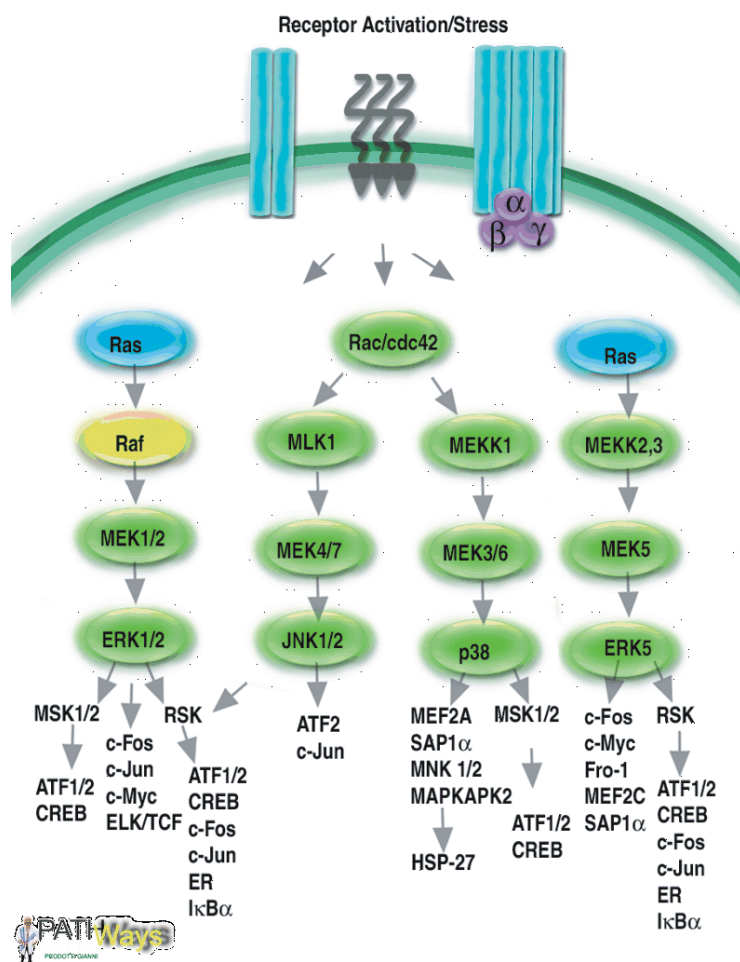


Figure 4: The MAPK pathways in higher organisms and in yeast. (A) Schematic diagram of the different MAPK pathways: ERK, JNK and p38. The pathways are activated by growth factors or stress. Activated Ras or Rac/cdc-42 leads to the sequential activation of downstream kinases that ultimately leads to activation of transcription factors and cytokine induction. Crosstalk amongst the different MAPK pathways is avoided by scaffold-like proteins such as KSR for the ERK pathway and JNK-interacting protein (JIP) for the JNK pathway. **(B)** Schematic representation of the HOG and the pheromone response MAPK pathways in yeast. YopJ inhibits these pathways at the level of MAPK kinases. [Taken from: *Journal of Biological Chemistry* 2003, 278: 2131]

Review of the NF κ B pathway

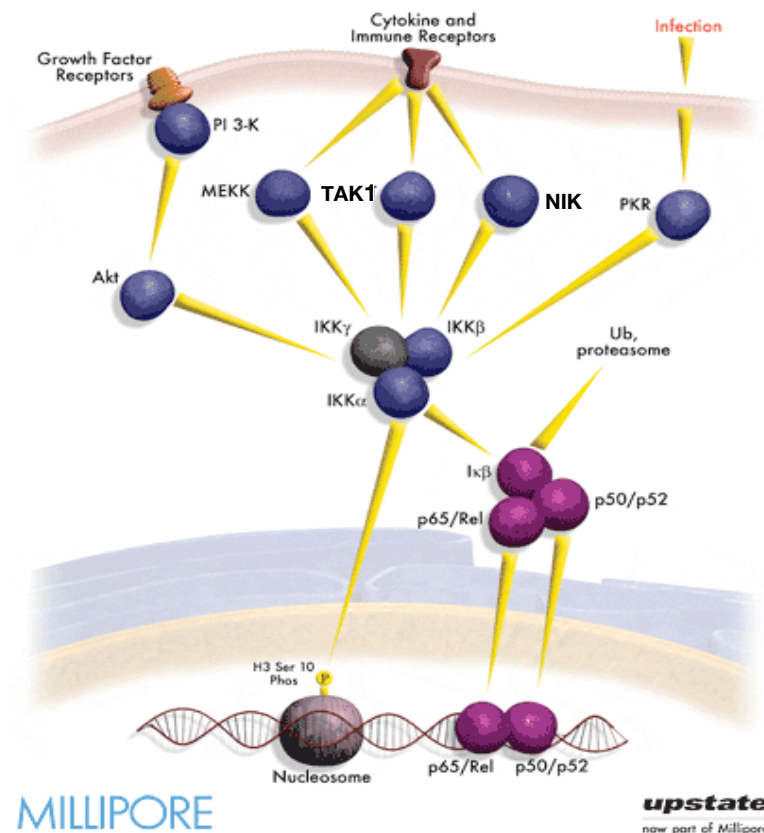
The other pathway that is disrupted upon *Yersinia* infection by YopJ is the NF κ B pathway. This pathway plays an important role in inflammation, cell proliferation, autoimmune response and apoptosis. Unlike the MAPK pathways, the NF κ B pathway can be activated by different upstream stimuli such as inflammatory cytokines, UV light and bacterial or viral toxins that finally converge at a common point, the IKK complex. The complex then phosphorylates its downstream target I κ B, which sequesters NF κ B in the cytoplasm in an inactive form. Phosphorylation of I κ B by the IKK complex leads to ubiquitin mediated degradation of I κ B, thereby allowing the release and subsequent translocation of NF κ B into the nucleus for transcriptional activation (Figure 5A) [34].

The IKK complex is a large complex of proteins (~700kD) that consists of two kinases, IKK α and IKK β , and a regulatory component, IKK γ , also known as NF κ B essential modulator (NEMO). Heat shock protein 90 (Hsp90) and cell

division cycle 37 (*cdc37*) also form part of the integral components of this pathway [35]. Although IKK α and IKK β share about 50% sequence homology, IKK β activates the canonical NF κ B pathway in response to proinflammatory signals that results in the release of NF κ B from I κ B, whereas IKK α activates the non-canonical NF κ B pathway leading to the processing of NF κ B2/p100 to p52 [36]. *In vitro* GST-pull down experiments demonstrated that YopJ binds to the IKK β component and not the IKK α component of the IKK complex [8].

Depending upon the extracellular stimuli, the IKK complex is activated by different upstream kinases including NF κ B inducing kinase (NIK), MEKK1 or TGF- β activated kinase (TAK1) [34]. NIK can activate both the IKK α - and the IKK β -dependent pathways. MEKK1 is the direct upstream kinase for IKK β , which can also activate the JNK pathway. An upstream activator molecule, TNF α receptor associated factor 6 (TRAF6), controls the TAK1-dependent activation of the IKK complex. Deng and colleagues dissected the TRAF6-mediated IKK activation using biochemical fractionation experiments [37]. They identified TRAF6 as an E3 ubiquitin ligase that ubiquitinates and activates the downstream kinase complex consisting of TAK1, TAB1 and TAB2 (TAK1 binding proteins) and then upon activation, TAK1 activates IKK β by phosphorylation (Figure 5B). Hence, the IKK complex is the central, converging point in the NF κ B pathway that is activated by different upstream kinases and previous studies have showed that YopJ inhibits the NF κ B pathway at the level of the IKK complex [8].

Another protein that activates the NF κ B pathway is the phospho-oncoprotein, Tax from the retrovirus, human T-cell leukemia virus-1 (HTLV-1) [13]. This 40kD protein, unlike the above kinases, does not activate the IKK complex by phosphorylation. It binds to the IKK γ component and it has been predicted that Tax activates the IKK complex by inducing a conformational change [17]. However, different groups have also linked the activity of serine threonine protein phosphatase 2A (PP2A) with Tax-mediated activation of IKK [15, 16]. Carter and colleagues went on to demonstrate that YopJ inhibits the activation of the IKK complex by Tax, using transfection studies [18].



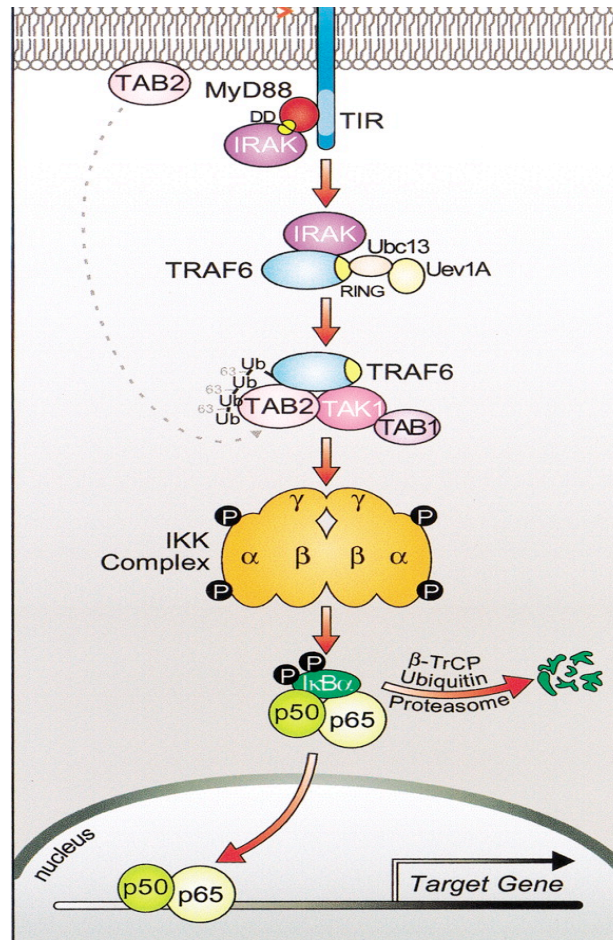


Figure 5: The NFκB pathway. (A) The NFκB pathway is activated by growth factors or inflammatory cytokines and during infection by bacterial or viral toxins. TAK1, NIK and MEKK1 are the three well-studied upstream kinases that phosphorylate and activate the IKK complex, thereby leading to phosphorylation and degradation of IκB, which then allows the translocation of NFκB/p65 to the nucleus for transcriptional activity. (B) TRAF6-mediated activation of the IKK complex. TRAF6 acts as an E3 ligase to ubiquitinate the downstream TAK1-TAB1-TAB2 protein complex in association with ubiquitin, E1 and E2 (a heterodimeric protein complex of Uev1a/Ubc13). Upon activation, the kinase TAK1 phosphorylates and activates the IKK complex. [Taken from: *Genes and Development* 2001, 15]

A single point mutation abrogates YopJ's inhibitory activity

Based on the observations from other *Yersinia* effectors, YopJ was predicted to mimic the activity of a eukaryotic protein that inhibits these signaling machineries. To identify this activity, alignment and comparison of the YopJ family of proteins to known secondary structures derived from crystallographic data predicted that the secondary structure of YopJ was similar to that of adenoviral protease (AVP), a cysteine protease from adenovirus [9]. Alignment of YopJ-like proteins with AVP revealed that all of the catalytic residues found in AVP were also present in YopJ and its homologues, with minor gaps, including the histidine (109), glutamate (128) and cysteine (172) residues that form the catalytic triad of a cysteine protease. This indicated that YopJ encodes a hydrolase.

Li and Hochstrasser in 1999 demonstrated that AVP is very similar to a eukaryotic cysteine protease Ulp1 (ubiquitin like protein protease) from yeast [38]. Sequence alignment of YopJ with AVP and Ulp1 demonstrated the conservation of the catalytic residues including histidine, aspartate or glutamate and cysteine in all the three proteins (Figure 6) [9]. Mutation of the putative catalytic cysteine at position 172 or histidine at position 109 to alanine (YopJC172A or YopJH109A) rendered YopJ catalytically inactive because the YopJ mutants lost their ability to inhibit either the MAPK pathways or the NFκB pathway [9]. In addition, similar mutations in other YopJ family of proteins like AvrRxv or AvrA also resulted in dead enzymes that could no longer mediate their inhibitory effects [9, 11]. Two members of the YopJ family of effector proteins,

VopA and AopP, have recently been characterized [10, 12]. VopA inhibits the MAPK pathway but has no effect on the NFκB pathway [12]. In contrast, AopP, like AvrA [11], inhibits the NFκB pathway downstream of IKK activation and does not affect the MAPK pathway [10]. Mutation of the catalytic cysteine in any one of these proteins resulted in dead, inactive enzymes. Thus, mutational analyses further support the model that the YopJ family of proteins function as hydrolases to cripple the host-signaling machineries in both plant and animal systems.

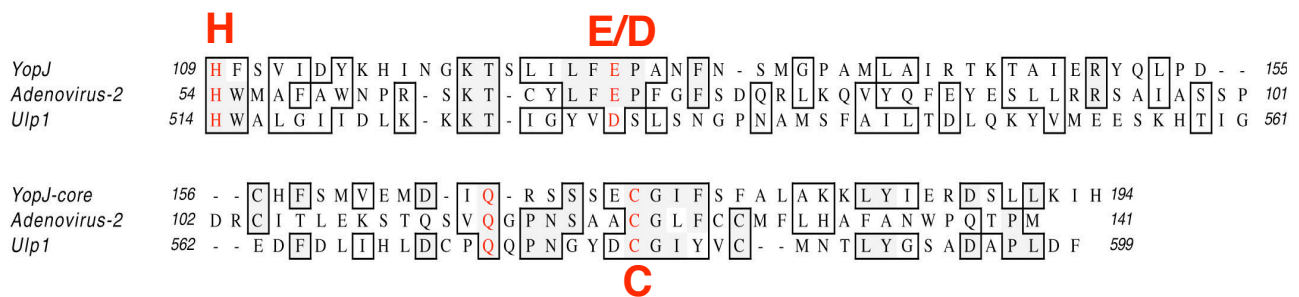


Figure 6: YopJ is grouped under Clan CE of cysteine proteases. Sequence alignment of YopJ with AVP and Ulp1 reveals the highly conserved catalytic residues- histidine (109), glutamate or aspartate (128) and cysteine (172), highlighted in red. The conserved glutamine residue at position 166 forms the oxyanion hole during the catalytic process. [Adapted from: *Science* 2000, 290: 1475]

Review of SUMOylation

The similarity of YopJ with Ulp1 and AVP placed YopJ under Clan CE of cysteine proteases. Ulp1 cleaves the carboxyl terminus of small ubiquitin-related

modifier (SUMO), just after the motif X-X-Gly-Gly [39]. SUMO in its processed form, with two glycine residues on its C-terminus, then modifies its target proteins in a manner similar to that used by ubiquitin to modify target proteins. The glycine on the C-terminus of SUMO forms an isopeptide bond with the -amino group of a lysine residue in the target protein [40]. SUMOylation, just like ubiquitination, involves three unique steps. First, SUMO is activated by a heterodimeric E1 activating enzyme (Uba2/Aos1 for yeast and SAE1/SAE2 for humans). This E1 enzyme forms a high-energy thioester intermediate with SUMO in the presence of ATP. Second, an E2 conjugating enzyme transfers the SUMO moiety from E1 to either the next enzyme E3 ligase or directly onto a variety of cellular targets. Third, only in some cases, an E3 ligase facilitates SUMOylation of specific substrates by transferring SUMO to a target protein, thereby forming an isopeptide bond (Figure 7). Deconjugation of SUMO from target proteins, in order to recycle SUMO monomers, is catalyzed by cysteine proteases such as Ulp1, which cleave the isopeptide bond between SUMO and the target protein. Thus, Ulp1 functions both as a peptidase and as an isopeptidase in the maturation step of SUMO and in the removal of SUMO from modified substrates, respectively (Figure 7).

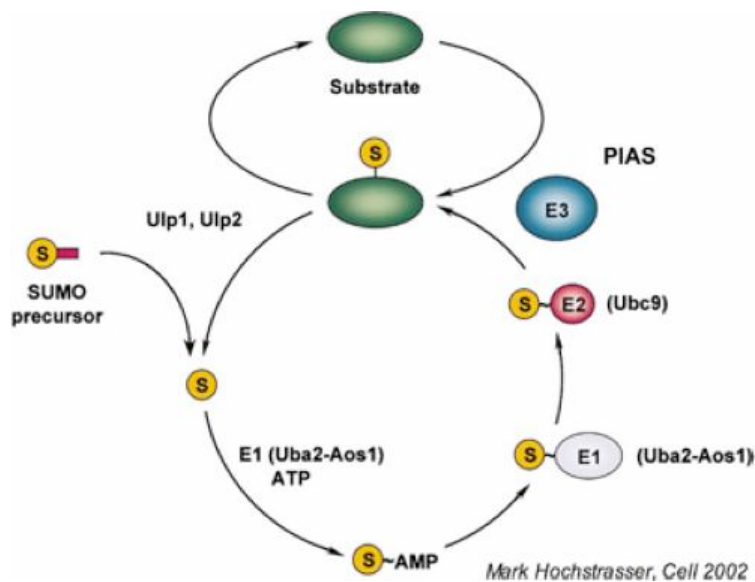


Figure 7: Mechanism of SUMOylation. SUMO is first activated by the E1 activating enzyme in the presence of ATP, resulting in the formation of a thioester intermediate. Next, SUMO gets transferred to the E2 conjugating enzyme and is subsequently transferred onto the target protein, sometimes in the presence of a specific SUMO E3 ligase. Isopeptidases cleave off SUMO from substrates to replenish the pool of SUMO monomers. [Taken from *Cell* 2002:]

The post-translational modification by SUMO or ubiquitin can be compared to the post-translational modification by phosphorylation in several aspects (Figure 8). Both of these processes require ATP as the energy source, they are both reversible due to the activity of isopeptidases and phosphatases and both of them alter the function of the target protein upon modification such as the activation of an inactive enzyme (MKK phosphorylation) or localization of a protein to the nucleus (RanGAP SUMOylation) [41, 42]. These post-translational modifications play an important role in different cellular events such as signal

transduction cascades, cell cycle progression, autophagy and DNA repair [39, 43].

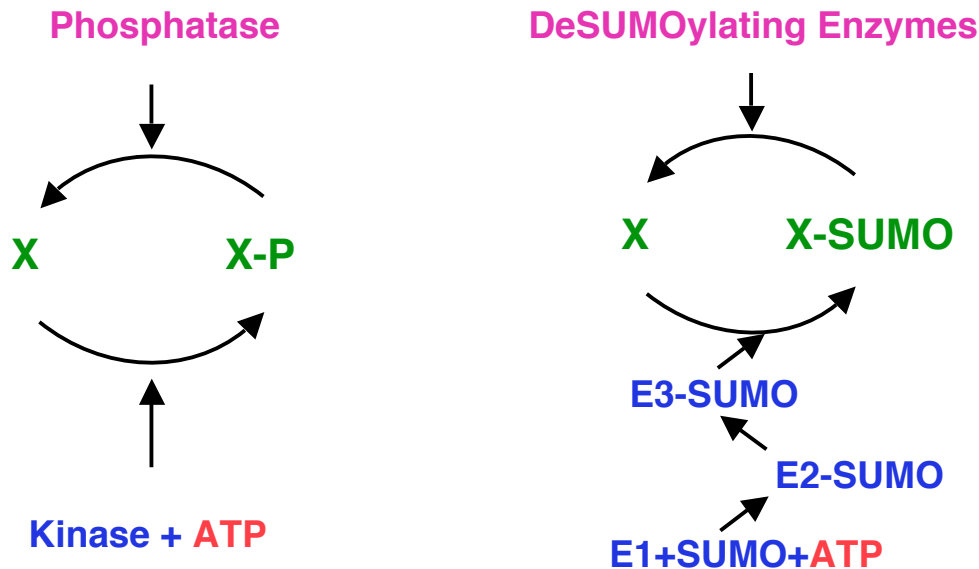


Figure 8: Phosphorylation vs. SUMOylation. Phosphorylation is depicted on the left and SUMOylation on the right. Both of these post-translational modifications require energy in the form of ATP, marked in red. A kinase adds a phosphate group (P) onto its substrate and in a similar manner the SUMOylation machinery comprising of E1, E2 and E3 enzymes adds a SUMO moiety to its substrate. Phosphatases or deSUMOylating enzymes participate in cleaving the P or SUMO groups, respectively, from their substrates. [Adapted from *Current Opinion in Microbiology* 2002, 5: 38]

YopJ: a DeSUMOylating enzyme or a DUB?

YopJ's similarity to Ulp1 predicted that YopJ maybe functioning in a manner similar to Ulp1 and led to the model that YopJ maybe mimicking the activity of some deSUMOylating enzyme. This idea was supported by the work of

Orth and colleagues [9], in which they showed that YopJ decreases the expression of SUMO and SUMO-conjugated proteins (Figure 9). However, it is important to note here that this study was done in an overexpression system. Epitope-tagged SUMO was overexpressed in mammalian cells in the presence and absence of YopJ-Flag and as such it is highly possible that the effect observed by YopJ might be a global cellular effect and not specific to YopJ's inhibitory activity.

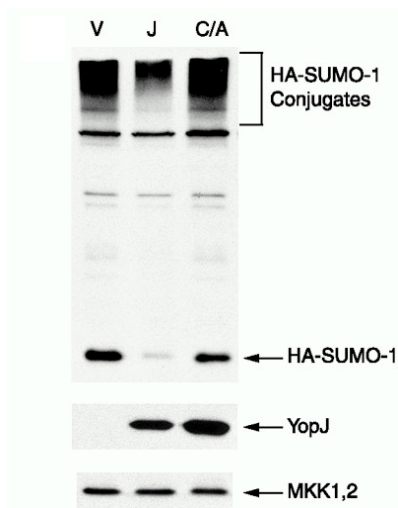


Figure 9: Inhibition of SUMO conjugation of proteins by YopJ. HEK293 cells were transfected with control vector (V), YopJ (J) and the catalytically inactive YopJ mutant, YopJC172A (C/A) in the presence of HA-SUMO and GST-B-Raf. SUMO and SUMOylated proteins were detected by immunoblotting with anti-HA antibody. [Taken from: *Science* 2000, 290: 1475]

Using a similar hypothesis, two other groups reported deubiquitinating (DUB) activities for YopJ [44, 45]. Carter and colleagues ectopically expressed

IKK β -Flag, IKK γ , HA-Ub, Tax and YopJ in HEK293 cells and detected an IKK β -Ub band in YopJ-deficient cells, but failed to detect the same IKK β -Ub band in the presence of YopJ, after immunoblotting with anti-HA antibody [44]. Likewise, Zhou and colleagues demonstrated that YopJ functions as a promiscuous DUB by acting on upstream TRAF molecules and on downstream I κ B to inhibit the NF κ B pathway [45]. This result contradicts the established model that YopJ inhibits both the MAPK and the NF κ B pathways at a common point, which is upstream or at the level of MAPK kinases [8]. Studies from both these groups were also done in an overexpression-based system by transient transfections and neither of them could explain the ability of YopJ to specifically inhibit the NF κ B pathway or all the MAPK pathways at the level of MAPK kinases. Although Zhou and colleagues demonstrated *in vitro* DUB activity for YopJ using Ub-AMC as the substrate, the activity was extremely weak and they failed to provide an important control in their assay, using the catalytically inactive YopJ mutant, YopJC172A, [45]. Recombinant YopJ used here was purified from Sf9 cells and hence there is a high chance of a contaminating DUB being co-purified with YopJ and thereby contributing to this effect.

Goal of this dissertation

The main aim of this thesis project is to discover and characterize YopJ's mechanism of inhibition of the eukaryotic signaling machinery. YopJ blocks the MAPK and NF κ B pathways upstream of the activation of the MAPK kinases,

which includes MKK and IKK β , respectively. YopJ's inhibition of these pathways requires the maintenance of an active catalytic site (C172) and this predicted that YopJ may be functioning as a hydrolase. More specifically it might be acting as a protease since it shares similar secondary structure with two known proteases, AVP and Ulp1. There are essential components of the MAPK and NF κ B pathways that may be sensitive to the hydrolytic activity of YopJ and may be required for the activation via phosphorylation of the MAPK kinases.

As with the other *Yersinia* effectors, YopJ may have also captured a proteolytic activity from eukaryotes to deregulate signaling. The discovery of the mechanism of other *Yersinia* effectors has uncovered critical points of regulation in their respective signaling pathways. Since YopJ targets an evolutionarily conserved mechanism of regulation, its discovery will lead to a further understanding of essential regulatory mechanisms in eukaryotic signaling pathways.

CHAPTER THREE

Results

STUDY OF THE INHIBITORY EFFECTS OF YOPJ ON THE MAPK AND NF κ B PATHWAYS

Introduction

YopJ inhibits the MAPK and NF κ B pathways at a common point, upstream or at the level, of MKK activation [8]. Using yeast two-hybrid analyses and GST-pull down assays, Orth *et al* showed that YopJ specifically binds to mitogen activated protein kinase kinases (MKK1, MKK2 and MKK4/SEK1) and IKK β . Mutation of the catalytic cysteine residue (C172A) completely abrogates YopJ's ability to block signaling [9]. This supported the hypothesis that YopJ is working as a hydrolase and that its catalytic activity is essential for its function. More specifically, may be it is acting as a protease, because the deduced secondary structure of YopJ has strong resemblance to the Clan CE group of cysteine proteases that includes AVP and Ulp1. XopD, another type III bacterial effector protein in plants shares high sequence homology with Ulp1 and has been recently shown to hydrolyze plant SUMO conjugates [46]. This suggests the possibility of YopJ being a deSUMOylating enzyme. To understand YopJ's mechanism, which could be similar to the ones described above or could be a new, unidentified mechanism, it is important to study the effect of YopJ on the different components of the signaling complexes that are required for MKK or IKK β activation.

This study demonstrates *in vitro* SUMOylation of MKK. Modification of MKK by SUMO is never observed under *in vivo* conditions even after several experimental trials. In addition, recombinant YopJ purified from different sources also fails to show any deSUMOylating or DUB activities. In the NF κ B pathway, inhibition of the IKK complex by YopJ occurs regardless of the upstream stimulus and YopJ specifically inhibits the IKK β -dependent pathway. Lastly, YopJ has no effect on the localization or stability of any of the signaling components in the MAPK and NF κ B pathways.

Materials and Methods

Plasmids and reagents

pSFFV-YopJ-Flag, pSFFV-YopJC172A-Flag, pCMV5-MEKK1, pcDNA3-MEK-myc, pcDNA3-HA-B-Raf, HRasV12 and 5xNF κ B luciferase reporter are described previously [8]. pRK7-Flag-NIK, pcDNA3-Flag-p100, pcDNA3-Flag-IKK α , pcDNA3-Flag-IKK β , pcDNA3-Flag-IKK-EE, pcDNA3-Flag-I κ B, pEBG-IKK β were provided by Dr. Zhijian J. Chen. KSR was cloned into pCMV5 and pEF1 vectors with 5' and 3'. pCMV5-KSRC809Y and pCMV5-KSRC392A were provided by Dr. Rob Lewis. pRSV-Renilla was provided by Dr. Debabrata Saha. pET11c-Aos1, pET28b-Uba2 and pET28b Ubc9 expression plasmids were gifts from Dr. Chris Lima. The different mutants of pcDNA3-MEK-myc (K36R, K64R, K183R) were generated using the Stratagene QuikChangeTM site-directed mutagenesis kit in both and mutants were confirmed

by DNA sequence analysis (Table of Primers in the Appendix).

Antibodies for phospho-MKK1/2, phospho-I κ B, phospho-IKK, phospho-ERK, and MKK1/2 were purchased from Cell Signaling. Antibodies for I κ B, IKK β , HSP90, TRAF6, aldolase, IKK α , IKK γ and myc were purchased from Santa Cruz Biotechnology. Anti-Flag and anti-GST antibodies were purchased from SIGMA and Covance respectively. Anti-lamin and anti-Na⁺/K⁺ ATPase antibodies were purchased from Zymed Laboratories and BD Biosciences, respectively. EGF and Coumermycin A were purchased from Alexis. T6RZC cell line was provided by Dr. Zhijian J. Chen and KSR^{-/-} cell lines were provided by Dr. Rob Lewis.

Purification of recombinant proteins

pET11c-Aos1 was transformed into BL21DE3 CP (RIL) competent cells expressing pET28b-Uba2 since Aos1 and Uba2 exists as a heterodimeric protein. His-Aos1/Uba2, along with His-Ubc9, were purified by standard Ni²⁺-NTA affinity chromatography (Qiagen). Briefly, cells were lysed using Emulsiflex C-5 cell homogenizer (Avastin) in lysis buffer containing 50mM NaH₂PO₄ (pH: 8.0), 300mM NaCl, 10mM imidazole (Sigma) with 0.05% β -mercaptoethanol (β ME) (BioRad) and 1mM phenyl methyl sulfonyl fluoride (PMSF) (Sigma). Cell lysates were allowed to bind to Ni-NTA resin for 1 hour at 4C and then eluted from beads using 250mM imidazole-containing buffer. Recombinant His-Ulp1 and GST-YopJ were kindly provided by Dr. Renee Chosed. GST-SUMO was provided by Dr. George DeMartino.

Tissue culture and transfection experiments

HEK293, T6RZC and KSR^{-/-} cell lines were cultured in Dulbecco's modified Eagle's medium (DMEM from Invitrogen) with 10% cosmic calf serum (Gemini) and 5% CO₂. For most of the experiments, Fugene reagent from Roche was used and cells were lysed with HNT lysis buffer (10mM HEPES 7.4, 50mM NaCl and 1% TritonX-100) containing protease inhibitor cocktail tablet (Roche), 1mM DTT, 20mM NaF, 20mM β -glycerophosphate, 0.5mM sodium vanadate and 0.5mM EGTA.

T6RZC cell lines, transfected with pSFFV, pSFFV-YopJ-Flag or pSFFV-YopJC172A-Flag for 36 hours were treated with coumermycin A for 0, 10 and 15 min, lysed with SDS sample buffer and immunoblotted with anti-TRAF6 antibody. Longer time points were also performed and samples were immunoblotted with anti-I κ B antibody to assess I κ B degradation over time. KSR^{-/-} cells were transfected with pSFFV, pSFFV-YopJ-Flag or pSFFV-YopJC172A-Flag in the presence of HRasV12 and then starved overnight, 24 hours post-transfection. Samples were immunoblotted for phospho-ERK. HEK293 cells transfected with pCMV5-Flag-KSR wild type, pCMV5-Flag-KSRC809Y and pCMV5-Flag-KSRS392A in the presence of pSFFV-YopJ-Flag or pSFFV-YopJC172A-Flag were treated with 50ng/ml EGF for 5 min at room temperature and then immunoblotted with anti-Flag antibody to detect KSR levels. For the NF κ B pathway, HEK293 cells were transfected with pRK7-Flag-NIK or pEBG-IKK β in the presence of pSFFV-YopJ-Flag and pSFFV-YopJC172A-Flag. Lysates were immunoblotted with anti-phospho-I κ B and anti-phospho-IKK

antibodies. To distinguish between the IKK α - and IKK β -dependent pathways, HEK293 cells were co-transfected with pRK7-Flag-NIK and either pDNA3-Flag-I κ B or pDNA3-Flag-p100, in the presence of pSFFV-YopJ-Flag and pSFFV-YopJC172A-Flag for 36 hours. Immunoblotting of lysates with anti-Flag antibody was done to detect both Flag-I κ B degradation and Flag-p100 processing to p52, simultaneously.

Luciferase assay

HEK293 cells were transfected with pCMV5-MEKK1, pRK7-Flag-NIK, pcDNA3-Flag-IKK α , pcDNA3-Flag-IKK β or pcDNA3-Flag-IKK-EE in the presence of pSFFV-YopJ-Flag or pSFFV-YopJC172A using Fugene transfection reagent. Each plate was also transfected with pRSV-Renilla to serve as the internal standard control. 24 hours post-transfections, cell lysates were prepared using passive lysis buffer (Promega), and luciferase assay was performed using Fluostar Optima (BMG Labtech).

Immunoprecipitation

HEK293 cells, transfected with pcDNA3-MEK-myc or the K1 and K2 mutants in the presence of pSFFV-YopJ-Flag or pSFFV-YopJC172A-Flag, were lysed in HNT lysis buffer and immunoprecipitated with 1:400 anti-myc antibody for 1 hour at 4°C, followed by incubation with Protein A-sepharose beads (Invitrogen) for 30 min. Samples were resolved by SDS-PAGE and immunoblotted with anti-phospho-MKK antibody. pSFFV and pSFFV-YopJ-

FLAG expressing HEK293 cell lysates were immunoprecipitated with anti-IKK γ antibody for 2 hours at 4°C, followed by protein A-sepharose bead incubation for 1 hour at 4°C. Cell lysates were immunoblotted with anti-IKK β , anti-I κ B and anti-Hsp90 antibodies.

Nitrogen Cavitation

HEK293 cells, transfected with control vector pSFFV or pSFFV-YopJ-FLAG plasmids, were harvested with PBS+1mM EDTA and the cell pellets were resuspended in HNMEK buffer (20mM HEPES 8.0, 150mM NaCl, 2mM MgCl₂, 1mM EDTA and 10mM KCl). The cells were then transferred to the metal base of the nitrogen cavitation apparatus and pressurized to 450psi with nitrogen gas on ice [47]. After 15 min, the cells were slowly released into a conical centrifuge covered with parafilm and spun at 800g for 5 min to separate the nuclear fraction. The lysates were further subjected to differential centrifugation at 16,000g and 100,000g for 10 and 60 minutes respectively to separate the organelles and the membrane fractions. Fractions were first immunoblotted with fraction-specific markers to assess purity of the sub-cellular fractions and then with antibodies to endogenous MKK or IKK.

Glycerol density gradient centrifugation

HEK293 cell lysates, transfected with or without pEF1-FLAG-KSR, were subjected to glycerol density gradient centrifugation. Briefly, cells were lysed in 0.05M Tris 7.8 buffer using a Dounce homogenizer and spun down to remove cellular debris. Cleared lysate was then loaded on top of a 10-40% glycerol

column, prepared the night before, and the columns were spun at 100,000g for 3 hours at 4°C. 100µl fractions collected were then immunoblotted with anti-MKK antibody. For the NFκB pathway similarly, cells were transfected with pSFFV-YopJ-FLAG and immunoblotted with anti-IKKβ, anti-IKKα and anti-IKKγ antibodies.

In vitro translation and SUMOylation

pcDNA3-MEK-myc, pcDNA3-MEK-myc-K1, pcDNA3-MEK-myc-K2 and pcDNA3-FLAG-IκB were *in vitro* translated in the TNT coupled rabbit reticulocyte lysate (RRL) system (Promega) with L-[³⁵S]-methionine (Amersham). Translation of the proteins was confirmed by running SDS gels, followed by autoradiography. pcDNA3-YopJ-FLAG was *in vitro* translated cold, without -[³⁵S]-methionine.

In vitro SUMOylation was performed in a 15µl reaction by incubating ³⁵S-labeled MEK-myc or ³⁵S-labeled FLAG-IκB with 1 µg purified Aos1/Uba2 (E1), 0.3µg purified Ubc9 (E2) and 2µg GST-SUMO in the presence of an ATP regenerating system (10xARS stock: 10mM ATP, 350mM creatine phosphate, 20mM Hepes pH 7.2, 10mM MgCl₂ and 500µg/ml creatine kinase) for 2 hours at 37°C. Samples were resolved by SDS-PAGE, fixed in solution containing 50% MeOH, 40% dH₂O and 10% acetic acid for 30 min, amplified using Amplify reagent (Amersham) for 15 min, and finally analyzed by autoradiography.

To assess YopJ's role as a deSUMOylating enzyme, GST-YopJ or cold *in vitro* translated YopJ-Flag was incubated with SUMO-³⁵S-IκB and SUMO-³⁵S-

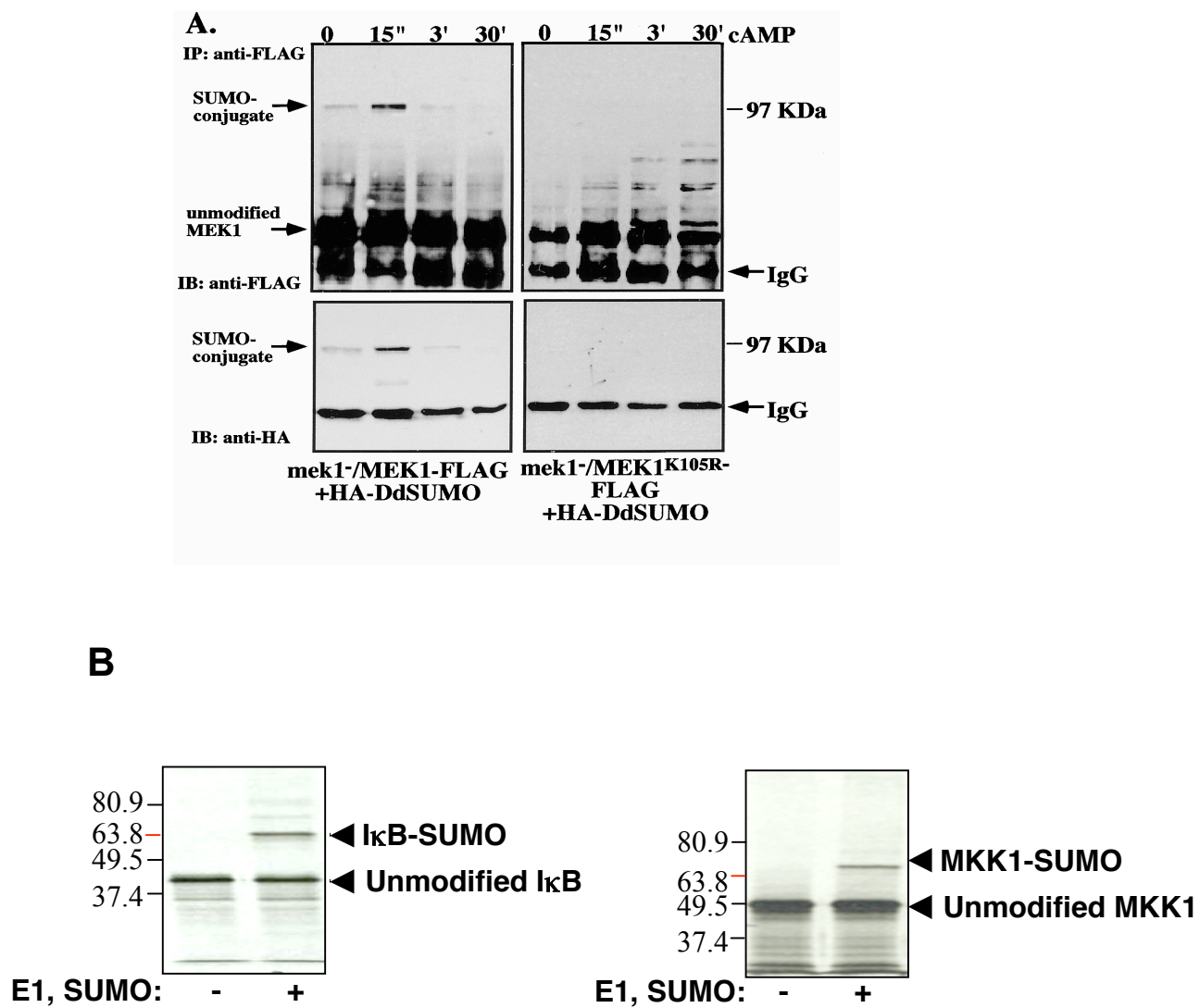
MKK1 for 1 hour at 37°C. SUMO-³⁵S-MKK1 was also incubated with recombinant His-Ulp1 for 1 hour at 37°C to ensure cleavage of the SUMO moiety from ³⁵S-MKK1.

Results

In vitro SUMOylation of MKK

Modification of MKK by SUMO has been observed in *Dictyostelium* (Figure 10A) and has been shown to be important for its activation [48]. Since MKK is one of the known interacting partners of YopJ and since the secondary structure of YopJ is similar to Ulp1, it is possible that MKK modification by SUMO may be sensitive to the hydrolase activity of YopJ. Thus, *in vitro* SUMOylation assays were set up to first test whether mammalian MKK1 indeed gets SUMOylated. MKK1 was *in vitro* transcribed and translated in a rabbit reticulocyte lysate (RRL). The *in vitro* translated ³⁵S-labeled MKK1 was then used in an *in vitro* SUMOylation assay with recombinant SUMO conjugation system, consisting of purified heterodimeric protein complex of His-Aos1/Uba2 (E1), His-Ubc9 (E2), GST-SUMO and an ATP regenerating system (ARS). Like IκB, which was used as a positive control in this assay [49], MKK1 also gets modified by SUMO, as detected by a ~17kD upward shift in mobility on a SDS-PAGE gel (Figure 10B). This indicates that MKK from other species can also be modified by SUMO. To ascertain that the observed band was indeed MKK1-SUMO, recombinant Ulp-1 protein was incubated with MKK1-SUMO and as

observed in Figure 10C, lane 4, Ulp-1 was able to remove the SUMO moiety from MKK1.



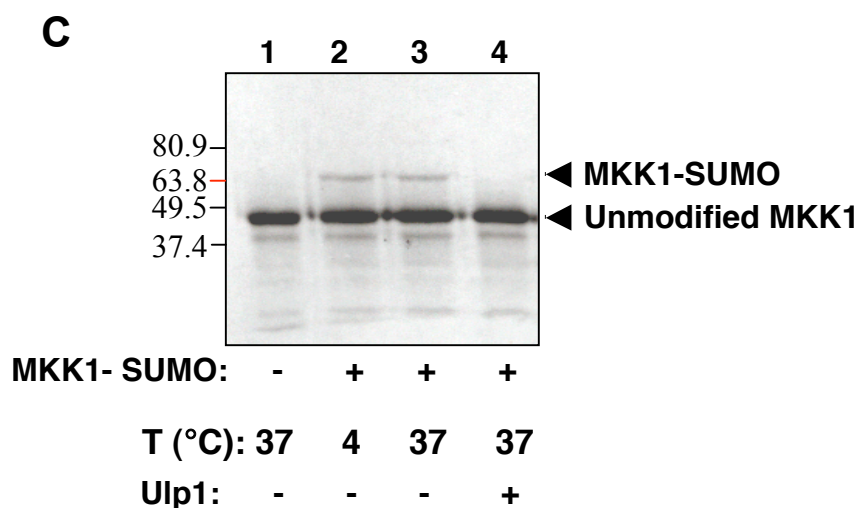
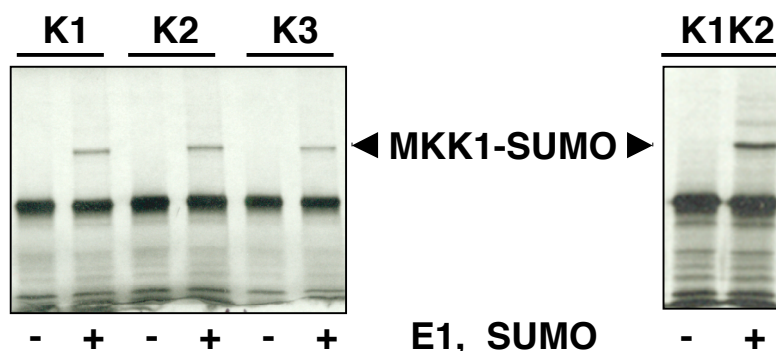


Figure 10: *In vitro* SUMOylation of MKK is sensitive to Ulp1 hydrolase activity. (A) SUMO modification of *Dictyostelium* MEK1 on lysine105. *mek1* null cells coexpressing HA-DdSUMO and either MEK1-FLAG (left panel) or MEK1K105R-FLAG (right panel) were stimulated with 30 mM cAMP for the indicated time intervals. Immunoprecipitated MEK1 was subjected to immunoblot analysis with anti-FLAG and anti-HA antibodies. [Taken from: *Dev. Cell*, 2002, 2:745-56] (B) *In vitro* SUMOylation of IκB and MKK1. ³⁵S-IκB (left panel) and ³⁵S-MKK1 (right panel) were incubated with or without the SUMO conjugation machinery for one hour at 37°C. Reactions were stopped by adding 5x-SDS SB and samples were separated by SDS-PAGE and analyzed by autoradiography. (C) Incubation of SUMO modified MKK1 with recombinant Ulp1 for 1 hour at 37°C, removed the SUMO moiety from MKK1 (lane 4).

Next, to determine which lysine in MKK1 is modified by the SUMO conjugation system, several candidate lysine mutations were made, based on the consensus site for SUMO modification (I/L-K-X-E/D) in MKK1, and were tested for SUMOylation *in vitro*- K1 (K36R), K2 (K64R) and K3 (K183R). These lysine mutants were also used in transfection-based assays to determine whether they can be activated by EGF stimulus and/or whether they are resistant to YopJ's

inhibition. Unfortunately, none of the lysine mutants were able to abolish MKK1 modification by SUMO *in vitro* (Figure 11A). In addition, upon transfection in HEK293 cells, all the mutants were inhibited when coexpressed with YopJ (Figure 11B). Analyses of MKK-SUMO under *in vivo* conditions were quite challenging and after several experimental trials, however, conjugation of MKK with SUMO was never observed. From these observations, questions arise regarding the importance of SUMO modification in the regulation of mammalian MAPK signaling.

A



B

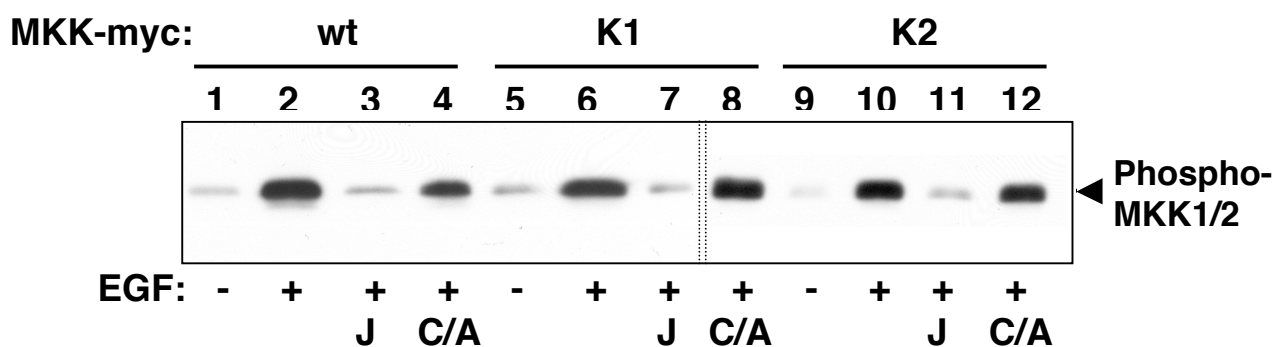


Figure 11: Assays to test different candidate MKK1 lysine mutants for SUMOylation and activation. (A) Three single lysine mutants K1 (K36R), K2 (K64R) K3 (K183R) and one double lysine K1K2 (K36R, K64R) mutant were made using site-directed mutagenesis. The mutants were *in vitro* translated in RRL and used in *in vitro* SUMO conjugation assay as described in Figure 1B. (B) HEK293 cells were transfected with wt MKK1, K1 and K2, with or without YopJ-Flag, using Fugene reagent. 24 hours post-transfection, cells were starved with serum-free media for 3 hours and lysed with HNT lysis buffer. Lysates were immunoblotted with anti-phospho-MKK1/2 antibody after separation on a SDS-PAGE gel.

YopJ is neither a deSUMOylating enzyme nor a DUB

Having developed an *in vitro* SUMOylation system using MKK1 as the substrate, the next important question is whether this modification is sensitive to the hydrolase activity of YopJ. *In vitro* SUMOylated MKK1 (^{35}S -MKK1-SUMO) was incubated with recombinant YopJ purified from different sources including yeast, bacteria and insect cells. *In vitro* translated ^{35}S -labeled YopJ was also used as one of the sources. In all the experiments, cleavage of the MKK1-SUMO band was never observed (Figure 12), in contrast to incubation with Ulp-1 as seen in lane 4, Figure 10C.

The possibility of YopJ being a DUB was also tested using several different approaches. For example, a transfection-based assay using HEK293 cell lines stably expressing a modified form of TRAF6 were utilized. TRAF6 is an E3 ligase that activates the downstream TAK1 kinase complex to activate IKK signaling. Activation of this stable cell line (also known as T6RZC), where the N-terminal fragment of gyrase B (inducible dimerization domain) replaces the C-terminal TRAF domain of TRAF6 (Figure 13A), by coumermycin A leads to

dimerization and auto-ubiquitination of T6RZC, resulting in activation of the NF κ B pathway [37]. Figure 13B shows anti-TRAF6 immunoblot of T6RZC cell lysates that were transfected with vector control, YopJ or YopJC172A plasmids and treated with coumermycin A for 10 and 15 minutes to activate NF κ B signaling. The high M.W. bands, in the form of a ladder, correspond to TRAF6-ubiquitin chains. Comparing lanes 3, 6 and 9, it was obvious that there was no reduction in TRAF6-ubiquitin bands in the presence of YopJ. This implies that YopJ inhibits the NF κ B pathway downstream of TRAF6 activation (see below) and that it does not affect TRAF6 auto-ubiquitination.

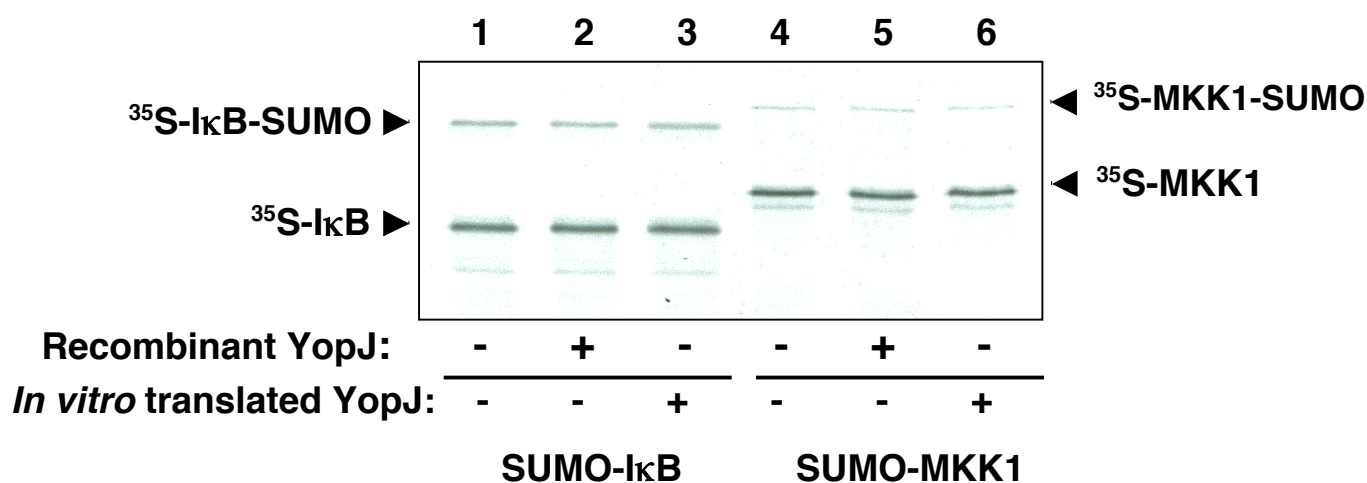


Figure 12: YopJ does not function as a deSUMOylating enzyme. 35 S-I κ B and 35 S-MKK1 modified with SUMO were incubated with either GST-YopJ purified from *E. coli* (lanes 2 and 5) or with cold, *in vitro* translated YopJ-Flag (lanes 3 and 6) for 1 hour at 37°C. Samples were resolved on a 12% SDS gel and visualized by autoradiography.

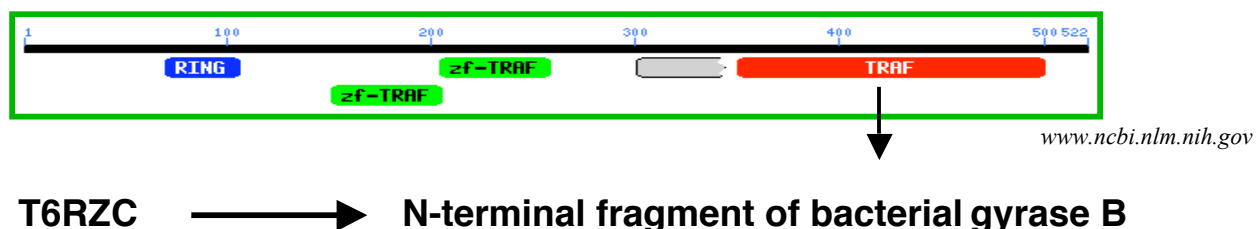
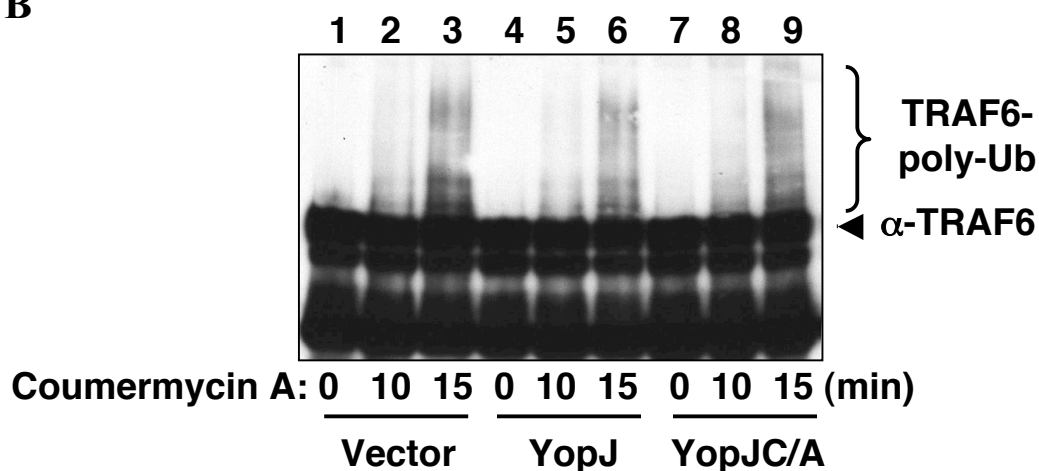
A**B**

Figure 13: YopJ does not function as a deubiquitinating enzyme. (A) Schematic of TRAF6 molecule with its domains. T6RZC is constructed by replacing the C-terminal TRAF domain by the N-terminal fragment of bacterial gyrase B. [Taken from *ncbi.nlm.nih.gov*] (B) T6RZC stable HEK293 cells were transfected with pSFFV control vector, YopJ-Flag and YopJC172A-Flag for 36 hours, treated with Coumermycin A for 0, 10 and 15 minutes and lysed with HNT lysis buffer. Samples were run on a SDS gel, transferred to PVDF membrane and then immunoblotted with anti-TRAF6 antibody.

Vinyl sulfones (VS) are functional groups that act as potent, irreversible inhibitors of cysteine proteases including DUB's and ubiquitin-specific proteases [50]. They are useful for inhibiting the hydrolysis of poly-ubiquitin or ubiquitin-like chains on substrate proteins *in vitro* and thus enhances polyubiquitin chain accumulation. Potential DUBs have been identified in the past using ubiquitin-VS (Ub-VS) adduct wherein protein conjugates with Ub-VS are visualized on a SDS-PAGE gel [51]. To determine whether YopJ functions as a DUB or deSUMOylating enzyme, experiments were done by incubating Ub-VS or SUMO-VS [*Courtesy: Dr. Keith Wilkinson, Emory University*] with YopJ cell extracts. Unfortunately, there was no such appearance of bands consistent with YopJ-Ub-VS or YopJ-SUMO-VS adducts on a SDS-PAGE gel. The details of this experiment are described later in chapter five. Thus, these studies further rule out the possibility of YopJ functioning as a DUB or a deSUMOylating enzyme.

YopJ inhibits IKK activation irrespective of the upstream stimulus

The NF κ B pathway, in contrast to the MAPK pathway, is activated by different stimuli that converge at a common point, the IKK complex, which then phosphorylates its downstream target I κ B, thereby releasing NF κ B into the nucleus for transcriptional activity. TAK1, NIK and MEKK1 are three kinases that independently lead to IKK phosphorylation and activation [34]. To determine whether these kinases utilize a common mechanism to activate the IKK complex and whether this mechanism is sensitive to YopJ's inhibitory activity, luciferase

assays were performed by over expressing TAK1, NIK and MEKK1 in the presence of either YopJ or YopJC172A (*Courtesy: Gladys Keitany*). Figure 14A demonstrates that YopJ, but not YopJC172A, inhibited the induction of a NF κ B luciferase reporter gene, thereby blocking NF κ B pathway activation, by all of these kinases. In transfection-based assays, using NIK as the upstream stimulus, immunoblotting with anti-phospho-I κ B antibody showed that YopJ, in contrast to YopJC172A, resulted in a decrease in I κ B phosphorylation (Figure 14B). Activation of YopJ-expressing T6RZC cell lines with coumermycin A, revealed stabilization of I κ B levels when immunoblotted for endogenous I κ B, implying inhibition of the NF κ B pathway (Figure 14C, middle panel). By contrast, in T6RZC cells expressing YopJC172A, I κ B gets phosphorylated and subsequently degraded over time, similar to vector control (Figure 14C, upper and lower panels). All these results indicate that YopJ may be affecting the ability of all the upstream stimuli to activate this complex.

Immunoprecipitation of the IKK complex with α -IKK γ antibody from cells over-expressing NIK or MEKK1, in the presence or absence of YopJ, also revealed that the IKK complex isolated from YopJ lysates had decreased kinase activity as demonstrated by diminished phosphorylation of the GST-I κ B α substrate *in vitro* (data not shown). Thus, this implies that in the presence of YopJ, the IKK complex is inactive and can no longer activate its downstream target.

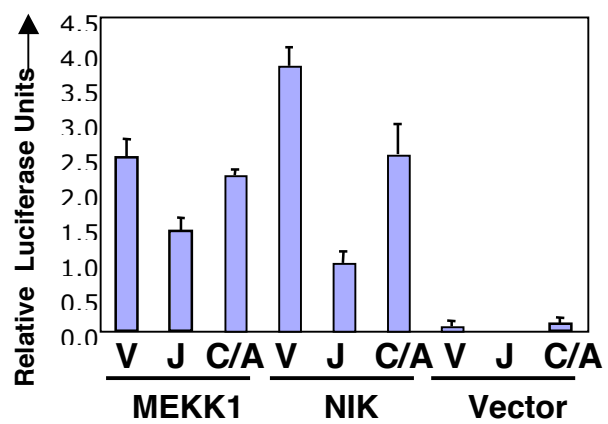
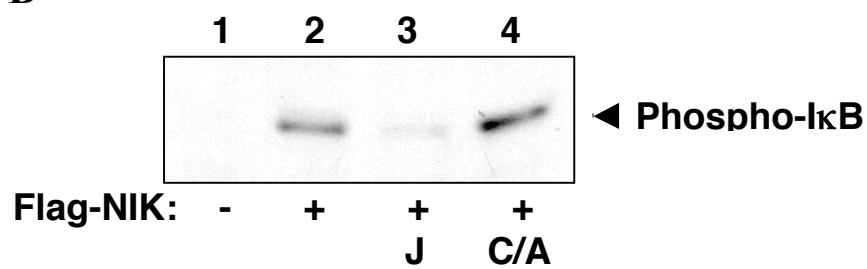
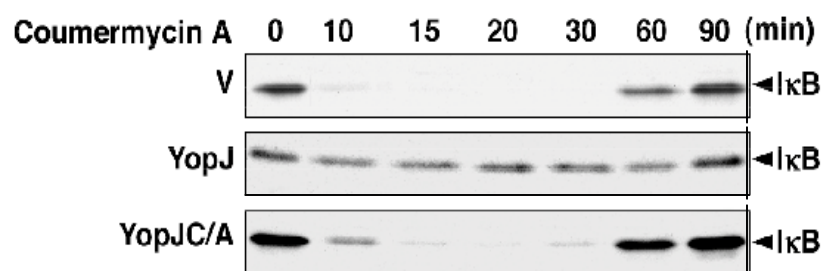
A**B****C**

Figure 14: Inhibition of the NF κ B pathway by YopJ occurs regardless of the upstream stimuli. (A) Luciferase assay of extracts from HEK293 cells cotransfected with a NF κ B luciferase reporter plasmid, expression plasmids for MEKK1 or NIK (as inducers), and vector (V), YopJ (J), or YopJC172A (C/A) as indicated. Renilla luciferase activity served as the internal control and was used to normalize all reactions for transfection efficiency. [Courtesy: Gladys Keitany] (B) HEK293 cells were transfected with Flag-NIK in the presence of YopJ (J) or YopJC/A (C/A) for 24 hours using Fugene transfection reagent. Cells were lysed with HNT lysis buffer and samples were resolved on a SDS gel, followed by immunoblotting with antibody to endogenous phospho-I κ B. (C) T6RZC cell lines were transfected with vector control (V), YopJ (J) or mutant (C/A) for 36 hours and then treated with Coumermycin A for the times indicated. Activation of the NF κ B pathway was detected by immunoblotting with anti-I κ B antibody. [Courtesy: Huaqun Chen]

YopJ specifically inhibits the IKK β -dependent pathway

The IKK complex includes two kinases, IKK α and IKK β and a regulatory component, IKK γ . IKK β activates the canonical NF κ B pathway, in response to pro-inflammatory signals, which results in the release of NF κ B from I κ B whereas IKK α activates the non-canonical NF κ B pathway wherein it leads to the processing of NF κ B2/p100 to p52 [36]. *In vitro* GST-pull down experiments has shown that YopJ binds IKK β but not IKK α [8]. Luciferase reporter assays using these two kinases in the presence of YopJ showed that YopJ specifically inhibited the IKK β -mediated activation of NF κ B and had no effect on the IKK α -dependent pathway (Figure 15A). However, YopJ was unable to inhibit the NF κ B pathway when stimulated by the overexpression of constitutively active IKK β (IKK β -EE). This suggests that YopJ is acting at the level of IKK β activation and

that it cannot inhibit the NF κ B pathway when IKK β is constitutively active. In transfection-based assays, NF κ B signaling was also activated by the overexpression of GST-tagged IKK β in HEK293 cells. YopJ, but not YopJC172A, inhibited both IKK and I κ B phosphorylation (Figure 15B) when co-expressed with GST-IKK β . These results indicate that YopJ is specific to the IKK β -dependent pathway.

NIK is an upstream kinase that not only activates IKK β , leading to I κ B phosphorylation and degradation, but also activates IKK α , resulting in the phosphorylation-dependent processing of NF κ B2/p100 to p52. Keeping this in mind, an experiment was designed to simultaneously study the activation of both IKK α - and IKK β -dependent pathways by NIK in the presence of YopJ. HEK293 cells were transfected with Flag-NIK and either Flag-p100 or Flag-I κ B in the presence of either wild type YopJ or the catalytically inactive form, YopJC172A. As observed in Figure 15C (lanes 3 and 8), I κ B was phosphorylated and NF κ B2/p100 was processed to p52 respectively, in the presence of NIK. Although YopJ inhibited I κ B phosphorylation (lane 4), it did not affect NF κ B2/p100 processing to p52 (lane 9). The effect of YopJ is more convincing when looking at the phosphorylated state of I κ B (lane 4, lower panel) as compared to the steady state level of I κ B (lane 4, upper panel). All these experiments suggest that YopJ is only able to inhibit the activation of that molecule to which it binds.

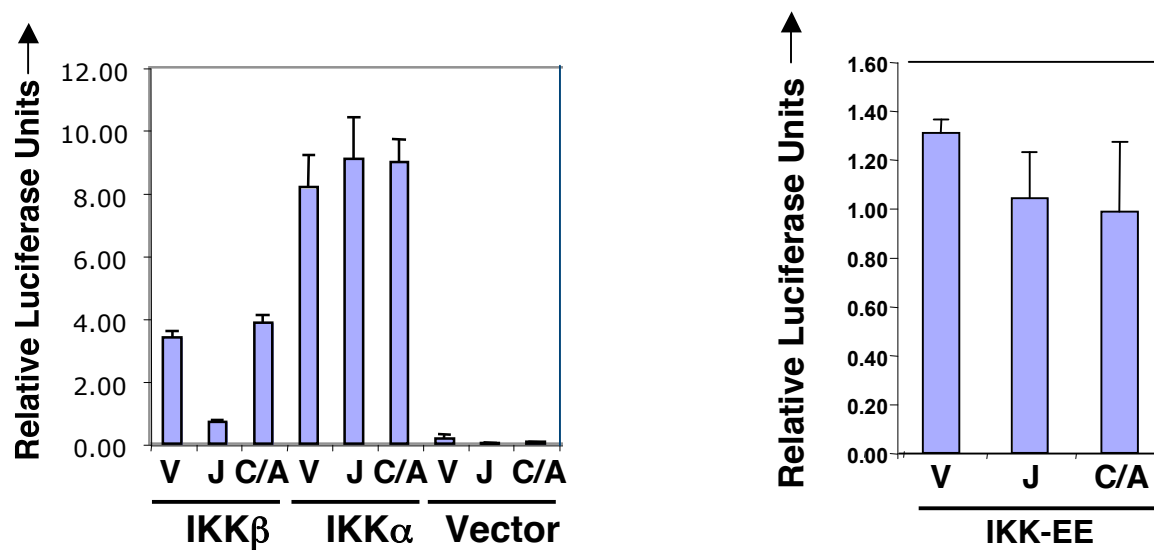
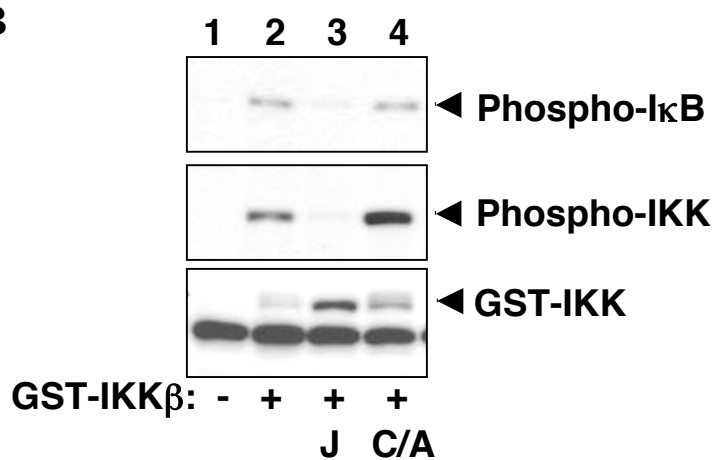
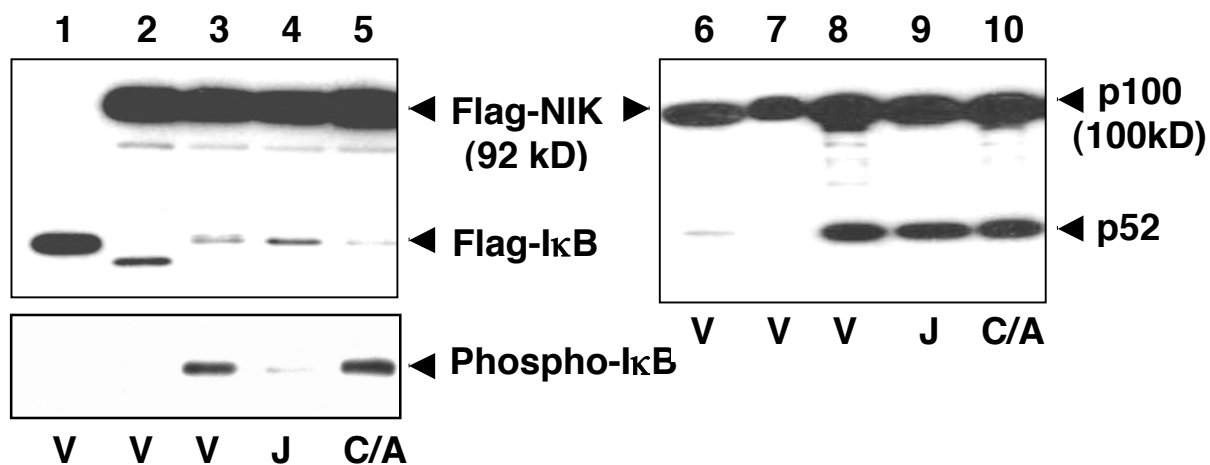
A**B****C**

Figure 15: YopJ specifically inhibits the IKK β -dependent pathway. (A) Luciferase assay of extracts from HEK293 cells cotransfected with a NF κ B luciferase reporter plasmid, expression plasmids for IKK β , IKK α or IKK-EE (as inducers), and vector (V), YopJ (J), or YopJC172A (C/A) as indicated. Renilla luciferase activity served as the internal control and was used to normalize all reactions for transfection efficiency. (B) HEK293 cells were transfected with GST-IKK β in the presence of YopJ (J) or YopJC/A (C/A) for 24 hours using Eugene transfection reagent. Cells were lysed with HNT lysis buffer and samples were resolved on a SDS gel, followed by immunoblotting with antibodies to endogenous phospho-I κ B (upper panel), endogenous phospho-IKK (middle panel) and GST (lower panel). (C) HEK293 cells were co-transfected with Flag-NIK and either Flag-I κ B (left panel) or Flag-p100 (right panel) in the presence of YopJ-Flag (J) or YopJ inactive mutant (C/A). After lysis with HNT buffer, samples were resolved by SDS-PAGE and immunoblotted with anti-Flag antibody (upper two panels) and anti-phospho-I κ B antibody (lower left panel).

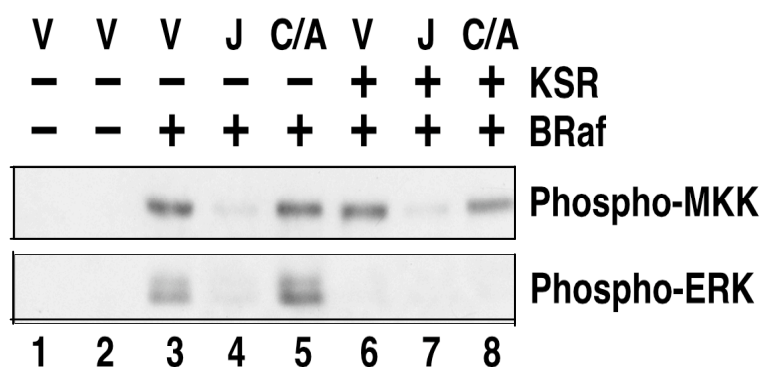
Effect of YopJ on the MKK signaling complex

MKK is known to associate with a scaffold protein, called kinase suppressor of Ras (KSR) [31]. KSR acts as a scaffold by promoting the phosphorylation of MKK. Upon activation, the scaffold brings MKK to the membrane and binds to Raf that can then activate MKK by phosphorylation [52]. KSR also interacts with downstream ERK, thereby placing MKK in close proximity to its substrate ERK. To assess the role played by KSR on the ability of YopJ to inhibit MKK phosphorylation, the effects of YopJ on the activity of this signaling machinery was investigated. Experiments were done by transfecting Flag-KSR, with or without YopJ and YopJC172A, in HEK293 cells. Previous studies have demonstrated that overexpression of KSR inhibits ERK activation [31]. As seen in lanes 6 and 7 (Figure 16A, lower panel), overexpression of KSR and/or YopJ inhibited the phosphorylation of endogenous ERK by B-Raf (Figure

16B). However, activation of endogenous MKK was inhibited only by overexpression of YopJ but not by overexpression of KSR (Figure 16A, upper panel, lanes 6 and 7). This suggests that YopJ maybe acting upstream of the inhibitory activity of the scaffold protein. Another interesting observation made was that in the presence of wild type YopJ, but not YopJC172A mutant, the migration pattern of KSR was altered as shown by immunoblotting with a α -Flag antibody (Figure 16B). When cells were induced with EGF or B-Raf, KSR migrated with slower mobility and YopJ inhibited even this mobility shift. It is possible that this shift is due to a change in the phosphorylation state of KSR, which is sensitive to YopJ's inhibition.

To further explore whether KSR is involved in the inhibitory activity of YopJ, the effect of YopJ on the MAPK pathway was observed in KSR knockout cells (*Courtesy: RE Lewis, Univ. of Nebraska*). After transfecting KSR^{-/-} cells with RasV12, in the presence or absence of YopJ, the cell lysates were analyzed for MAPK activation by immunoblotting for endogenous phospho-ERK. YopJ failed to block ERK phosphorylation in KSR^{-/-} cells, thereby implying an important role played by KSR in YopJ's inhibitory activity (Figure 16B).

A



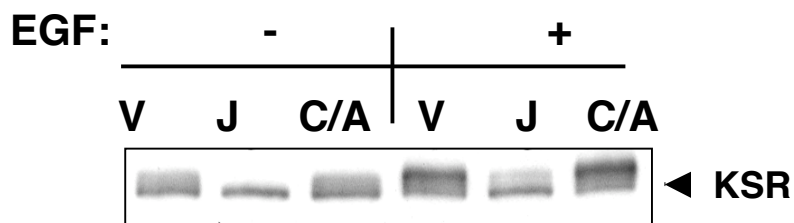
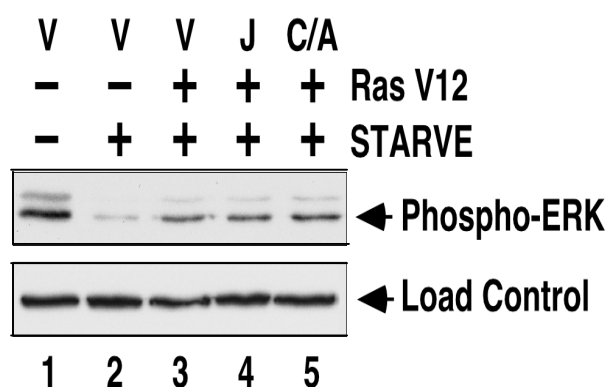
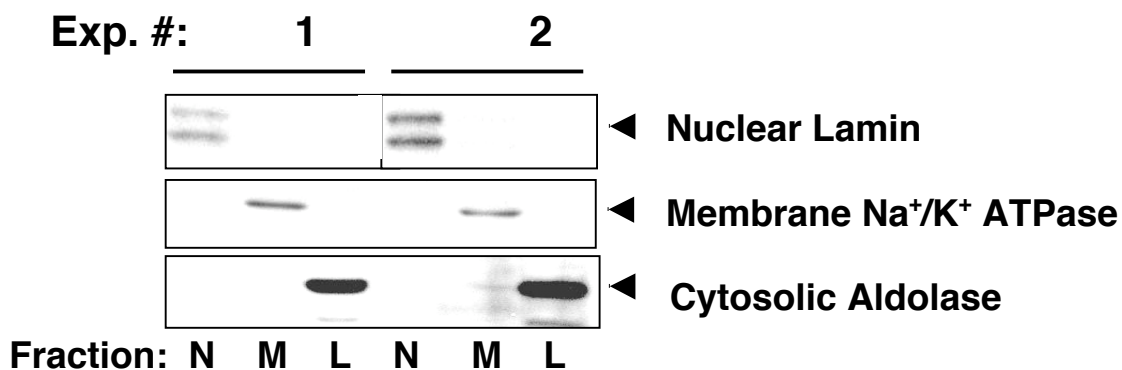
B**C**

Figure 16: Study of the inhibition of MAPK pathway by YopJ in the presence of the scaffold protein, KSR. (A) HEK293 cells were transfected with Flag-KSR in the presence of YopJ-Flag (J) or YopJC172A (C/A) and with B-Raf to induce the pathway. Cell lysates were immunoblotted with antibodies to endogenous phospho-MKK (upper panel) and phospho-ERK (lower panel). (B) Same experiment as in (A) where EGF, instead of B-Raf, was used as upstream stimulus and lysates were immunoblotted with anti-Flag antibody to analyze KSR levels. (C) KSR ^{-/-} cells were transfected for 48 hours with RasV12 in the presence and absence of YopJ and YopJC172A, followed by serum starvation for 3 hours. Cells were harvested with SDS sample buffer and analyzed by immunoblotting for endogenous phospho-ERK. [Courtesy: Huaqun Chen and Dr. Kim Orth]

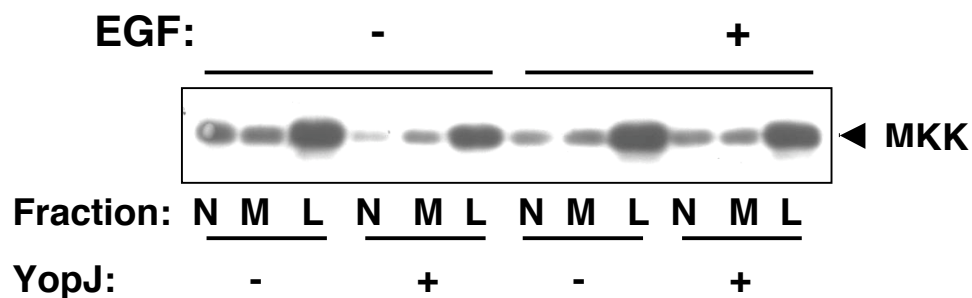
Next, the effect of YopJ on the machinery used to transfer MKK from the cytosol to the upstream signaling machinery located at the membrane was investigated. The localization of KSR and MKK to different cellular compartments has been reported to modulate MAPK signaling. Both KSR and MKK are known to undergo nucleocytoplasmic shuttling and in the presence of a growth stimulus the KSR-MKK signaling complex is recruited to the membrane [32]. To determine whether YopJ affects the ability of MKK to be recruited to the membrane, subcellular fractionation techniques, such as nitrogen cavitation, was utilized. This technique involves lysing cells under low oxygen conditions and then separating the nuclear, membrane and cytosolic fractions by differential centrifugation [53]. The advantage of using this technique is that it is highly reproducible and that it reduces contamination between different sub-cellular fractions, by keeping the nuclear and membrane fractions intact. Western blotting with different marker proteins assessed the purity of each of the sub-cellular fractions (Figure 17A). Under both uninduced and induced states, MKK was predominantly found in the cytosolic fraction and YopJ did not affect its recruitment to the membrane or even affect its localization pattern (Figure 17B). Experiments to detect KSR localization were technically very challenging due to its high M.W. (92kD) and, in addition, different KSR constructs (pEF1-KSR and pCMV5-KSR) gave different, contradicting results. Two KSR mutants, C809Y and S392A, known to disrupt the sub-cellular localization and phosphorylation state of KSR respectively [32], were also investigated for their effects on YopJ's inhibitory activity. Unfortunately, localization studies with these mutants in the presence of YopJ failed to provide any clue, however, the migration pattern of

these mutants on a SDS-PAGE gel were similar to that observed with wild-type KSR in the presence of YopJ (compare Figures 17C and 16B). These studies, thus, suggest that YopJ is not disrupting the sub-cellular localization of this complex to the membrane; rather it is inhibiting the KSR-MKK complex at the level of its activation, thereby affecting the phosphorylation states of these molecules.

A



B



C

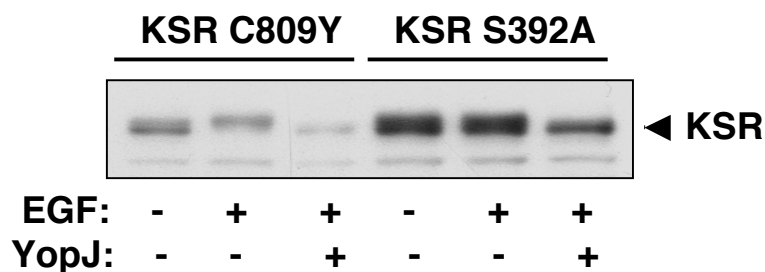


Figure 17: Sub-cellular fractionation studies of the MKK-KSR complex in the presence of YopJ. (A) Immunoblotting of nuclear, membrane and cytosolic fractions with marker proteins lamin, Na⁺/K⁺ ATPase and aldolase respectively, after nitrogen cavitation to assess the purity of each subcellular fraction. (B) Analysis of subcellular localization of endogenous MKK in cells with and without YopJ, in the absence or presence of EGF by immunoblotting with anti-MKK antibody. (C) YopJ affects the migration pattern of the two KSR mutants, C809Y and S392A as seen by immunoblotting with anti-Flag antibody to detect KSR. C809Y is phosphorylated in the presence of EGF in contrast to S392A, the phosphorylation-deficient KSR mutant.

Glycerol density gradient techniques were also utilized to determine YopJ's effect on the stability of the KSR-MKK signaling complex. When KSR was overexpressed, endogenous MKK came out in a higher density fraction (Figure 18), consistent with previous observations [8], thereby implying KSR-MKK complex formation. YopJ, however, did not alter the migration pattern of the high M.W. KSR-MKK complex and therefore this indicates that YopJ does not disrupt or affect the composition of the MKK-KSR complex in order to prevent its activation by the upstream signaling machinery.

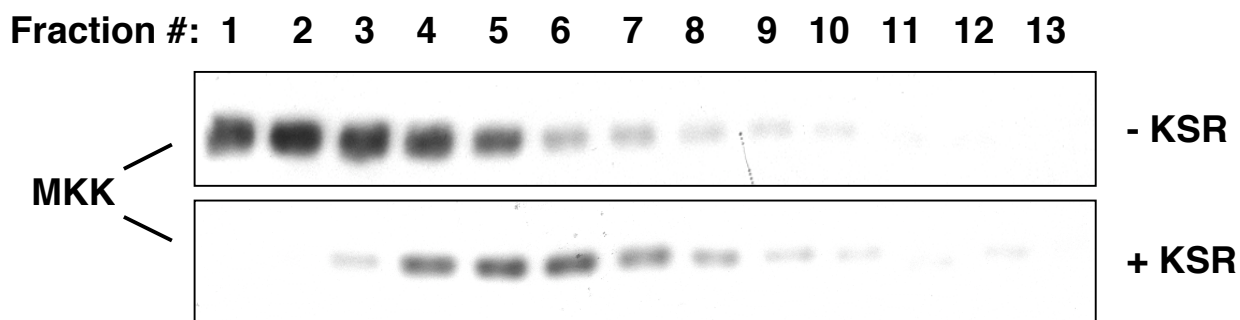


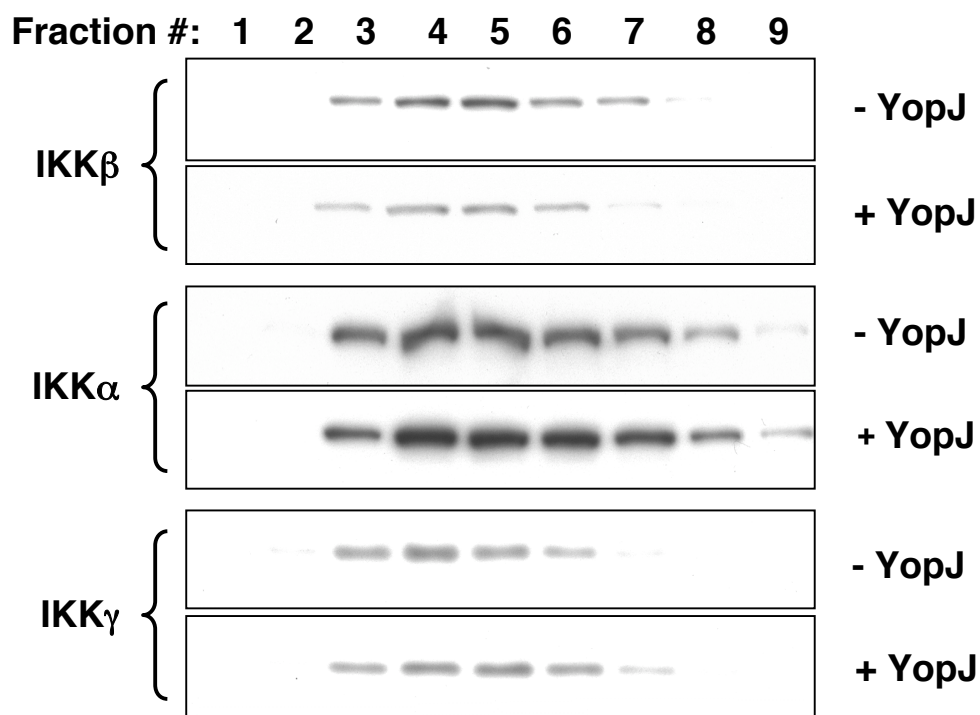
Figure 18: MKK forms a high molecular weight complex in the presence of KSR. HEK293 cell lysates, expressing or not expressing KSR, were subjected to 10-40% glycerol density gradient centrifugation for 3 hours at 4°C. Fractions collected were resolved on SDS-PAGE gel and analyzed by immunoblotting with anti-MKK antibody.

Effect of YopJ on the IKK Signalosome

The IKK signalosome is a large complex of different proteins with a M.W. of ~ 700- 900kDa. IKK α , IKK β , IKK γ , Hsp90 and cdc37 are some of the integral components of this complex. Sub-cellular fractionation studies were also carried out for the IKK signaling machinery in the presence and absence of YopJ. Similar to the experiments performed with the MAPK pathway, no obvious changes were observed in the localization pattern of the components of the IKK complex in the presence of YopJ. In addition, even through glycerol density gradient studies, the migration patterns of the different components were indistinguishable in the absence and presence of YopJ (Figure 19A). To determine if YopJ affects the

stability of the complex, the endogenous IKK complex was immunoprecipitated with IKK γ antibody from HEK293 cells expressing YopJ. Immunoblotting for different components of the IKK signalosome showed that YopJ did not disrupt the integrity and stability of the IKK complex (Figure 19B). All these observations indicate that YopJ is not affecting the localization or stability of the IKK signalosome and is instead using some other mechanism to inhibit its activation by the upstream stimuli.

A



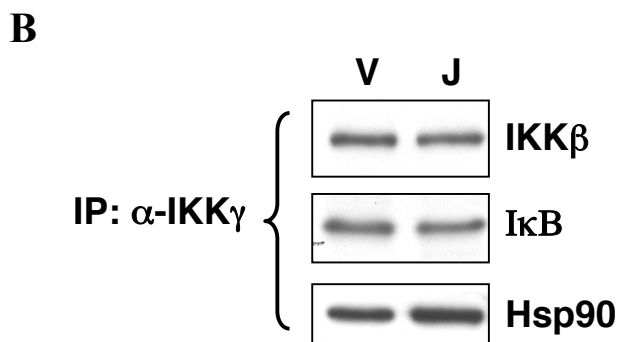


Figure 19: Effect of YopJ on the localization and stability of the IKK signalosome. (A) HEK293 cell lysates, expressing or not expressing YopJ, were subjected to 10-40% glycerol density gradient centrifugation for 3 hours at 4°C. Fractions collected were resolved on SDS-PAGE gel and analyzed by immunoblotting with antibodies to endogenous IKK β , IKK α and IKK γ . (B) Endogenous IKK complex immunoprecipitated with anti-IKK γ antibody from HEK293 cells, in the presence and absence of YopJ, was immunoblotted with anti-IKK β , anti-I κ B and anti-Hsp90 antibodies.

Discussions

Previous studies have indicated that YopJ is using a common mechanism to inhibit the activation of MKK and IKK β [8]. This study describes in detail the inhibitory effect of YopJ on the MAPK and NF κ B pathways simultaneously using mainly *in vivo* transfection-based experiments. The initial aim was to confirm YopJ's role as a deSUMOylating enzyme based on previous observations where overexpression of YopJ decreased levels of SUMO and SUMO-conjugated proteins [4]. YopJ's similarity to Ulp1, a deSUMOylating enzyme, further strengthened this model. To prove this hypothesis, an *in vitro* assay system was

developed to check for SUMOylation of known YopJ-interacting partners, MKK and IKK β . Although SUMOylation of MKK was observed *in vitro*, *in vivo* studies failed to demonstrate MKK SUMOylation. In addition, recombinant YopJ purified from different sources such as yeast, bacteria and Sf9 cells failed to cleave the SUMO moiety from MKK. Other transfection-based experiments and assays using Ub-VS or SUMO-VS adducts further ruled out YopJ's possibility of being a DUB or a deSUMOylating enzyme.

Studies with the NF κ B pathway showed that YopJ inhibited the activation of the IKK complex irrespective of the upstream stimulus. This suggested that YopJ is blocking a common mechanism utilized by all upstream activators to activate the IKK complex or that it is modifying the IKK complex such that it can no longer be activated by any stimulus. YopJ was also shown to specifically inhibit the IKK β -dependent pathway. Since YopJ binds to IKK β and not to IKK α [8], this implied that YopJ inhibits the activation of only that molecule to which it binds.

To further investigate YopJ's mechanism of inhibition of the MAPK and NF κ B pathways, the signaling components associated with each pathway were analyzed and studied in detail. For example, KSR in the MAPK pathway recruits MKK to the membrane for its activation upon phosphorylation by upstream B-Raf. Glycerol density gradient assays and sub-cellular localization experiments were utilized to determine whether YopJ disrupted MKK-KSR association and prevented MKK from relocating to the membrane. These techniques were also used in analyzing the NF κ B pathway components and all these assays failed to

show any effect of YopJ on the stability or localization of these signaling molecules. Preliminary studies with KSR^{-/-} cells did indicate that KSR may be playing an essential role in YopJ's inhibitory effect but future experiments involving KSR proved to be very challenging because of technical difficulties and as such were not continued.

Thus, the *in vivo* studies so far indicate that YopJ is neither a DUB nor a deSUMOylating enzyme and that it does not disrupt the signaling complexes or affect their localization. These were some of the possibilities by which YopJ could have been inhibiting the activation of MKK and IKK β . Ultimately, all experiments point to the common observation and that is, in the presence of YopJ, MKK and IKK β are in an inhibited state. Alternatively, YopJ is using a common, yet to be identified, mechanism to repress these kinases from both the pathways so that they can no longer be activated by upstream signaling machinery. To decipher how is YopJ bringing about this common inhibitory effect and in order to develop a physical model for YopJ's activity, an *in vitro* cell-free signaling system needed to be established.

CHAPTER FOUR

Results

DEVELOPMENT OF AN *IN VITRO* BIOCHEMICAL ASSAY TO STUDY YOPJ'S MECHANISM OF ACTION

Introduction

YopJ is using a novel, evolutionarily conserved and common mechanism to block the signaling of the MAPK and NFκB pathways at a common point and this requires the maintenance of the catalytic site of YopJ. This hypothesis is based on previous published observations [7, 9, 33] and also on the results from chapter four. However, to date, all studies on the inhibitory activity of YopJ have been *in vivo* transfection-based assays and on the basis of the proposed model, no activity for YopJ as a protease has been detected *in vitro*. Thus, the main goal is to take an unbiased approach and first establish an *in vitro* biochemical assay to study the mechanism of inhibition by YopJ. This would then help establish a physical model for YopJ's inhibitory role on the MAPK and NFκB pathways and also identify its substrate(s).

This study demonstrates the development of an *in vitro* assay to study YopJ's mechanism of action. RasV12 and B-Raf were used as the upstream stimuli for the MAPK pathway and TRAF6, NIK and MEKK1 served as the upstream activators for the NFκB pathway. The inhibitory effect of YopJ was demonstrated *in vitro* using all the above stimuli and YopJ-C172A was used as

the negative control in these assays. The observations from this study are consistent with previous genetic, microbial and cellular studies on the activity of YopJ and provide a method for analyzing inhibition of signaling by YopJ *in vitro*.

Materials and Methods

Plasmids and Reagents

pSFFV-YopJ-Flag and pSFFV-YopJC172A-Flag are described previously [8]. pGEX-I κ B and pRK7-Flag-NIK were provided by Dr. Zhijian J. Chen and pDCR-HA-RasV12 was provided by Dr. Mike White.

Antibodies for phospho-ERK1/2, phospho-MKK, phospho-I κ B, phospho-IKK, phospho-MKK6 and MKK1/2 were purchased from Cell Signaling, for IKK β and aldolase were purchased from Santa Cruz Biotechnology, for anti-HA antibody was purchased from Covance and for anti-FLAG antibody was purchased from SIGMA. B-Raf kinase and MEKK1 were purchased from Upstate. EGF and okadaic acid were purchased from Alexis. Anti-Flag M2 resin was purchased from Sigma. His-YopJ protein was provided by Dr. Chris Lima and HA-Ub-VS and HA-SUMO-VS adducts were kindly provided by Dr. Keith Wilkinson.

Purification of recombinant proteins

pFast-Bac-T6RZC virus was kindly provided by Dr. Zhijian J. Chen and the recombinant protein was purified from Sf9 cells using Ni²⁺ affinity

purification (Qiagen). Briefly, cells were lysed using Emulsiflex C-5 cell homogenizer (Avastin) in lysis buffer containing 20mM Tris (pH: 7.5), 10mM KCl, 1.5mM MgCl₂, 10mM NaF, 40mM EGTA, 0.05% β ME (BioRad) and a protease inhibitor cocktail tablet (Roche). Cell lysate was allowed to bind to Ni-NTA resin for 1 hour at 4°C and then eluted from beads using 250mM imidazole-containing buffer. GST-I κ B was expressed and purified from bacteria using standard GST purification protocol [54]. Briefly, cells were grown to an O.D. of 0.6-0.8 in 2xYT media and then induced with 0.4mM IPTG for 5 hours at 30°C. The cells were lysed in PBS, pH: 8.0, 1% Triton X-100 (Fisher) containing 0.05% β ME and 1mM PMSF. All purified His and GST proteins were analyzed by SDS-PAGE and quantified using a modification of the Lowry's method [55]. Recombinant YopJ-FLAG and YopJC172A-FLAG, purified from Sf9 cells, were provided by Dr. Renee Chosed.

Mammalian cell culture, transfection and immunoprecipitation

HEK293 cells were used for all experiments. The cells were cultured in Dulbecco's modified Eagle's medium (Invitrogen) with 10% cosmic calf serum (Gemini) and 5% CO₂. For preparing large-scale V, J or C/A lysates, cells were cultured in 150 mm plates and transfected with 10 μ g of either empty pSFFV, pSFFV-YopJ-FLAG or pSFFV-YopJ-C/A-FLAG using the calcium-phosphate-based transfection method [56]. Cells transfected with pRK7-Flag-NIK were performed using Fugene transfection reagent (Roche). Both YopJ-Flag and Flag-NIK were immunoprecipitated from HEK293 cell lysates with anti-Flag M2 resin

for 1 hour at 4°C and the washed beads were then used in the *in vitro* assays.

Lysate immunodepleted off YopJ was saved and also used in assays.

Lysate and membrane preparation for in vitro assays

Large scale vector-transfected (V), YopJ-transfected (J) and YopJC/A-transfected (C/A) lysates were prepared based on a protocol developed by Sturgill and colleagues [57], with slight modifications. Briefly, cells were washed with cold 1x PBS, harvested with PBS +1mM EDTA and lysed with equal amount of HTX buffer (10mM HEPES pH: 7.4, 0.5% Triton-X 100, 10mM MgCl₂, 1mM MnCl₂, 0.1mM EGTA and protease inhibitor cocktail tablet from Roche) for 20-60 min on ice. Scraping off cells from plates was avoided during harvesting in order to prevent cell shearing. Membrane-free cell lysates were obtained by performing three consecutive centrifugation steps at 800xg, 16,000xg and 100,000xg for 5, 10 and 60 minutes, respectively. Lysates were stored at -80°C at a concentration of 10mg/ml. Cells used in the *in vitro* MAPK assays were starved overnight with serum-free media, ~24 hours post-transfection.

HEK293 cells, treated with EGF for 5 min at room temperature or transfected with pDCR-HA-RasV12, were lysed as described above. Membranes from these cells were isolated after spinning the lysate at 100,000xg for 60 min at 4°C, resuspended in HTX buffer and stored at -80°C for future experiments.

In vitro MAPK and NFκB assays

For the *in vitro* MAPK assays, V, J or C/A lysates (10mg/ml) were incubated with either EGF for 5 min at room temperature, or with EGF-treated or

RasV12-transfected membranes for 10 minutes at 37°C or with 0.2 units of recombinant B-Raf for 10 minutes at 37°C, in the presence of an ATP regenerating buffer [58]. Reactions were stopped by adding 5x SDS sample buffer and analyzed by immunoblotting with phospho-ERK or phospho-MKK specific antibody to detect endogenous ERK and MKK activations, respectively. For the *in vitro* NFκB assay, recombinant T6RZC (0.5μM) or MEKK1 (0.4 μg) proteins were incubated with cleared lysates for 10 or 60 min, respectively. Activation by NIK was performed using NIK attached to anti-Flag beads by immunoprecipitation from HEK293 cells overexpressing pRK7-FLAG-NIK. NFκB activation was detected by immunoblotting with phospho-IκB or phospho-IKK specific antibodies. Lysate immunodepleted of YopJ was also activated similarly with either TRAF6 or RasV12 membranes. For *in vitro* assay with phosphatase inhibitors, 0.5μM okadaic acid or 10mM sodium fluoride were added to the lysates before addition of His-T6RZC. To check phosphorylation of exogenous IκB, 1μg of recombinant GST-IκB was added to the lysates and then incubated with 0.5μM His-T6RZC for 10 min at 37°C.

Immunoprecipitated YopJ-FLAG beads were added in increasing amounts to V lysate, followed by addition of RasV12-activated membranes or TRAF6. MAPK and NFκB activation were detected by immunoblotting with anti-ERK and anti-phospho-IκB antibodies, respectively. For *in vitro* assays with recombinant protein, His-YopJ from bacteria or YopJ-FLAG purified from Sf9 cells were added in increasing amounts to V lysate and incubated for either 10 min at 37°C or for 1 hour at 30°C.

Assay with Vinyl sulfone adducts

1 µg of HA-ubiquitin-VS or HA-SUMO-VS were incubated with 10mg/ml of V and J lysates for 1 hour at 30°C. Reactions were terminated by addition of 5x SDS sample buffer and samples were resolved on a SDS gel, followed by transfer to polyvinylidene difluoride (PVDF) membranes. Formation of YopJ-VS adducts were analysed by immunoblotting with antibody to the HA epitope.

Results

Development of an *in vitro* assay system for the activation of the MAPK pathway

The MAPK signal transduction cascade involves phosphorylation of MAPKs (such as ERK) by upstream MAPK kinases (MKK1, 2) that are in turn activated and phosphorylated by MAPK kinase kinases (Raf). In the presence of stimulus, such as EGF, Ras located at the membrane is activated and binds to Raf, a serine/threonine kinase that phosphorylates MEK, a dual-specificity protein kinase, which phosphorylates both threonine and tyrosine residues on ERK. In order to dissect the EGF-Ras-Raf-MKK-ERK signaling machinery, an *in vitro* assay system was established to reconstitute this signaling cascade. Since YopJ inhibits this pathway at the level of MKK, this *in vitro* cell-free system will ultimately help decipher YopJ's mechanism of action.

A modified version of a previously established protocol [57] was adopted for setting up the *in vitro* assay. Lysates from starved HEK293 cells were

prepared by adding equal volume of Triton X-100 containing Hepes buffer (cells: buffer::1:1) and incubating the mixture on ice for 20-60 min. Addition of only equal volume of 0.5% triton-containing lysis buffer results in a very concentrated lysate (~10mg/ml) and helps to maintain the signaling complexes in their native state. A separate plate of cells was activated with EGF for 5 min at room temperature, cooled to 4°C and lysed in Triton X-100 buffer. Membranes from these cells were isolated by differential centrifugation. Incubation of the membranes from the EGF-treated cells with the crude cell extract for 10 min at 37°C, in the presence of an ATP regenerating system (ARS), resulted in the activation of the MAPK pathway as detected by immunoblotting with anti-phospho-ERK antibody (Figure 20, lane 3). In this assay, it is very important to keep the background phosphorylation of ERK to a minimum so that a difference can be observed upon addition of stimulus. To achieve this, cells are starved overnight with serum-free media before harvesting and every step thereafter is strictly performed at 4°C. Scraping off cells from plates is avoided as it leads to shearing of cells and induces stress, resulting in increased background phospho-ERK levels. The background activity of the cell extracts usually varies between different cell preparations and also depends on the cell passage number (Figure 20, lane 2). Crude cell lysates can similarly be activated using Ras-V12 membranes or B-Raf as the stimuli (discussed in detail in the next section). Thus, these assays reconstitute the MAPK signaling cascade whereby addition of EGF, RasV12-activated cell membranes or B-Raf leads to the phosphorylation of the downstream substrate ERK by MKK.

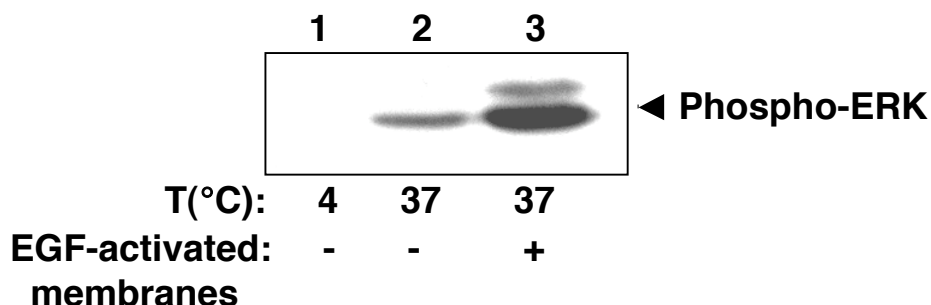


Figure 20: *In vitro* activation of the MAPK pathway by EGF-treated membranes. Crude cell extracts were incubated at 4°C or 37°C for 10 minutes with membranes isolated from cells that were treated with EGF for 4-5 minutes at room temperature. Activation of the MAPK pathway was detected by immunoblotting with anti-phospho-ERK antibody.

Effect of YopJ on the activation of the MAPK pathway *in vitro*

To assess whether YopJ can exert its inhibitory effect on MAPK activation in the *in vitro* assay, HEK293 cells were transfected with either a vector control plasmid or YopJ expression plasmid. As a positive control, cells were also transfected with the catalytically inactive mutant, YopJC172A (YopJC/A). Cells were harvested 24-36 hours post-transfection and lysates were prepared using the same protocol as described above but with slight modifications. Differential centrifugation was performed on these crude cell-extracts, to get rid off the nuclear and membrane fractions in order to obtain cleared lysate (at a concentration of ~10mg/ml) that can be stored at -80°C with multiple freeze thaw cycles. Membranes were isolated from cells treated with EGF or from cells transfected with the active form of Ras, RasV12. Incubation of RasV12

membranes with vector-transfected cleared lysate (V) for 10 min at 37°C led to the activation of the MAPK pathway as observed by immunoblotting with anti-phospho-ERK and anti-phospho-MKK antibodies (Figure 21, A and B, lane 2). However, addition of the activated membranes to YopJ-transfected lysate (J) diminished both ERK and MKK phosphorylation levels (Figure 21, A and B, lane 3). By contrast, ERK phosphorylation in YopJC/A lysate (C/A) was activated to the same extent as the vector-transfected lysate upon addition of stimulus (Figure 21B, lane 4). The *in vitro* assay was repeated using recombinant purified B-Raf as the upstream stimulus (Figure 21C) and similar results were observed. Addition of B-Raf to both vector- and YopJC/A-transfected lysates led to robust activation of the MAPK pathway, as indicated by ERK phosphorylation (Figure 21C, lanes 2 and 6). However, YopJ-transfected lysates showed decreased ERK phosphorylation when activated by B-Raf (Figure 21C, lane 4). To determine the level of MKK in these lysates, the samples were immunoblotted with antibody to endogenous MKK. No obvious changes were observed in the molecular weight or the stability of MKK in these lysates (Figure 21D). Thus, although there is decreased MKK phosphorylation in YopJ lysate, the total levels of full length MKK are indistinguishable in the V, J and C/A lysates and therefore YopJ does not appear to be acting as a protease to disrupt MKK activation. All these results indicate that the MAPK pathway is defective in YopJ lysates in that the lysate can no longer be activated by any of the upstream stimulus including EGF, RasV12 and B-Raf.

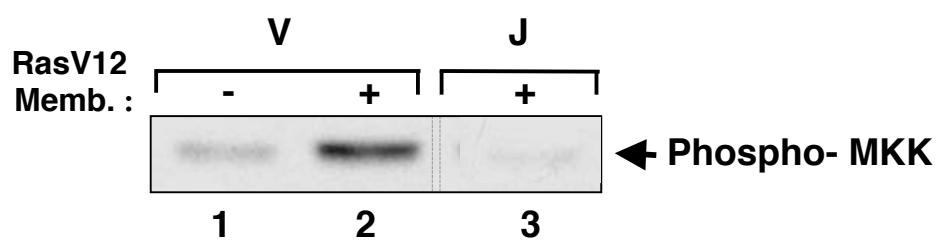
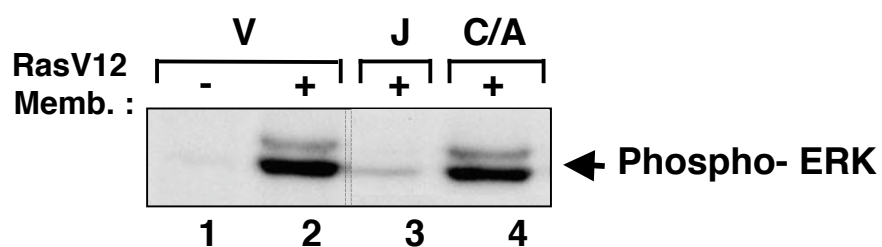
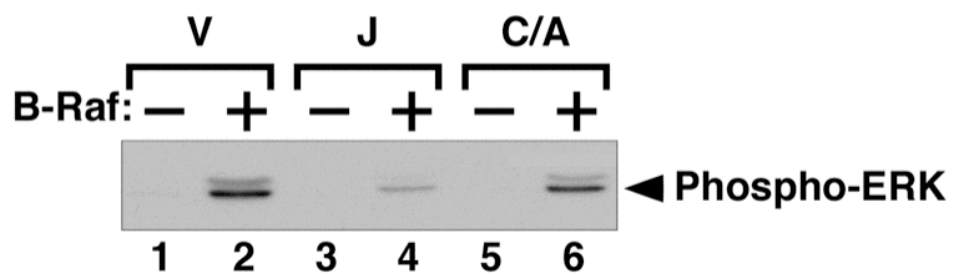
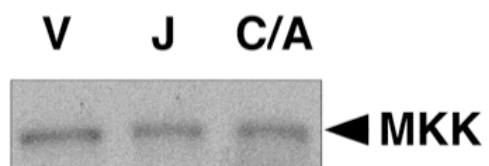
A**B****C****D**

Figure 21: YopJ inhibits MAPK activation *in vitro*. Membrane cleared lysates were harvested from HEK293 cells transfected with pSFFV empty vector (V), pSFFV-FLAG-YopJ (J) or pSFFV-FLAG-YopJ-C172A (C/A). **(A)** Lysates were incubated with membranes isolated from RasV12-transfected cells for 10 min at 37°C, followed by immunoblotting with antibody to phospho-MKK. **(B)** Membranes isolated from cells transfected with RasV12 were incubated with V, J and C/A lysates for 10 min at 37°C. Activation of ERK by phosphorylation was detected by immunoblotting with anti-phospho-ERK antibody. **(C)** Lysates were incubated with purified B-Raf for 10 min at 37°C and samples were immunoblotted with antibody to phospho-ERK. **(D)** V, J and C/A lysates were immunoblotted with antibody to MKK. The lines in the gels indicate lanes that have been deleted from the immunoblot.

Further experiments were done in which membranes isolated from cells co-transfected with RasV12 and YopJ were tested for activation of the MAPK pathway. Although there is background activity in the control lysate (Figure 22, lane 2), stimulation by RasV12-activated membranes was clearly detected as observed in lane 3. Stimulation with membranes isolated from RasV12 and YopJ co-transfected cells induced ERK phosphorylation to levels similar to that with membranes isolated from RasV12-transfected cells (Figure 22, lanes 3 and 4). These results support previous epistasis experiments because YopJ does not affect the RasV12 membrane complex that activates MAPK signaling. Instead YopJ affects the components that are to be activated by the RasV12 membrane complex. Previous studies and results from chapter four indicate that YopJ is acting at the level of MKK and IKK β since it cannot block signaling in the presence of the constitutively active form of these kinases [8]. All these results together suggest several different hypotheses. YopJ maybe modifying the MAPK kinases by the addition of some inhibitory factor or by changing the conformation of the signaling complex or by keeping an activator in a repressed state so that the

MAPK kinases can no longer be activated by upstream kinases.

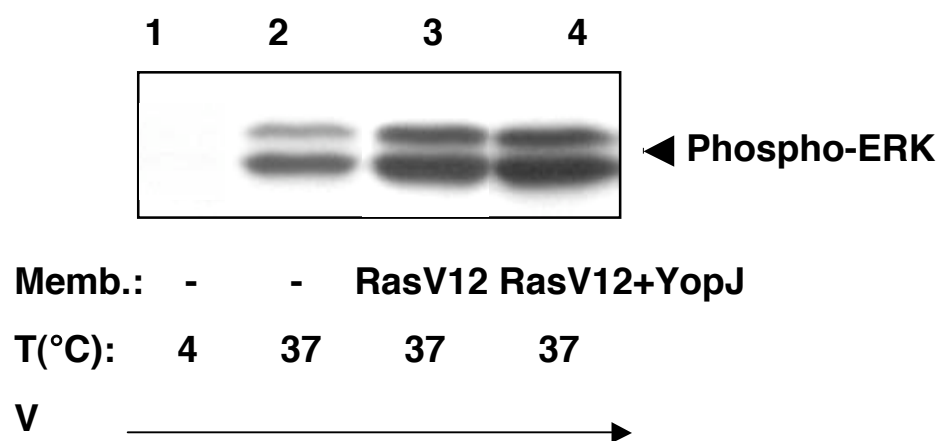
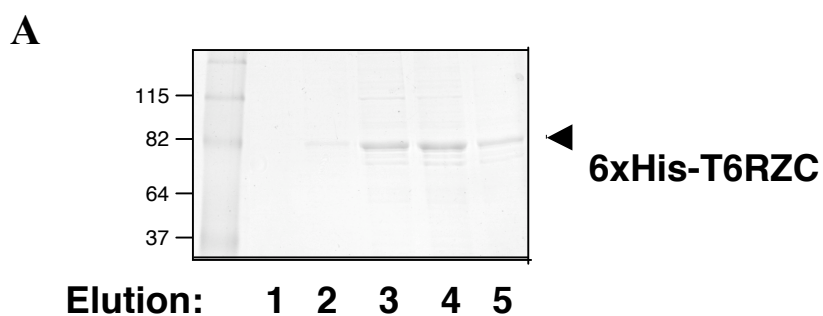


Figure 22: YopJ does not inhibit the active membrane complex that activates downstream MKK-ERK signaling. Membranes were isolated from cells transfected with either RasV12 alone or with YopJ and used to activate cleared lysates by incubation for 10 min at 37°C. MAPK activation was assessed by immunoblotting with anti-phospho-ERK antibody. Background of lysates was high at 37°C, even in the absence of membranes, and this varies according to the cell-preparations.

Effect of YopJ on the activation of the NFκB pathway

In vitro assays for activation of the NFκB pathway have been developed by different groups using different protocols [37] [59]. After the successful reconstitution of the MAPK pathway *in vitro*, the same cell-free signaling system was used to recapitulate YopJ's inhibition of the NFκB signaling pathway. The first stimulus tested was TRAF6. A modified version of TRAF6, T6RZC

(discussed in detail in chapter three), with a histidine tag on its N-terminus, was purified from insect cells using nickel affinity chromatography (Figure 23A). Addition of recombinant TRAF6 to membrane-free cytosolic lysate transfected with vector control activated the pathway, as indicated by the phosphorylation of I κ B and IKK (Figure 23, B and C, lane 2). By contrast, activation of I κ B signaling was diminished in cleared lysate isolated from cells transfected with YopJ (Figure 23, B and C, lane 4). As expected, the catalytic activity of YopJ was required for this inhibition, because addition of T6RZC to cells expressing YopJ-C/A led to activation of the NF κ B pathway (Figure 23, B and C, lane 6). The total IKK β levels in all the three lysates, V, J and C/A were exactly the same with no molecular weight shifts or stability issues (Figure 23D) similar to that observed for MKK in the *in vitro* MAPK assay (Figure 21D).



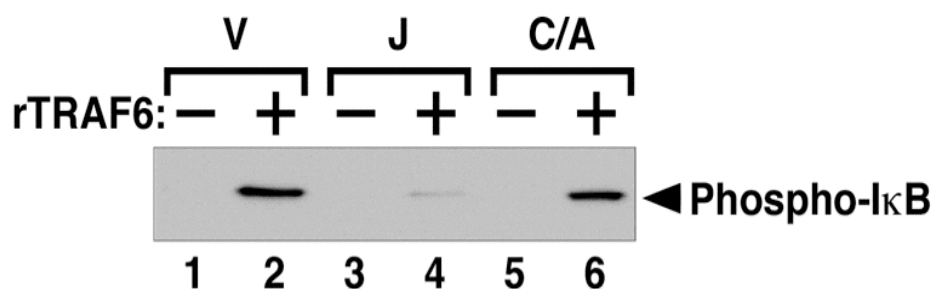
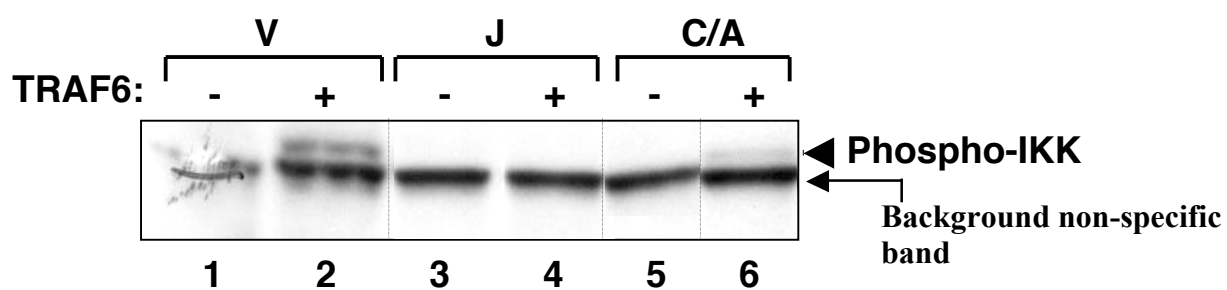
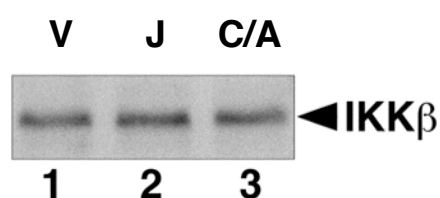
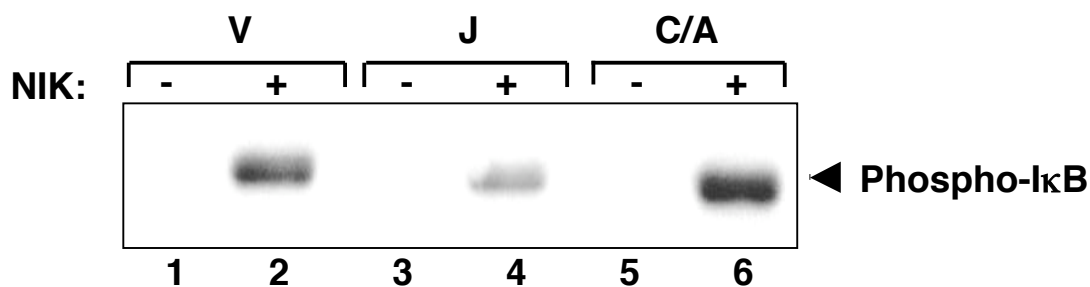
B**C****D**

Figure 23: YopJ inhibits NFκB activation *in vitro*. (A) Purification of His-T6RZC from Sf9 cells using nickel affinity chromatography. (B) V, J and C/A lysates were incubated with T6RZC for 10 min at 37°C, followed by immunoblotting with antibody against phospho-IκB. (C) Same experiment as in (B) but immunoblotting with anti-phospho-IKK antibody instead. (D) V, J and C/A lysates were immunoblotted with antibody to IKKβ. The lines in the gels indicate lanes that have been deleted from the immunoblot.

NIK, the second stimulus tested, gave similar results as T6RZC in that, YopJ, but not YopJ-C/A inhibited NIK-dependent activation of NF κ B signaling *in vitro* (Figure 24A). FLAG-tagged NIK is overexpressed in HEK293 cells, isolated by immunoprecipitation with anti-FLAG beads, and then used to activate the NF κ B pathway. Elution of NIK from the FLAG beads with a FLAG peptide produced a soluble, but inactive, kinase that failed to activate the pathway.

When a third exogenous stimulus used in this study, MEKK1, was added to the lysates, as expected, signaling was blocked only in the YopJ lysates (Figure 24B). Assays using recombinant MEKK1 to study YopJ's effect were very challenging because the activation of the NF κ B pathway by this kinase was never as robust as TRAF6 or NIK. In most cases, the purified kinase preparation was observed to be inactive. Thus, these *in vitro* assays are consistent with previous transfection- or luciferase-based assays in which YopJ inhibits IKK β signaling irrespective of the upstream stimulus. All these kinases utilize different mechanisms to activate NF κ B signaling but converge at a common point, the IKK complex. This again proves YopJ's inhibition at the level of IKK β .

A



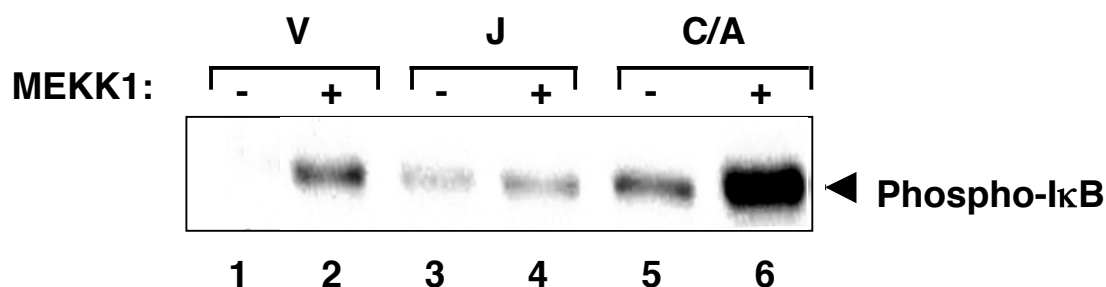
B

Figure 24: YopJ inhibits *in vitro* activation of the NFκB pathway by NIK and MEKK1. (A) FLAG-NIK overexpressed in HEK293 cells was immunoprecipitated out with anti-FLAG beads and incubated with V, J or C/A lysates for 10 min at 37°C. Activation of the pathway was observed by immunoblotting with anti-phospho-IκB antibody. (B) V, J and C/A lysates were incubated with recombinant MEKK1 for 1 hour at 30°C, followed by immunoblotting with antibody against phospho-IκB.

Effect of YopJ on the activation of exogenous GST-IκB

In the *in vitro* assays above, activation of the NFκB pathway was mostly assessed by immunoblotting with anti-phospho-IκB antibody. To determine whether YopJ could block the phosphorylation of exogenously added IκB, recombinant N-terminal GST-IκBα (1-36) [60] was purified from bacteria. TRAF6 incubated with GST-IκBα alone was unable to induce its phosphorylation (Figure 25, lane 4). However, addition of TRAF6 and GST-IκBα to cleared lysates from vector- or YopJ-C/A-transfected cells led to robust phosphorylation

of GST-I κ B α (Figure 25, lanes 3 and 8). By contrast, addition of GST-I κ B α to lysates transfected with YopJ, inhibited the ability of TRAF6 to phosphorylate this exogenously added GST-I κ B α (Figure 25, lane 6). This indicates that the signaling machinery, which allows the phosphorylation of exogenous GST-I κ B α in a TRAF6-dependent manner- the IKK complex, is crippled in the YopJ lysate. This is consistent with the hypothesis that YopJ is producing a dead IKK signalosome by either some modification or by change in conformation such that the upstream stimulus, such as TRAF6, can no longer phosphorylate downstream I κ B.

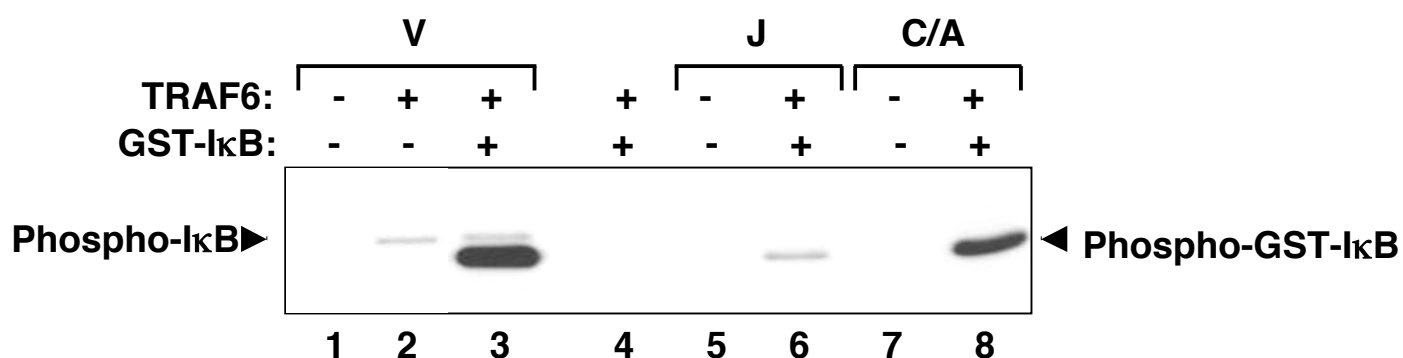


Figure 25: YopJ inhibits phosphorylation of exogenous I κ B in the *in vitro* signaling assay. GST-I κ B was purified from bacteria and added to V, J and C/A lysates in the presence of TRAF6 and incubated for 10 min at 37°C. Immunoblotting with anti-phospho-I κ B antibody not only detected phosphorylation of GST-I κ B but also phosphorylation of endogenous I κ B (lanes 2 and 3, top bands).

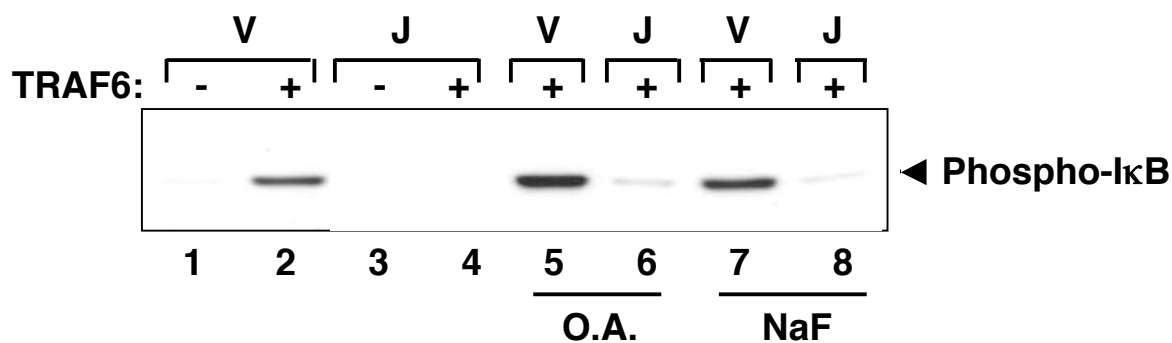
Effect of YopJ is independent of phosphatase or DUB activities

The *in vitro* assays demonstrate YopJ's inhibitory effect on the MAPK and NF κ B pathways. To ascertain whether this effect involves any phosphatase activity, the assays were done in the presence of a panel of phosphatase inhibitors including sodium fluoride, sodium vanadate, β -glycerophosphate, and okadaic acid (OA). Upon addition of these inhibitors, such as OA and sodium fluoride, to lysates isolated from YopJ-transfected cells, either during lysate preparation or during the ten minutes *in vitro* assay, YopJ's inhibitory effect was reversed to some extent (Figure 26A, compare lane 4 to lanes 6 and 8). Initially, this implied that YopJ maybe carrying a weak phosphatase activity or that YopJ might be associated with a phosphatase. However, upon closer analysis it was revealed that the addition of OA mildly increased the overall background of the *in vitro* signaling reaction and that this activity is attributed by an increase in basal stimulation due to inhibition of serine/threonine phosphatases. This is evident from Figure 26A, where in the presence of OA and sodium fluoride, TRAF6-dependent I κ B phosphorylation of control lysates was increased (compare lane 2 to lanes 5 and 7) to a similar extent as of YopJ lysates (lanes 4, 6 and 8). These results, thus, indicate that the inhibitory effect by YopJ is independent of any phosphatase activity and that phosphatase inhibitors do not influence YopJ's activity.

On the basis of the results from chapter three, this *in vitro* cell-free signaling system was also utilized to rule out the possibility that YopJ maybe functioning as a DUB or a deSUMOylating enzyme. Potential DUBs and deneddylases have been identified in the past using ubiquitin-VS (Ub-VS) and

Nedd8-VS adducts wherein protein conjugates with Ub-VS or Nedd8-VS are visualized on a SDS-PAGE gel [50, 51]. The vinyl sulfone adducts of ubiquitin (Ub-VS) and SUMO (Ub-SUMO) were obtained from Dr. Keith Wilkinson at Emory University. Cleared lysates isolated from vector-transfected or YopJ-transfected HEK293 cells were incubated with HA-tagged Ub-VS or SUMO-VS for 1 hour at 30°C. Reactions were terminated by the addition of SDS SB and samples were resolved on a SDS-PAGE gel, followed by immunoblotting with anti-HA antibody. No specific band corresponding to either YopJ-Ub-VS or YopJ-SUMO-VS adducts were observed (Figure 26B). Setting up the assay with recombinant purified YopJ protein also failed to show any band (data not shown). Thus, these results further confirm that YopJ is not functioning as a DUB or a deSUMOylating enzyme.

A



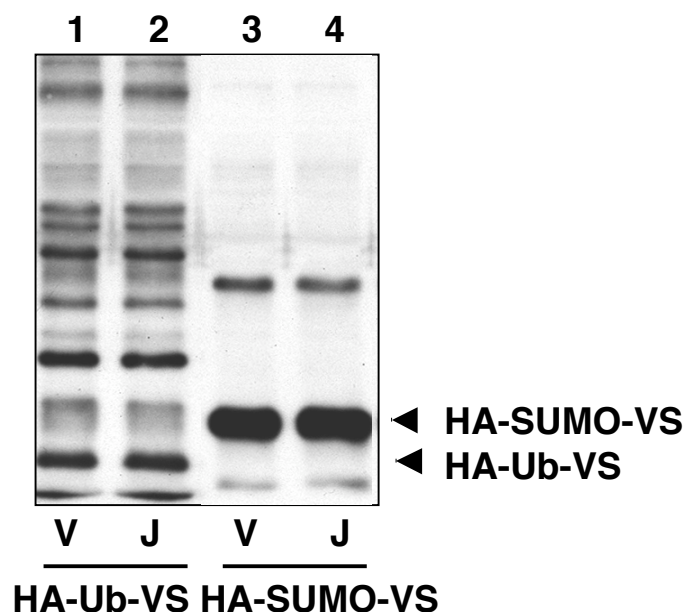
B

Figure 26: Inhibition of the signaling pathways by YopJ is independent of phosphatase or DUB activities. (A) V and J lysates were incubated with TRAF6 in the absence or presence of Okadaic acid (0.5 μ M) and sodium fluoride (10 mM) for 10 min at 37°C, followed by immunoblotting with anti-phospho-I κ B antibody. (B) V and J lysates were incubated with HA-Ub-VS or HA-SUMO-VS for 1 hour at 30°C. The formation of YopJ-VS adducts were looked for by immunoblotting with antibody to the HA epitope.

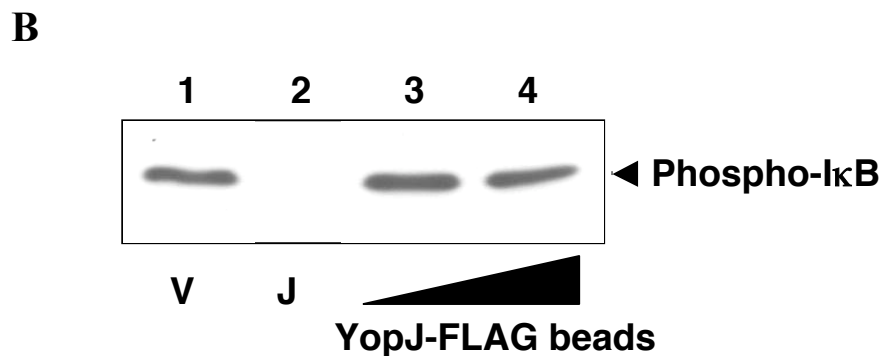
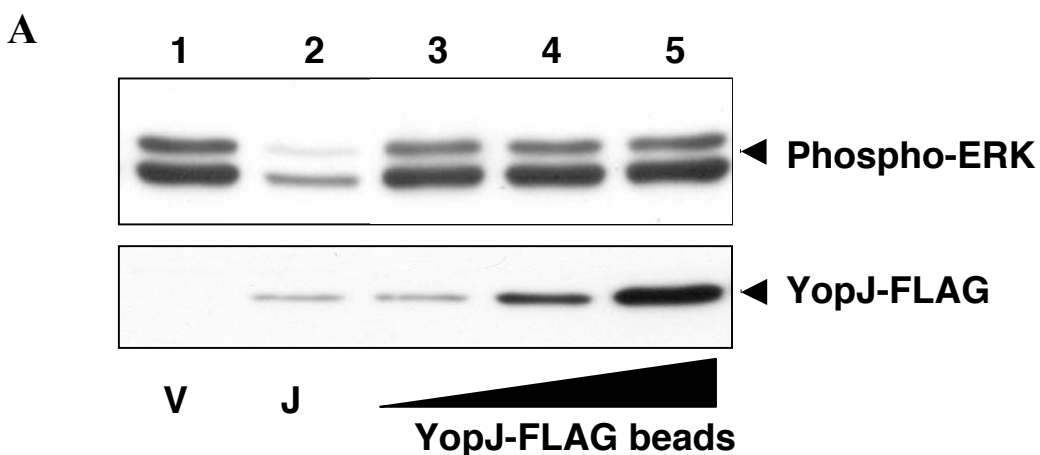
Experimental trials to study the effect of adding YopJ from different sources on the activation of the MAPK and NF κ B pathways *in vitro*

The inhibitory effect of YopJ on the MAPK and NF κ B pathways, recapitulated in the *in vitro* assays above, were observed in lysates that had been transfected with YopJ. To determine whether the YopJ lysate has the ability to

inhibit TRAF6-dependent activation of the control lysate, *in vitro* assays were set up by adding TRAF6 to control lysate that had been pre-incubated with YopJ lysate. The inhibitory effect of the YopJ lysate on the control lysate was hardly observed and due to the high variability and lack of consistency of the results; further conclusions could not be drawn.

The YopJ lysate served as the source of enzyme in the above assays, however, since lysates are mixtures of all the different proteins inside a cell, the next important step was to narrow down the experiment by using just the YopJ protein as the enzyme source. YopJ was immunoprecipitated out with FLAG beads from HEK293 cells transfected with YopJ-FLAG. Addition of increasing amounts of YopJ beads to control lysates did not inhibit the phosphorylation of either I κ B by TRAF6 or of ERK by RasV12 membranes (Figure 27, A and B). Recombinant YopJ, purified from several different sources such as yeast, bacteria and Sf9 cells with different tags like GST-, His- or FLAG-, or *in vitro* transcribed and translated YopJ using the rabbit reticulocyte lysate, were also used in the assays. The catalytically inactive mutant, YopJ-C/A was prepared simultaneously at all times to serve as a negative control. Under all of the above conditions, YopJ was never able to inhibit the MAPK and NF κ B pathways *in vitro* (Figure 27C). Several times, the inhibitory effect observed with YopJ was also seen with YopJ-C/A (Figure 27D, lanes 4 and 6). This implied that the observed inhibitory activity was maybe due to some contaminant being co-purified with YopJ or YopJ-C/A. All these studies indicate that YopJ, on its own, cannot inhibit the signaling pathways *in vitro* and, thus, suggests the requirement of some factor or activator to demonstrate its inhibitory effect.

Studies with lysates that have been immunodepleted of YopJ showed that these lysates, even in the absence of YopJ, were no longer activated either by TRAF6 or by RasV12 membranes (Figure 27E). This indicates that the physical presence of YopJ is not required for its inhibitory effect on the signaling pathways and that YopJ, according to the proposed hypothesis, may have already added an inhibitory molecule to the IKK complex or modified IKK β such that it cannot be activated by upstream TRAF6.



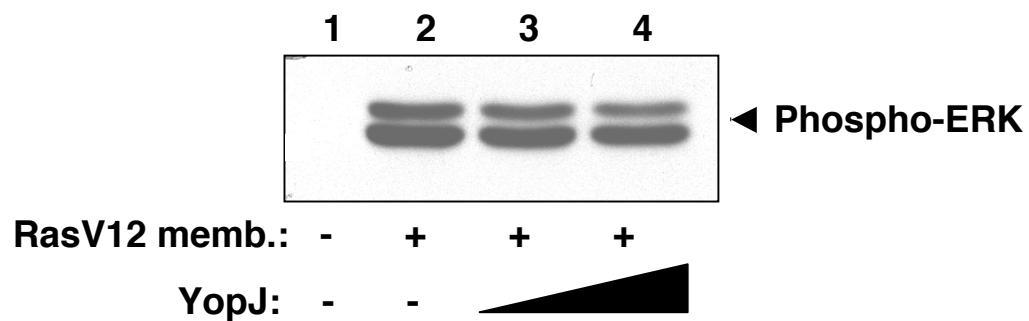
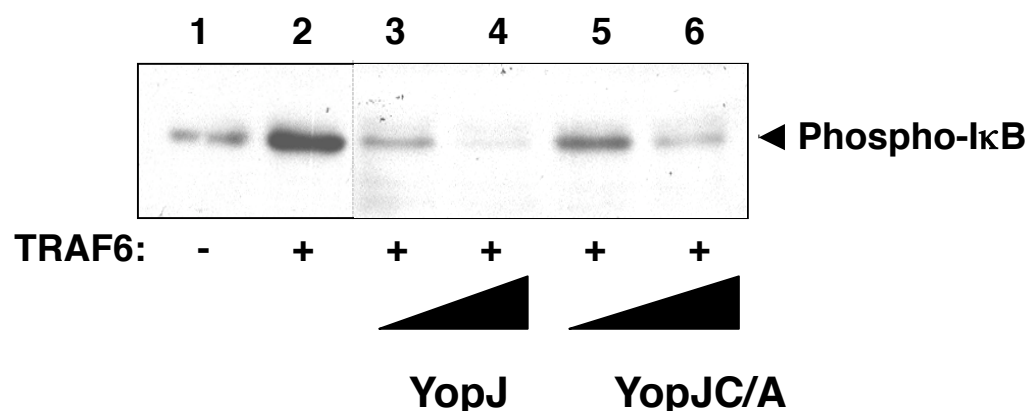
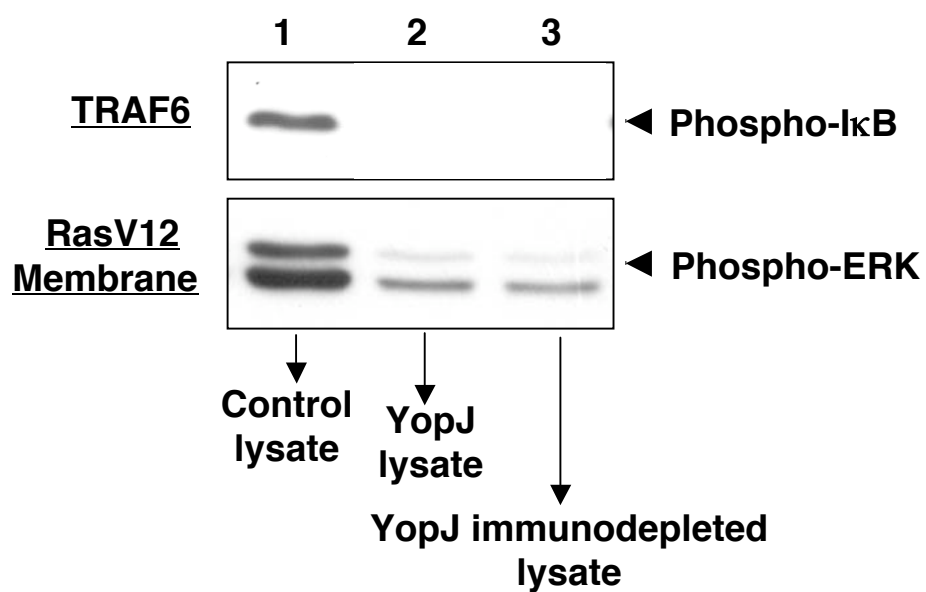
C**D****E**

Figure 27: Recombinant YopJ might be requiring some activator or inhibitory factor to exert its inhibitory effect on the MAPK and NFκB pathways. (A) YopJ was immunoprecipitated with anti-FLAG antibody from HEK293 cells expressing YopJ-FLAG and incubated in increasing amounts with lysate transfected with vector control (lanes 3, 4 and 5), in the presence of RasV12-activated membranes for 10 min at 37°C. Lanes 1 and 2 represent RasV12 membrane-mediated activation of V and J lysates respectively. Samples were analyzed by immunoblotting with anti-phospho-ERK antibody (upper panel) and with anti-Flag antibody (lower panel) to detect YopJ levels in the assay. (B) YopJ isolated on beads as in (A) was incubated in increasing amounts with V lysate in the presence of TRAF6 for 10 min at 37°C. NFκB activation was detected by immunoblotting with antibody to phospho-IκB. (C) Control lysate was incubated with recombinant Hisx6-YopJ, purified from bacteria, in the presence of RasV12-activated membranes for 10 minutes at 37°C. Samples were analyzed by immunoblotting with anti-phospho-ERK antibody. (D) Recombinant FLAG-YopJ and FLAG-YopJC/A purified from insect cells were incubated in increasing amounts with control lysate in the presence of TRAF6 and samples were immunoblotted with anti-phospho-IκB antibody (E) Lysate immunodepleted of YopJ was stimulated either with TRAF6 (upper panel) or with RasV12-activated membranes (lower panel) and activation of the pathways was detected by anti-phospho-IκB and anti-phospho-ERK immunoblots respectively. Lanes 1 and 2 represent activation of V and J lysates respectively.

Experimental trials to understand YopJ's mechanism of inhibition of the NFκB pathway in the *in vitro* assay

As demonstrated in Figure 27E, YopJ immunodepleted lysate was still able to inhibit TRAF6- or RasV12-mediated phosphorylation of IκB or ERK, respectively. This suggested the presence of some inhibitory factor, other than YopJ, that maybe causing the inhibition of the signaling pathways. Thus, in order to isolate the factor from YopJ extracts, biochemical fractionation technique was employed. The aim of this experiment was to fractionate the YopJ lysate by FPLC and then add back all the different fractions to the control lysate and lastly, assess the activation of the control lysate by TRAF6. The fraction that would be able to

block signaling by TRAF6 in the control lysate, would then be resolved on a SDS-PAGE gel and bands would be sent to mass spectrometric facility for identification. Unfortunately, due to technical difficulties associated with biochemical fractionation and other challenges, this study was abandoned. For example, fractionation of the YopJ lysate by gel filtration diluted each fraction to a large extent and as such it was difficult to detect the inhibitory effect when added back to control lysate upon activation by any upstream stimulus. In addition, it was almost impossible to even detect and follow YopJ in any of the fractions since only minimal amounts of YopJ plasmid are used to transfect cells, which ensures that YopJ functions at enzymatic levels. Trosky and colleagues have performed dilution assays and have showed that as little as 1ng of YopJ was enough to inhibit the MAPK pathway [12].

In-depth experiments for characterization of the activation of the IKK complex by TRAF6 in the presence and absence of YopJ were also carried out to decipher YopJ's mechanism. TRAF6, an E3 ligase, requires E1, E2 and ubiquitin to activate the IKK complex via the TAK1-TAB1-TAB2 complex and reconstitution of the NFκB pathway using all of these components has been established previously [37]. To understand inhibition by YopJ, different components such as the E2 (TRIKA1), TAK1 complex (TRIKA2) and the IKK complex were purified from YopJ extracts by biochemical fractionation. Each of these components was then used in *in vitro* reconstitution assays to test which component is inhibited in a YopJ-dependent manner. Unfortunately, after several experimental trials the TRAF6-dependent NFκB activation pathway could not be reconstituted in control lysates and as such experiments involving YopJ were also

not carried out further.

Discussions

In vivo studies from the previous chapter indicated that YopJ maintains MKK and IKK β , two of the MAPK kinases to which it binds, in a repressed state such that they can no longer be activated by the upstream signaling machinery. In order to understand YopJ's mechanism of inhibition of the MAPK and NF κ B pathways, this study was embarked upon to establish an *in vitro* cell-free signaling assay system. The MAPK pathway was reconstituted by using EGF, Ras or Raf as the upstream stimulus, whereas TRAF6, NIK and MEKK1 were used as upstream activators for the reconstitution of the NF κ B pathway. In all the *in vitro* assays it was observed that lysates expressing YopJ had lost their ability to be activated by any of the upstream stimuli and this inhibitory effect by YopJ required the maintenance of its catalytic site. Alternatively, the different activators were unable to activate MKK or IKK β signaling in lysates expressing YopJ, but not YopJC172A. Although the phosphorylated states of MKK and IKK β were reduced in the presence of YopJ, the total amounts of these kinases remained unchanged and this was revealed by SDS-PAGE where MKK or IKK β from V, J or C/A lysates were indistinguishable from each other. This indicated that YopJ does not affect the stability or shift the molecular weights of these kinases, which would be the usual expected result for proteases and isopeptidases. Assays with Ub-VS and SUMO-VS adducts further confirmed that YopJ does not function as a

DUB or a deSUMOylating enzyme. To determine whether the decreased phospho-levels of these kinases could be due to the association of some phosphatase activity with YopJ, a panel of different phosphatase inhibitors was tested in the *in vitro* assays. The presence of these inhibitors in the assay failed to alter YopJ's inhibition of the signaling pathways and as such discounted the phosphatase model.

After recapitulating YopJ's inhibitory activity using YopJ-transfected cell lysates, assays were set-up wherein recombinant YopJ was utilized. Addition of YopJ, purified from different sources such as bacteria, yeast, Sf9 cells or mammalian cells, failed to inhibit TRAF6- or RasV12-mediated NF κ B or MAPK activation, respectively. Pre-incubation of the lysate with YopJ, before the addition of the stimulus, also failed to show any inhibition of these pathways. Thus, these results clearly suggested that YopJ requires some unknown factor or an activator to exert its inhibitory effect on IKK β or MKK or it changes the conformation of these kinases so that they can no longer be phosphorylated for activation. Studies were next initiated to identify the missing factor, if any, using biochemical fractionation techniques. After several experimental trials using different strategies, unfortunately, the missing factor could not be identified. One of the major hurdles, for example, was the isolation of a purified, active MAPK kinase complex that would be used as the substrate in the assays.

One fact that was clear from all these results was that the IKK or MKK complexes were different in the presence of YopJ. This difference could be due to the presence of some factor, due to the absence of some required component, some kind of modification being added or subtracted or just a conformational

change. Thus, the next approach, to analyze the differences in the MKK or IKK β signaling complexes in the presence and absence of YopJ or YopJC172A, is to utilize mass spectrometric methods. This would help reveal the presence or absence of any inhibitory molecule, in a YopJ- dependent manner, on these signaling complexes or even recognize any modification or cleavage of a modification and this approach is discussed in detail in chapter six.

CHAPTER FIVE

Results

***IN VITRO* ACTIVATION OF THE IKK COMPLEX BY HTLV-1 TAX**

Introduction

The first identified pathogenic retrovirus, Human T-cell leukemia virus type-1 (HTLV-1), the causal agent for adult T-cell leukemia (ATL), expresses Tax, a 40 kD phospho-oncoprotein, that plays a pivotal role in growth and transformation of T-cells [13]. Tax chronically stimulates the IKK complex via NEMO/IKK γ , resulting in sustained phosphorylation and degradation of I κ B and activation of NF κ B [14, 61, 62]. It has been proposed that Tax activates the NF κ B pathway by inducing a conformational change [17]. Results from chapter four demonstrated that YopJ inhibits the activation of the NF κ B pathway irrespective of the different upstream stimuli that converge at a common point, the IKK complex. Since Tax also serves as one of the activators of the IKK complex, it will be interesting to determine whether YopJ can inhibit Tax-mediated activation of the NF κ B pathway. Tax, unlike all the other upstream stimuli, is not a kinase that phosphorylates and activates the IKK complex. It activates the complex by direct interaction via a mechanism not clearly understood. Understanding Tax-induced activation of the NF κ B pathway could serve as an alternate approach to help reveal the mechanism used by YopJ to block the activation of the IKK β

component in the IKK complex.

This study demonstrates the development of an *in vitro* cell-free signaling assay system for activation of the NF κ B pathway by recombinant, semi-purified HTLV-1 Tax protein. Although the mechanism for IKK activation by Tax was not completely deciphered, studies from the *in vitro* assays indicate that Tax-mediated IKK activation is independent of phosphatases, in contrast to previous studies [15, 16]. Preliminary studies using this assay confirmed the proposed model that Tax activates the IKK complex by inducing a conformational change [17]. Both *in vivo* and *in vitro* assays showed that YopJ inhibits Tax-mediated activation of the IKK complex and that YopJ does not disrupt the interaction of Tax with the IKK complex via IKK γ . Thus, this study further strengthens the hypothesis that YopJ maybe acting at the level of MAPK kinases and blocking their activation by some kind of modification or by inducing a conformational change.

Materials and Methods

Plasmids and Reagents

pSFFV YopJ-FLAG and pSFFV YopJC172A-FLAG are described previously [8]. Tax was cloned into pET28a and pcDNA3 vectors using 5' BamH1 and 3' Xho1. The four Tax mutant constructs, M22, H41Q, H43Q and K85N in pET28a and pcDNA3 vectors were created using the Stratagene mutagenesis kit (Appendix, Table of Primers). pcDNA3-FLAG-I κ B and pGEX-I κ B α were kindly provided by Dr. Zhijian Chen.

Anti-phospho-I κ B and anti-IKK γ antibodies were obtained from Cell Signaling and Santa Cruz respectively. Okadaic acid and Geldenamycin were purchased from Alexis.

Expression and purification of recombinant proteins

Wild type and the various mutants of Tax (M22, H41Q, H43Q and K85N) were expressed as His-tagged proteins in BL21/DE3 cells, grown to an O.D. of 0.6-0.8 and induced at room temperature with 0.2mM IPTG for 8-12 hours. The bacterial pellet was then lysed by an Emulsiflex C5 cell disruptor (Avestin) and purified using standard protocols for Ni²⁺-NTA purification (Qiagen). Purification of recombinant His-TRAF6 from Sf9 cells and GST-I κ B from *E. coli* are described in detail in chapter four.

Tissue culture and lysate preparation

HEK293 cells were cultured in DMEM medium supplemented with 10% cosmic calf serum and 100 units/ml penicillin/streptomycin/glutamine (Invitrogen) in the presence of 5% CO₂. For the *in vitro* assays, untransfected cells or cells transfected with 10 μ g pSFFV YopJ-FLAG or pSFFV YopJC172A-FLAG using Eugene (Roche), were grown up to 100% confluency, harvested using PBS-EDTA and lysed with equal volume of HTX lysis buffer (10mM 7.4 pH Hepes, 10mM MgCl₂, 1mM MnCl₂, 0.5% Triton X-100, 0.1mM EGTA) containing protease inhibitor cocktail tablet (Roche). Lysate was first spun down at 800xg to remove nuclei and then at 100,000xg to obtain a cleared lysate that is then stored at -80°C at a protein concentration of 10mg/ml.

Luciferase assay

HEK293 cells were transfected with 200ng of wt Tax or the different Tax mutants (M22, H41Q, H43Q and K85N) and 5xNF κ B luciferase reporter, in the absence or presence of pSFFV YopJ-FLAG or pSFFV YopJC172A-FLAG for 24 hours using Fugene transfection reagent. Each plate was also transfected with pRSV-Renilla to serve as the internal standard control. Lysates were prepared using passive lysis buffer (Promega), and luciferase assay was performed using Fluostar Optima (BMG Labtech).

Transfection and Immunoprecipitation

In vivo activation of the NF κ B pathway was demonstrated by transfecting HEK293 cells with pcDNA3-wt-Tax or mutant Tax and pcDNA3-FLAG-I κ B in the absence or presence of 100ng of pSFFV-YopJ-FLAG for 24 hours.

The IKK complex was immunoprecipitated from HEK293 cell lysate, expressing pcDNA3-Tax, with or without pSFFV-YopJ-Flag, using anti-IKK γ antibody for 2 hours at 4°C, followed by binding to Protein A sepharose beads for 1 hour at 4°C. Beads were washed and used in a kinase assay by incubating with recombinant GST-I κ B as the substrate for 1 hour at 30°C, in the presence of an ATP regenerating system (10x stock: 10mM ATP, 350mM creatine phosphate, 20mM Hepes pH 7.2, 10mM MgCl₂ and 500 μ g/ml creatine kinase).

In vitro assay using recombinant Tax

Cleared lysates (10mg/ml) were incubated with or without 30ng of

recombinant wt Tax and/or all the mutants or 0.5 μ M TRAF6 in the presence of an ATP regenerating system for 10 minutes at 37°C. 0.5 μ M Okadaic acid and 2 μ M Geldanamycin were added to cleared lysates before the addition of the recombinant protein. Reactions were terminated by addition of 5x SDS sample buffer. Proteins from the reaction samples were resolved by SDS-PAGE and transferred to PVDF membranes.

Results

***In vitro* activation of the NF κ B pathway by recombinant Tax**

Tax constitutively activates the IKK complex. To reconstitute and thereby analyze Tax-induced NF κ B signaling *in vitro*, Tax was first cloned into a protein expression vector, pET28a, with a 6xHis tag. Recombinant protein, 6xHis-Tax, was obtained by expression in *E. coli* and purified using nickel affinity chromatography (Figure 28). In the *in vitro* assay that was developed similar to that in chapter five, recombinant Tax served as the upstream stimuli and phosphorylation of I κ B served as the readout to assess the activation of the IKK signaling complex. Cell-free cleared lysate, which served as a source for unstimulated IKK complex, was prepared as before. Briefly, HEK293 cells were lysed with equal volume of Triton X-100-containing lysis buffer and the lysate was centrifuged at 800xg to remove nuclei followed by 100,000xg to obtain a membrane-cleared lysate that can be stored at -80°C at a protein concentration of

10mg/ml.

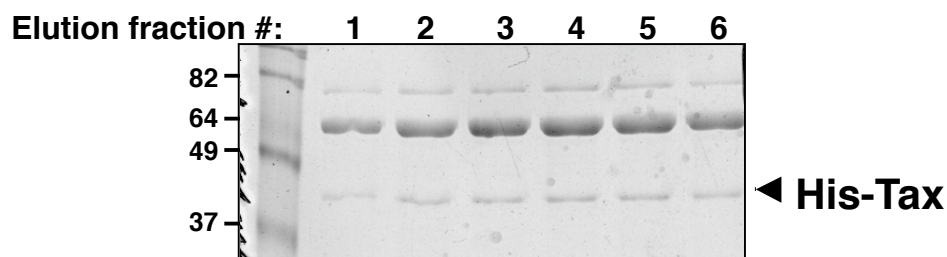
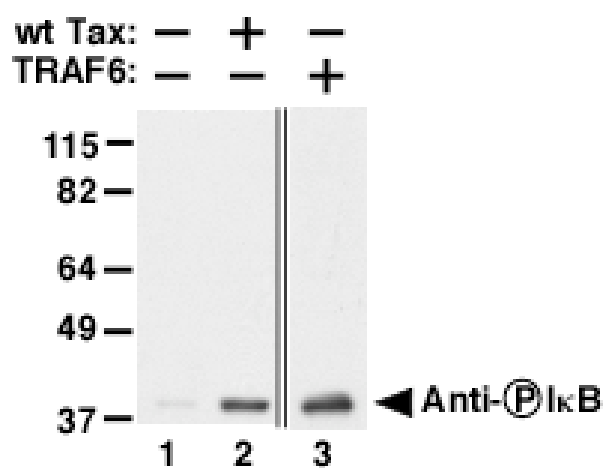


Figure 28: Purification of recombinant 6xHis-Tax. Recombinant 6xHis-Tax protein was expressed in bacteria and purified using nickel affinity chromatography. Protein was eluted as 1ml fractions from nickel beads with 250mM imidazole-containing buffer, resolved by SDS-PAGE and detected by Coomassie blue staining.

In the *in vitro* assay system, partially purified recombinant 6xHis-Tax protein was incubated with cleared lysate for 10 minutes at 37°C, in the presence of an ATP regenerating system followed by termination of the reaction by the addition of SDS sample buffer. To ascertain IKK activation, the reaction samples immunoblotted with anti-phospho-IkB antibody. Addition of Tax protein to cleared lysate resulted in the activation of the NFκB pathway as indicated by robust phosphorylation of IkB (Figure 29A, lane 2). Similarly, addition of partially purified recombinant TRAF6, which served as the positive control in this assay, also activated the NFκB pathway (Figure 29A, lane 3). Furthermore,

addition of serial dilutions of recombinant Tax to the *in vitro* signaling system showed that the activation of the NF κ B pathway could be detected with as little as 800nM of Tax demonstrating a concentration dependence of Tax on the activation of the NF κ B pathway (Figure 29B).

A



B

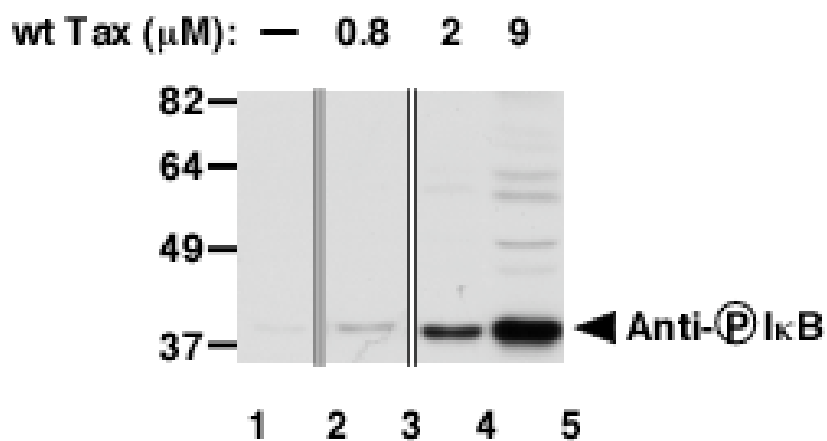


Figure 29: *In vitro* activation of the IKK complex by recombinant HTLV-1 Tax. Activation of the IKK complex was detected by immunoblotting with anti-phospho-I κ B antibody. **(A)** IKK activation by wild-type (wt) Tax and TRAF6: lane 1, lysate control; lanes 2 and 3, addition of 1 μ M Tax and 0.5 μ M TRAF6 respectively to lysate. **(B)** Concentration dependence of Tax-mediated I κ B phosphorylation: lane 1, lysate control; lanes 2-4, increasing amounts of Tax (0.8 - 9.0 μ M) added to lysate.

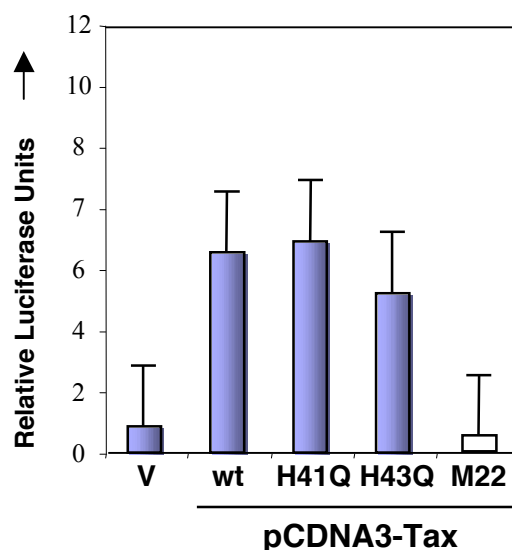
Tax-mediated IKK activation is independent of phosphatases

Previous studies have identified several different Tax-interacting partners, such as MEKK1 and IKK γ in the IKK complex [61, 63]. The catalytic subunit of the serine threonine protein phosphatase 2A (PP2A) was recently identified to bind Tax to form a ternary complex together with IKK γ [15]. PP2A's role in inhibiting the activation of the IKK complex has been established in the past [64] and currently there are two opposing models to explain Tax-mediated activation and regulation of the IKK complex. According to the first model, PP2A negatively regulates the catalytic activity of IKK and the binding of Tax to PP2A relieves the negative inhibition by PP2A resulting in an active complex [15]. According to the second model, Tax-mediated activation of IKK requires the association of active PP2A with the IKK complex [16].

To test the above models, several Tax mutants were made, such as M22, H41Q, H43Q and K85N [65, 66], and used in both *in vitro* and *in vivo* signaling assays. Initial studies to determine the effect of the different Tax mutants were first done by performing transfection-based luciferase assays with a NF κ B luciferase reporter (Figure 30A). These results were confirmed using

immunoblotting experiments with anti-phospho-I κ B antibody after transfecting HEK293 cells with wt Tax and its mutants. The NF κ B pathway could be activated by wt Tax, in contrast to M22, that failed to cause any activation (Figure 30B). M22 is the inactive mutant form of Tax (M22) and the effect seen by M22 is consistent with previous studies where it has been shown to be unable to activate the NF κ B pathway [15]. Tax mutants, H41Q and H43Q, activated the NF κ B pathway similar to the way wt Tax did (Figure 30, A and B, Table 1). Since H41Q and H43Q, which are defective in binding PP2A, were able to activate the NF κ B pathway, the binding of PP2A to Tax does not appear to be essential for Tax-mediated activation of the IKK complex, and therefore refutes the first model.

A



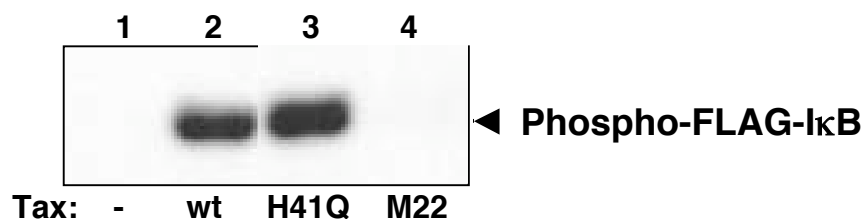
B

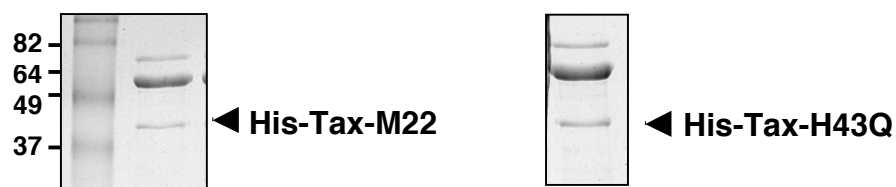
Figure 30: Study of the effect of Tax mutants on the NFκB pathway. (A) HEK293 cells were co-transfected with NFκB luciferase reporter construct and either wt pCDNA3-Tax, pCDNA3-Tax-H41Q, pCDNA3-Tax-H43Q or pCDNA3-Tax-M22. pRSV-Renilla was used as the internal standard control. Cells were lysed with passive lysis buffer and luciferase assay was performed following instructions in the Pierce dual luciferase assay kit. (*Technical assistance provided by Veera Singh and Gladys Keitany*) **(B)** HEK293 cells were transfected with FLAG-IκB and the wt or the mutant pCDNA3-Tax constructs. Activation of the NFκB pathway was assessed by immunoblotting the cell lysates with antibody against phospho-IκB.

<i>Mutant</i>	<i>Published Results (...)</i>	<i>Observed Results</i>
M22	Cannot activate the NFκB pathway	Cannot activate the NFκB pathway
H41Q	"	Activates NFκB pathway
H43Q	"	"

Table 1: Comparison of the activity of three Tax mutants from previous published results to those from the current study. The M22 mutant worked similar to previous results, in that, it no longer activated the NFκB pathway. The other two mutants, H41Q and H43Q however, in contrast to previous observations, were able to activate the NFκB pathway, similar to the way, wild type Tax does.

The Tax mutants were also expressed as recombinant His-tagged proteins in bacteria and purified using nickel affinity chromatography (Figure 31A). Consistent with previous *in vivo* observations, addition of the recombinant inactive mutant form of Tax (M22) to the *in vitro* signaling system was unable to induce phosphorylation of I κ B (Figure 31B, lane 5). However, addition of the other three recombinant mutants forms of Tax, H41Q, H43Q and K85N, which have previously been shown to be unable to bind PP2A [15], resulted in activation of the NF κ B pathway as indicated by phosphorylation of I κ B *in vitro*, albeit with varying potency (Figure 31B, lanes 3, 4 and 6). The profiles of partially purified wild type Tax and the inactive mutant, M22, proteins (Figures 28 and 31A, left panel) appear the same, supporting the proposal that differences in the activities can be attributed to the mutated amino acids in the various Tax proteins. Overall, these observations refute the first model, in that binding of PP2A to Tax is not essential for Tax activation of the IKK complex.

A



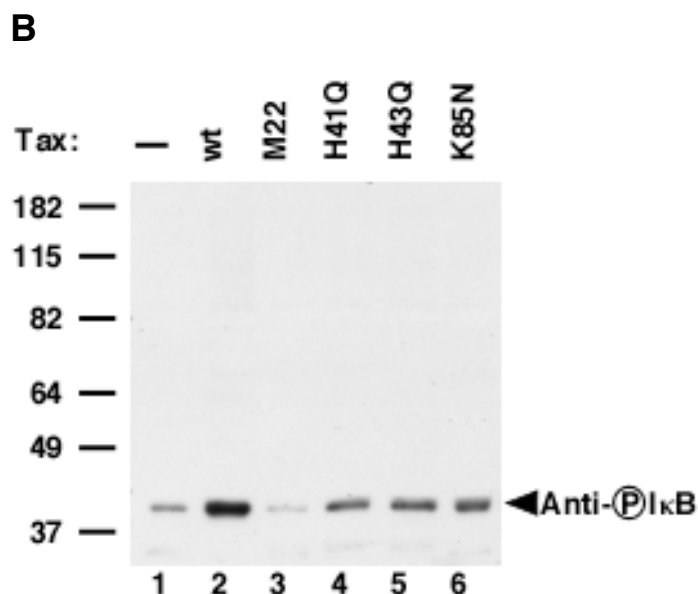


Figure 31: *In vitro* activation of the IKK complex by recombinant Tax mutant proteins. (A) Coomassie-stained gel of purified recombinant Tax mutant proteins expressed in bacteria. M22 and H43Q are shown here as examples. (B) IKK activation by wt and mutant forms of Tax: lane 1, cell free lysate control; lanes 2-6, addition of equal amounts (1 μ M) of recombinant wt Tax, M22, H41Q, H43Q and K85N respectively to lysate. Activation of the IKK complex was detected by immunoblotting with anti-phospho-I κ B antibody.

To further assess whether PP2A plays a role in the *in vitro* activation of the IKK complex by Tax, the Tax-induced activation of this complex was analyzed in the presence of okadaic acid (OA). Addition of 0.5 μ M OA did not alter the ability of wild type Tax to activate the IKK complex as observed by phosphorylation of I κ B (Figure 32, lane 4). Therefore, when PP2A activity is inhibited, Tax is still able to activate the IKK complex. The addition of OA mildly increased the overall background of the *in vitro* signaling reaction (Figure

32, compare lanes 1 and 2) and this activity is attributed to an increase in basal stimulation due to inhibition of serine/threonine phosphatases during the ten-minute *in vitro* assay. The increase in I κ B phosphorylation observed upon addition of TRAF6 to OA- supplemented lysate (Figure 32, lane 7) confirms that the treatment with OA does indeed inhibit background phosphatase activity. Similarly, addition of recombinant wt Tax to OA- supplemented lysate increased, rather than decreased, the phosphorylation state of I κ B. Based on these observations, it indicates that Tax can activate the IKK complex independent of PP2A activity, thereby discounting the second model which predicted that the interaction between IKK and PP2A is essential for Tax to be able to activate the IKK complex [16].

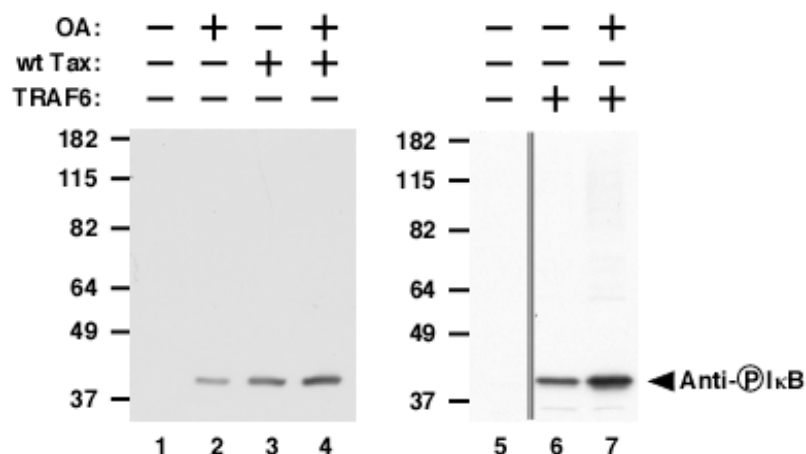


Figure 32: Effect of okadaic acid (OA) on Tax-dependent activation of IKK. Activation of the IKK complex was detected by immunoblotting with anti-phospho-I κ B antibody. Activation of IKK by wt Tax and TRAF6 in the presence

of 0.5 μ M OA: lane 1, lysate control; lane 2, lysate in the presence of OA; lane 3, addition of wt Tax to lysate; lane 4, wt Tax added to lysate in the presence of OA; lanes 6 and 7, addition of TRAF6 to lysate in the absence and presence of OA, respectively.

Tax mediates IKK activation by inducing a conformational change

Studies were initiated to further understand the requirements for activation of the IKK complex by Tax. The *in vitro* signaling system developed earlier, recapitulated the activation of the NF κ B pathway by Tax and also demonstrated that Tax-mediated IKK activation is independent of phosphatases. Based on the strategies utilized in chapter five involving reconstituting the activation of the IKK complex by TRAF6, similar experiments were set-up for Tax. Endogenous IKK complex was isolated and purified from HEK293 cells either by anion exchange and gel filtration chromatographies or by immunoprecipitation with anti-IKK γ antibody. In both cases, Tax was unable to activate the isolated IKK complex. This suggests that Tax requires some additional factor or missing component, besides binding to IKK γ , in order to activate the IKK complex. Several experimental trials were set-up to identify the factor and understand the mechanism used by Tax, but most of them failed to provide any relevant information. For example, since MEKK1 is also known to bind Tax, recombinant MEKK1 was added to the *in vitro* assay but this did not help Tax activate the isolated IKK complex and addition of the ubiquitin conjugation machinery also failed to reconstitute the assay.

Alternatively, it is possible that by binding to IKK γ , Tax is inducing a conformational change that results in the activation of the IKK complex. Hsp90, which is known to maintain the structural integrity of protein complexes [67], is an integral component of the IKK complex [68]. Geldanamycin (GA), an HSP90-specific inhibitor, was used in the *in vitro* signaling system to test whether it can affect the ability of Tax to activate the NF κ B pathway *in vitro*. Upon addition of 2 μ M GA to the *in vitro* signaling assay, it was observed that Tax could no longer activate IKK as indicated by the lack of I κ B phosphorylation (Figure 33, lane 4). GA also inhibited the TRAF6-dependent activation of the IKK complex (Figure 33, lane 7). This is consistent with previous observations where GA-dependent Hsp90 inhibition has been shown to interfere with IKK activation [68]. As Hsp90 is known to maintain the structural integrity of protein complexes, these observations support a new model that a preformed native complex requiring active Hsp90 is essential for the activation of the IKK complex by Tax. This supports the proposed model that binding of Tax to IKK γ in the IKK complex is causing a conformational change that induces autoactivation of the kinases in the complex [17].

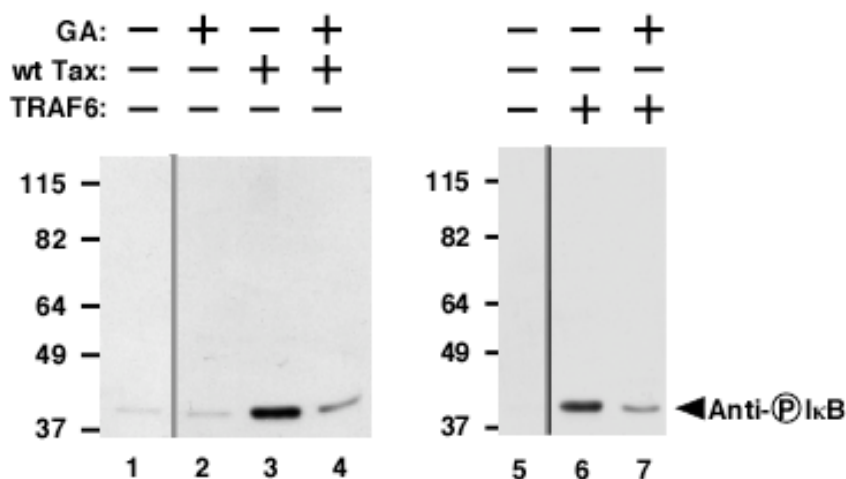


Figure 33: Effect of Geldanamycin (GA) on Tax-dependent activation of IKK. Activation of the IKK complex was detected by immunoblotting with anti-phospho-I κ B antibody. IKK activation in the presence of 2 μ M GA: lane 1, lysate control; lane 2, lysate in the presence of GA; lane 3, addition of wt Tax to lysate; lane 4, wt Tax added to lysate in the presence of GA; lanes 6 and 7, addition of TRAF6 to lysate in the absence and presence of GA, respectively.

Effect of YopJ on Tax-mediated activation of the IKK complex

Tax is one of the upstream activators of the IKK complex, however, the mechanism by which it activates IKK is not completely deciphered. Since YopJ inhibits IKK β activation regardless of the upstream stimuli, experiments were next designed to confirm whether YopJ could inhibit Tax-induced activation of the IKK β . HEK293 cells were transfected with Tax in the presence and absence of YopJ-FLAG and activation of the NF κ B pathway was first assessed by

luciferase assays with a NF κ B luciferase reporter. YopJ, but not the catalytically inactive mutant YopJC172A, inhibited Tax-mediated activation of NF κ B (Figure 34A). Immunoblotting with antibody against phospho-I κ B showed that YopJ inhibited I κ B phosphorylation (Figure 34B, lane 6). For this experiment, cells were overexpressed with FLAG-I κ B to detect phosphorylation of exogenous I κ B, because endogenous I κ B gets degraded upon activation of the NF κ B pathway (Figure 34B)

In another experiment, the IKK complex was immunoprecipitated out from cells expressing either Tax alone or in the presence of YopJ, and tested for its ability to phosphorylate recombinant GST-I κ B. The IKK complex isolated from Tax-expressing cells was able to phosphorylate exogenous I κ B (Figure 34C, lane 2). By contrast, the ability of the IKK complex to phosphorylate GST-I κ B was reduced in cells expressing both Tax and YopJ together (Figure 34C, lane 3). This indicates that YopJ inhibits Tax-induced IKK activation and modifies the IKK complex such that it has lost its ability to phosphorylate its downstream substrate, I κ B. Co-immunoprecipitation experiments of Tax and IKK γ in the presence of YopJ showed that YopJ does not disrupt the interaction between Tax and IKK γ (data not shown).

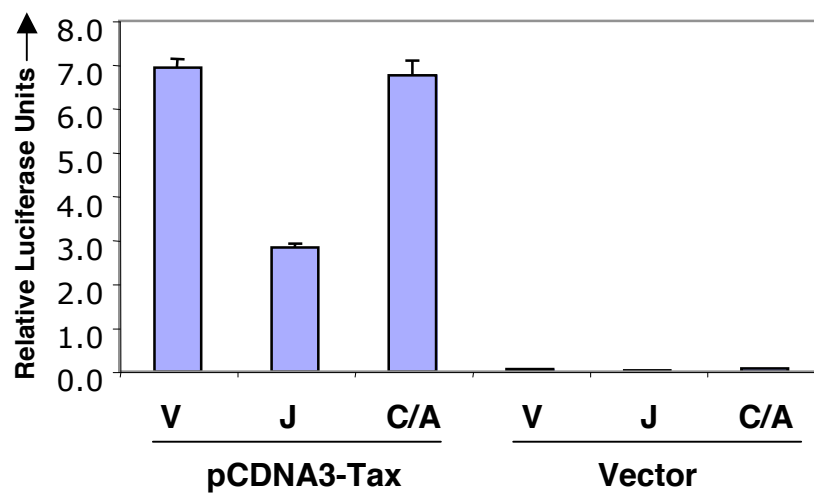
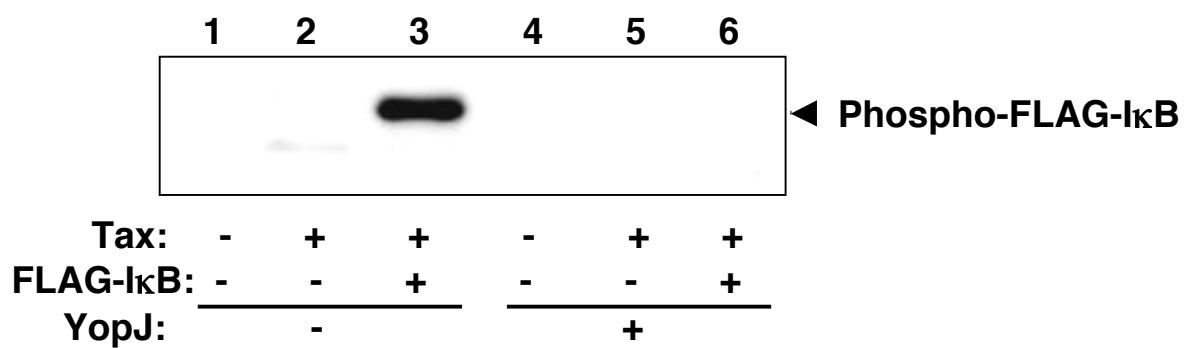
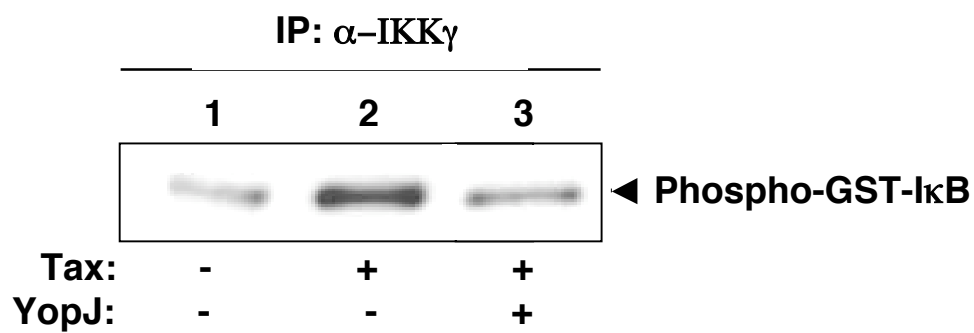
A**B****C**

Figure 34: Effect of YopJ on Tax-mediated activation of the NF κ B pathway.

(A) Luciferase assay was performed after transfecting HEK293 cells with NF κ B luciferase reporter along with either pSFFV vector control (V) or YopJ-FLAG (J) or YopJC172A-FLAG (C/A) in the presence or absence of pCDNA3-Tax. (B) HEK293 cells were transfected with pCDNA3-Tax and FLAG-I κ B in the presence or absence of YopJ. Samples were resolved on a SDS-PAGE gel and analyzed by Western blotting with anti-phospho-I κ B antibody. (C) The endogenous IKK complex was isolated from cells expressing either Tax alone or Tax in the presence of YopJ by immunoprecipitating with anti-IKK γ antibody. The isolated IKK complex on beads was then used in a kinase assay to phosphorylate GST-I κ B and phosphorylation was detected by immunoblotting with anti-phospho-I κ B antibody.

To gain insight into YopJ's inhibitory mechanism, the *in vitro* assay of Tax-mediated IKK activation was utilized. Recombinant Tax was used to activate V, J and C/A lysates. Tax was able to phosphorylate endogenous I κ B in both vector- and C/A-transfected cell lysates (Figure 35). By contrast and as expected, Tax had lost its ability to phosphorylate I κ B from cells expressing YopJ. The results from this *in vitro* assay confirm the *in vivo* results demonstrated earlier and are in accordance with the work by Carter and colleagues [18]. Thus, just like all the other upstream stimuli, YopJ blocks Tax-mediated activation of the IKK complex.

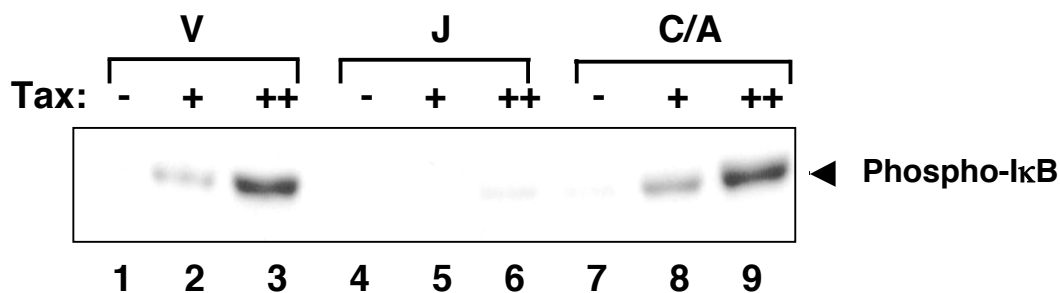


Figure 35: YopJ inhibits *in vitro* activation of the NFκB pathway by recombinant Tax. Increasing amounts of recombinant Tax was incubated with vector-transfected (V), YopJ-transfected (J) or YopJC172A (C/A) lysates for 1 hour at 30°C. Reaction was terminated by addition of SDS sample buffer. Samples were run on a SDS gel and immunoblotted with antibody against phospho-IκB.

Discussions

In this study, an *in vitro* signaling assay is used to analyze the activation of IKK by Tax. Recombinant Tax, purified from bacteria, is able to strongly induce IκB phosphorylation in cleared lysates. The PP2A-binding-deficient mutants of Tax were also able to activate NFκB signaling, although not as strongly as wt Tax. This indicated that the binding of this phosphatase, PP2A, to Tax is not essential for Tax-mediated activation of the IKK complex. In addition, experiments with okadaic acid added to the *in vitro* assay did not alter the ability of wt Tax to activate the IKK complex. These observations refute the proposed model that states that Tax-mediated IKK activation is positively regulated by PP2A [16]. By contrast, Tax was unable to activate the NFκB pathway when Hsp90, an integral component of the IKK complex, was inhibited by the addition of geldanamycin to the assay. Based on these results, a new model is proposed that Tax-dependent activation of the IKK signalosome utilizes an Hsp90-dependent IKK complex and is independent of phosphatase activity. Binding of Tax to IKKγ in the IKK complex may be causing a conformational change that is inducing autoactivation of the kinases in the complex. As more mutants

associated with the other activities of viral Tax are discovered, this system can be used to diagnose their role in the activation of IKK. Although this study did not provide the exact mechanism utilized by Tax to activate NF κ B signaling, the *in vitro* signaling system did provide an important tool that will facilitate the elucidation of the biochemical mechanism of Tax-induced activation of the IKK complex.

Experiments were next carried out to test YopJ's effect on Tax-mediated IKK β activation since Tax is also one of the activators of IKK β . Herein, both *in vivo* and *in vitro* studies revealed that YopJ blocks the activation of IKK by Tax. Tax, unlike MEKK1, NIK or TAK1, is not a kinase that phosphorylates IKK β for activation. Rather, based on GA-inhibited Hsp90 assays and the proposed model [17], Tax maybe activating the IKK complex by inducing a conformational change. Thus, according to the results, since YopJ blocks Tax-induced conformational change in IKK β , it confirms that IKK β itself is the target for YopJ. The following chapter describes how is YopJ inhibiting MKK or IKK β by utilizing a novel post-translational modification.

CHAPTER SIX

Results

CHARACTERIZATION OF THE *IN VITRO* ACTIVITY OF YOPJ

Introduction

The cell-free signaling system, developed in chapter five, recapitulates the inhibition of the NF κ B and MAPK signaling pathways by YopJ during infection and provides a method for analyzing inhibition of signaling by YopJ *in vitro*. Based on the results from transfection and luciferase assays (chapter three) and the *in vitro* signaling pathway assays (chapter four), it is quite clear that YopJ is inhibiting MAPK and NF κ B signaling at the level of MKK and IKK β , respectively. Studies with HTLV-1 Tax (chapter five) also showed that YopJ acts downstream of Tax-mediated IKK signaling. In contrast to other activators of the IKK complex, Tax is predicted to activate the NF κ B pathway by binding to the IKK complex and thereby induce a conformational change [17]. These results along with the observation that YopJ cannot disrupt NF κ B activation in the presence of constitutively active IKK β (IKK-EE in chapter three, Figure 15A), further pinpoints YopJ's activity at the level of or on the IKK complex. The analogous kinase, MKK, is predicted to be the target in the MAPK pathway.

A single point mutation in YopJ (C172A), completely abolishing the inhibitory activity of YopJ both *in vivo* and *in vitro* (chapters three and four),

supports the proposal that YopJ maybe functioning as a protease. The hydrolase activity of YopJ was predicted to be similar to that observed for AVP and Ulp1 [9]. SDS-PAGE gels did not show any molecular weight shifts or any effect on the stability of MKKs and IKK β in the presence of YopJ (chapter four), however, these kinases could no longer be activated by the upstream stimuli when YopJ was around. All these observations implicate that YopJ is altering the kinases, to which it binds, such that they are inactive. This leads to the hypothesis that YopJ is using its catalytic activity to either modify or change the conformation of its interacting partners, MKK and IKK β , such that they cannot be activated by the upstream signaling machinery (Figure 36).

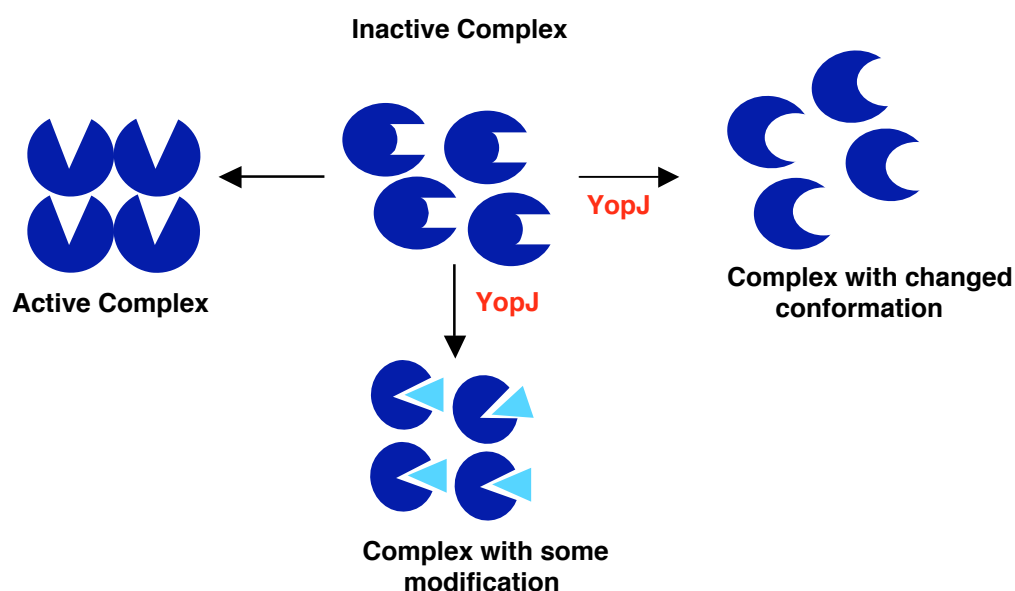


Figure 36: Model to explain YopJ's inhibitory activity. YopJ inhibits the MAPK and NF κ B pathways by blocking the activation of MKK and IKK β , respectively, and it maybe bringing about this effect by either modifying or changing the conformation of the signaling complexes, to which it binds.

The results described in this chapter demonstrate that YopJ blocks the phosphorylation and thereby the activation of the two kinases, MKK and IKK β , by functioning as an acetyltransferase. Using mass spectrometric studies, it has been revealed that YopJ modifies the critical serine and threonine residues in the activation loop of MKK6 by the addition of an acetyl group. The acetylation on MKK6 directly competes with phosphorylation, thereby preventing activation of the modified protein. This covalent modification may be used as a general regulatory mechanism in biological signaling.

Materials and Methods

Plasmids and Reagents

YopJ was cloned into pGEX-TEV vector that was kindly provided by Dr. YuhMin Chook. pGEX-TEV-YopJC172A was created using site-directed mutagenesis kit from Stratagene (Table 1, Appendix section). Human MKK6 (1-335), provided by Dr. Betsy Goldsmith, was cloned into pET28a vector using Nde1 and Not1. IKK β was cloned into pET28a vector using Not1 and HindIII. pSFFV YopJ-FLAG and pSFFV YopJC172A-FLAG are described previously [8]. MKK6-K/A, MKK6-ST/AA, MKK6-SKT/AAA and MKK6-ST/EE mutants were generated using the Stratagene QuikChangeTM site-directed mutagenesis kit and were confirmed by DNA sequence analysis (Refer to Table 1 in Appendix A).

Antibodies for phospho-ERK1/2, phospho-I κ B, phospho-MKK6, phospho-IKK and MKK1/2 were purchased from Cell Signaling, for IKK β and

aldolase were purchased from Santa Cruz Biotechnology, for GST was purchased from Covance, for anti-Hisx4 antibody was purchased from Invitrogen and for anti-FLAG antibody was purchased from SIGMA. ^{14}C -Acetyl CoA (10 μCi) and non-radioactive acetyl CoA were purchased from Amersham and Sigma, respectively. PP1 and λ phosphatases were purchased from Upstate.

Purification of recombinant proteins

pET28a-His-MKK6 (1-335) alone or in the presence of pGEX-TEV-YopJ or pGEXTEV-YopJC/A were transformed into Rosetta (DE3) cells (Novagen). Single colonies were grown to an O.D. of 0.6-0.8 followed by induction with 0.2mM IPTG (Roche) for 8-12 hours at room temperature. Cells were harvested, lysed using Emulsiflex C-5 cell homogenizer (Avastin) and the proteins (rMKK6, rMKK6-J, rMKK6-C/A) were purified using Ni²⁺ affinity purification (Qiagen) and then concentrated and charged onto a Superdex 75 size exclusion column (Amersham). Fractions corresponding to rMKK6 were pooled, concentrated and sent for mass spectrometric analyses either as a soluble sample (Q-star) or by cutting out bands (LC-MS/MS) from a Colloidal blue (Invitrogen) stained- SDS-PAGE gel. GST-YopJ and GST-YopJC/A were expressed and purified from bacteria using standard GST purification protocol [54]. Briefly, cells were grown to an O.D. of 0.6-0.8 in 2xYT media and then induced with 0.4mM IPTG for 5 hours at 30°C. The cells were lysed in PBS, pH: 8.0, 1% Triton X-100 (Fisher), 5mM DTT and 1mg/ml PeFa Bloc (Roche). Purified GST proteins were analyzed by SDS-PAGE and quantified using a modification of the Lowry's method [55]. Recombinant MKK1 protein was purchased from Upstate. For purification of His-

IKK β , cells were lysed as described above and purified as specified by Qiagen using Ni-NTA resin chromatography. Protein was eluted from Nickel beads with 250mM Imidazole containing buffer.

Mammalian cell culture and lysate preparation

HEK293 cells were cultured in DMEM (Invitrogen) with 10% cosmic calf serum (Gemini) and 5% CO₂. For preparing large-scale V, J or C/A lysates, cells were cultured in 150 mm plates and transfected with 10 μ g of either empty pSFFV, pSFFV-YopJ or pSFFV-YopJ-C/A using the standard calcium-phosphate-based transfection method [56]. Lysates for the *in vitro* assays were prepared as described in Chapter four.

In vitro assay with rMKK6, rMKK6-J and rMKK6-C/A

Equal amounts of purified His-MKK6, His-MKK6-J and His-MKK6-C/A were incubated with 10mg/ml serum-stimulated cleared lysate for 10 min at 37°C. Reactions were stopped by adding 5x SDS sample buffer and analyzed by immunoblotting with phospho-MKK6 specific antibody to detect MKK6 activation. To confirm equal loading of recombinant proteins and lysates, samples were immunoblotted with anti-Hisx6 and anti-aldolase, respectively.

In vitro Acetyltransferase assay

Acetyltransferase assays were performed as described previously [69]. In brief, 4-6 μ g of purified MKK6 (substrate) or was mixed with 50 μ M acetyl CoA or 2 μ l 14C-acetyl CoA (56 μ Ci/ μ M) in the absence or presence of 0.5 μ g of GST-

YopJ or GST-YopJC/A attached to glutathione beads in a 20 μ l or 50 μ l reaction containing 50mM HEPES (pH: 8.0), 10% glycerol, 1mM DTT and 1mM PMSF) and was incubated for 1 hour at 30°C. To test whether rMKK6 could be phosphorylated by endogenous signaling machinery, cleared lysate from serum stimulated cells (10 mg/ml) was added to each reaction in the presence of an ATP regenerating buffer, incubated at 37°C for 10 minutes followed by immunoblotting with phospho-MKK6 specific antibody. For the NF κ B pathway, GST-YopJ and GST-YopJC/A proteins were incubated with cleared lysate that had been supplemented with 50 μ M acetyl-CoA for one hour at 30°C. Reactions were stopped by the addition of 5x SDS sample buffer and the samples were resolved on a 12% SDS-PAGE gel, transferred to PVDF membranes and immunoblotted for phospho-I κ B. For the radioactive assays, the reaction mixtures were subjected to 15% SDS-PAGE gels, fixed with 50% methanol and 10% glacial acetic acid for 30 minutes and enhanced by impregnating with an enhancing solution, Amplify (Amersham) for 15 minutes. Gels were then dried and autoradiography was carried out at -80°C for 1-3 days. For the scintillation counting, beads were washed three times with 750 μ l of 1x reaction buffer and the supernatant was TCA precipitated with 10% TCA, applied to a nitrocellulose filter and washed with 5 ml of 6% TCA. Radiolabel associated with beads and filters was measured by liquid scintillation spectrometry. *In vitro* acetyltransferase assays with the different MKK6 mutants and MKK1 with GST-YopJ and GST-YopJC/A were performed as described above.

In vitro phosphatase assay

Partially purified His-IKK β was incubated with 0.1 units of PP1 or 100 units of λ -phosphatase for 1 hour at 37°C. Reactions were stopped by addition of SDS sample buffer, samples were resolved by SDS-PAGE and were analyzed by immunoblotting with anti-phospho-IKK β antibody.

Mass spectrometry

Samples were desalted with C4 Ziptip from Millipore (Billerica, MA). The eluted protein samples were made into a solution that contains 50% acetonitrile and 1% formic acid. The Proxeon nano-tips (Denmark) were used to infuse the samples into a QStar XL Q- TOF mass spectrometer (Applied Biosystems, Framingham, MA). Spectra were acquired with mass range m/z 500-2000. The molecular weights of proteins were calculated with the Bayesian Protein Reconstruct tool of the Analyst QS1.1 software.

Tandem Mass Spectrometry

Twenty micrograms of each sample were fractionated by 1D-SDS PAGE and the slices of rMKK6 protein were treated with DTT and iodoacetamide and were digested with trypsin. Samples from the digests were analyzed by nano-LC/MS/MS using a system that a Dionex LC-Packings HPLC (Sunnyvale, CA) was coupled with a QStar XL mass spectrometer (Applied Biosystems, Framingham, MA). Peptides were first desalted on a 300 μ M x 5 mm PepMap C18 trap column with 0.1% formic acid in HPLC grade water at a flow rate of 20

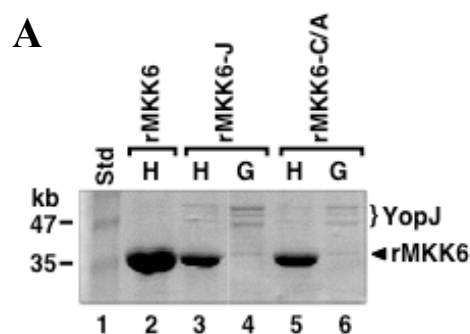
μl/min. After desalting for 6 min, peptides were backflushed onto a LC-Packings 75μm x 15cm C18 nano column (3 micron, 100Å) at a flow rate of 200 nl/min. Peptides were eluted with a 60 min gradient of 3-42% acetonitrile, in 0.1% formic acid. Mass ranges for the MS survey scan and MS/MS were m/z 300-1600 and m/z 50-1600, respectively. The scan time for MS and MS/MS were 1.0 s and 5.0 s, respectively. The top three multiple-charged ions with MS peak intensity greater than 40 counts/scan were chosen for MS/MS fragmentation with a precursor ion dynamic exclusion of 120 s.

Results

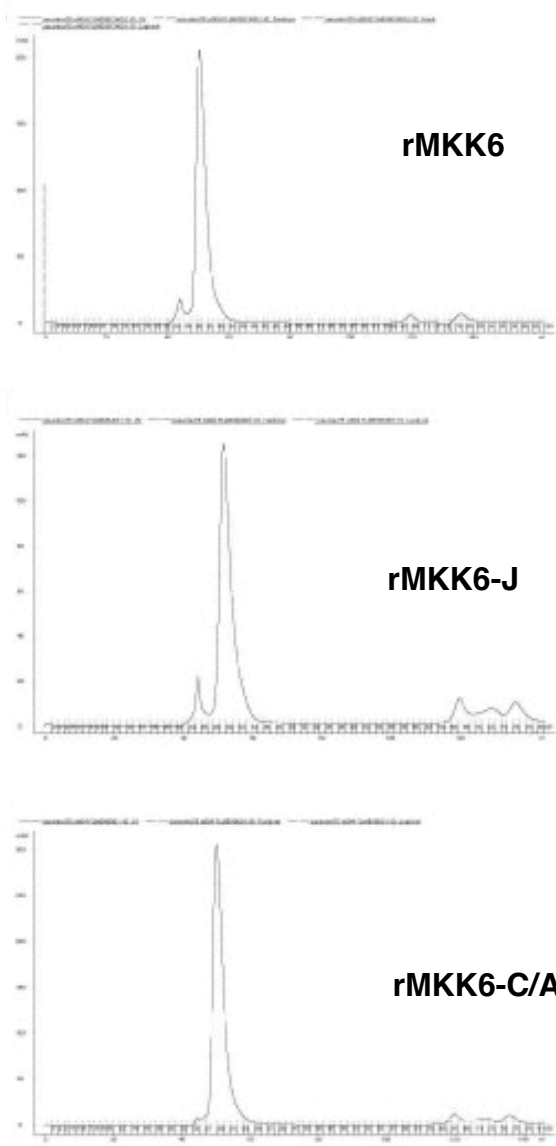
Analyses of MKK6 co-expressed with YopJ or YopJC172A in bacteria

To test whether YopJ directly acted on the MKKs and IKKβ, a bacterial system was utilized to express His-tagged MKK6 (rMKK6) alone or in the presence of GST-tagged wild type YopJ (rMKK6-J) or the catalytically inactive form of YopJ (rMKK6-C/A). MKK6 served as the representative member of the superfamily of MAPK kinases. The experiment was initially designed to express His-rMKK6, independent of other eukaryotic signaling components, with and without GST-YopJ or GST-YopJ-C/A. If no YopJ-mediated effect were observed on the activation of rMKK6, additional signaling components would be co-expressed with MKK6, together with YopJ. His-MKK6 from the three different sources (rMKK6, rMKK6-J and rMKK6-C/A) was purified by nickel affinity chromatography and run on a SDS-PAGE gel to check for protein expression. The

His-MKK6 expression was robust (>1 mg/L) (Figure 37A, lane 2) in comparison to the limited expression of the GST-tagged YopJ and YopJ-C/A (<0.1 mg/L) (Figure 37A, lanes 4 and 6) and no apparent differences were observed in the mobility of rMKK6, rMKK6-J and rMKK6-C/A proteins (Figure 37A, lanes 2, 3 and 5). The proteins were further purified by gel filtration on a Superdex75 column, where not only rMKK6 but also rMKK6-J and rMKK6-C/A were observed to elute as a dimer (Figure 37B). The gel filtration profiles for all the three recombinant proteins were indistinguishable. Even after gel filtration, when the protein samples were analyzed by SDS-PAGE, they looked the same (Figure 37C). Thus far, all biochemical analyses indicated that the three preparations of rMKK6 (rMKK6, rMKK6-J, rMKK6-C/A) were not different from each other.



B



C

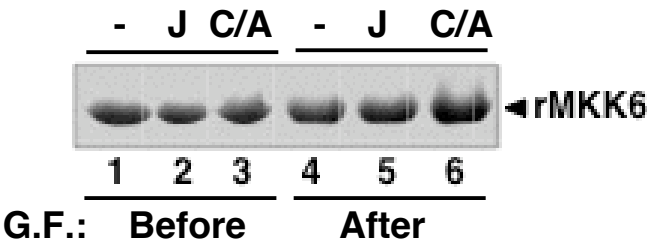


Figure 37: Purification and biochemical analyses of rMKK6, rMKK6-J and rMKK6-C/A. (A) Hisx6-MKK6 was expressed in the presence and absence of GST-YopJ (rMKK6-J) or GST-YopJ-C/A (rMKK6-C/A). Samples were split and proteins were isolated by either nickel affinity chromatography (H: lanes 1, 3, 5) or glutathione sepharose chromatography (G: lanes 2, 4, 6). (B) Gel filtration profiles for Hisx6-MKK6 (top panel), Hisx6-MKK6-J (middle panel) and Hisx6-MKK6-C/A (lower panel) indicating that all the rMKK6s elute as dimers. (C) rMKK6, rMKK6-J and rMKK6-C/A purified by nickel affinity chromatography (lanes 1-3, respectively), followed by gel filtration chromatography (lanes 4-6, respectively).

***In vitro* assay with rMKK6, rMKK6-J and rMKK6-C/A**

Since the various rMKK6s were indistinguishable by SDS-PAGE and gel filtration, the next question was whether these recombinant proteins could be activated in the *in vitro* signaling assay. To test this hypothesis, equal amounts of all of the three purified rMKK6 proteins were incubated with cleared, cell-free lysate derived from unstarved cells, thereby maintaining signaling machinery in an active state. Upon addition of rMKK6 or rMKK6-C/A to cleared lysate, both rMKK6 and rMKK6-C/A were robustly phosphorylated, as indicated by immunoblot analysis with a phospho-MKK6 antibody (Figure 38, lanes 2 and 6). By contrast, when rMKK6-J was incubated with cleared lysate (Figure 38, lane 4), MKK6 phosphorylation was completely abolished. This indicates that co-expression of MKK6 with YopJ maybe producing an inactive, dead kinase that can no longer be stimulated by upstream signaling machinery. These observations are consistent with previous cell free lysate studies that demonstrate YopJ functions in a catalytic manner to modify the MKK superfamily, without changing their levels or migration as assessed by SDS-PAGE (chapter four,

Figures 21D and 23D).

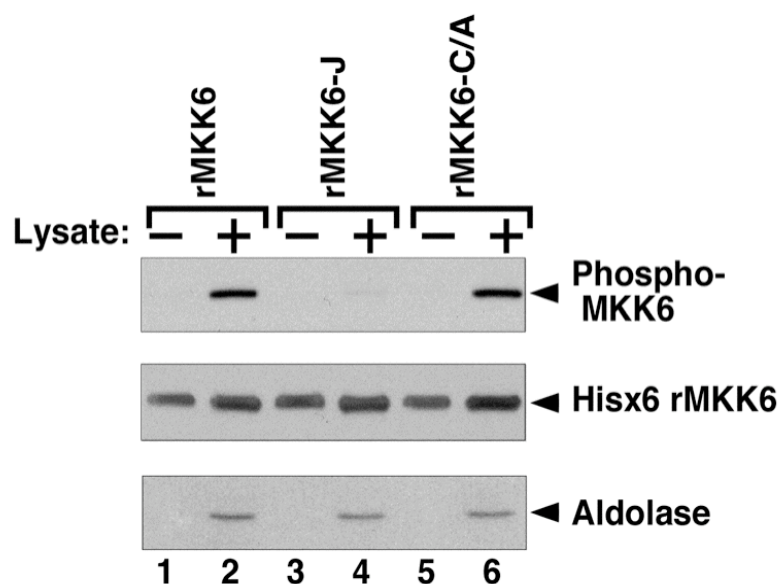


Figure 38: Expression of YopJ prevents the activation of MKK6 by phosphorylation *in vitro*. YopJ co-expressed with rMKK6 in bacteria is not phosphorylated by upstream signaling machinery. Purified rMKK6, rMKK6-J and rMKK6-C/A were incubated with serum-stimulated cleared lysate for 10 min at 37°C, followed by analysis with antibody to phospho-MKK6 (anti-phospho-MKK6) (lanes 2, 4 and 6). rMKK6 was detected by immunoblotting with antibody to Hisx4. Aldolase immunoblot was a load control for lysate.

Analysis of rMKK6-J by mass spectrometry

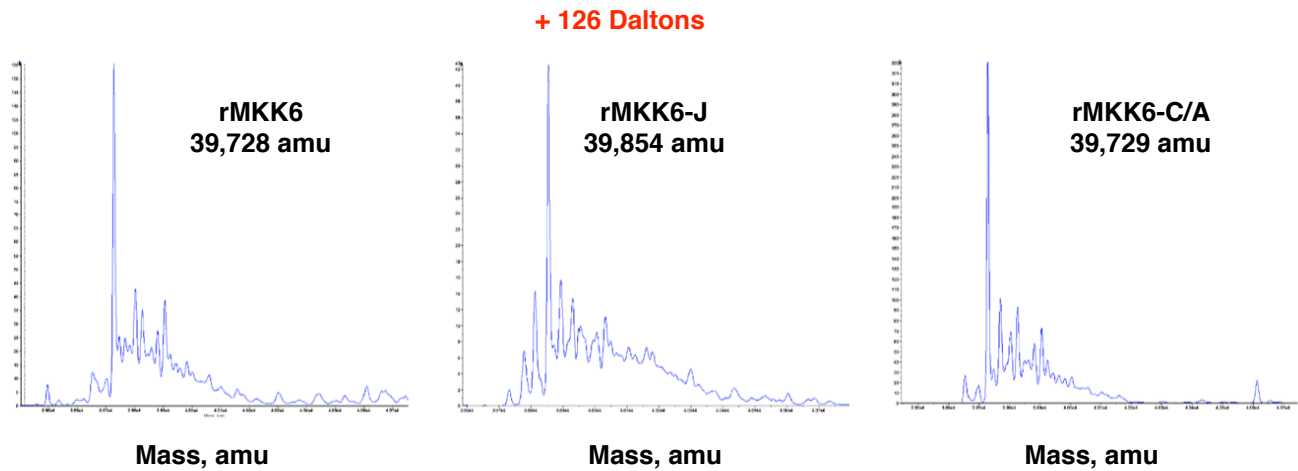
To determine why MKK6 co-expressed with YopJ was inactive when stimulated by upstream signaling machinery, studies were undertaken to determine the biochemical nature of the modifications in rMKK6-J, if any. N-terminal sequencing did not show any differences between rMKK6, rMKK6-J and

rMKK6-C/A. However, differences in the rMKK6 protein preparations became apparent when the total mass of each of the rMKK6s was determined by mass spectrometry. The ABI QSTAR XL machine used for this study revealed that the mass of rMKK6-J (39,854 amu) was larger than that of either rMKK6 or rMKK6-C/A (39,728-9 amu). The majority of YopJ-inactivated rMKK6 showed an increase in mass of 126 atomic mass units (amu), whereas smaller populations of rMKK6-J exhibited increases in mass of 84 amu or 42 amu (Figure 39A). These observations indicate that YopJ is altering the mass of rMKK6 by adding single, double, or triple post-translational modifications equal to a mass of 42 amu.

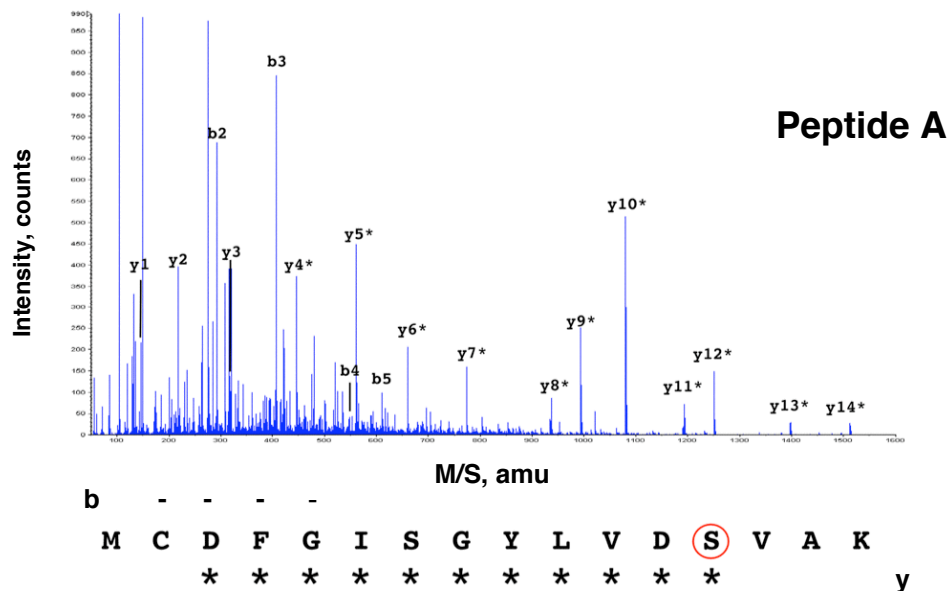
To determine what is contributing to the increase in the total mass of rMKK6-J, the tryptic peptides for all three rMKK6s (rMKK6, rMKK6-J, rMKK6-C/A) were analyzed by using liquid chromatography followed by tandem mass spectrometry (MS/MS). After obtaining a complete data set for all the predicted tryptic peptides, rMKK6-J, but not rMKK6 or rMKK6-C/A, was observed to contain two tandem peptides (peptide A, MKK6 195-210 amino acids, and peptide B, MKK6 211-224 amino acids) that were modified by acetylation with a consequent increase of 42 amu for each peptide (Figure 39, B and C). In another partially cleaved tryptic peptide (MKK6 195-224 amino acids), that contained both peptides A and B, multiple acetylated sites were observed. MS/MS data of “b” and “y” ions (Figure 39D) indicated that Peptide A in the rMKK6-J protein was modified by acetylation on Ser 207 (Figure 39B) and peptide B was modified by acetylation on Thr 211 (Figure 39C). In the third peptide, it appeared that Lys 210 and Ser 207 and/or Thr 211 were modified by acetylation. Modification of the lysine residue contributed to the inefficient cleavage of this peptide by trypsin.

These observations indicate that YopJ is adding acetyl groups onto MKK6 on three distinct sites resulting in a kinase that cannot be phosphorylated.

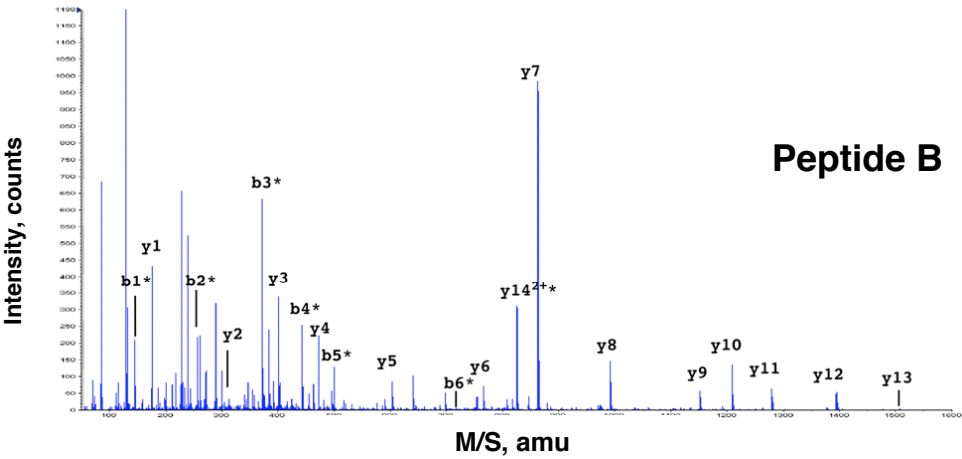
A



B

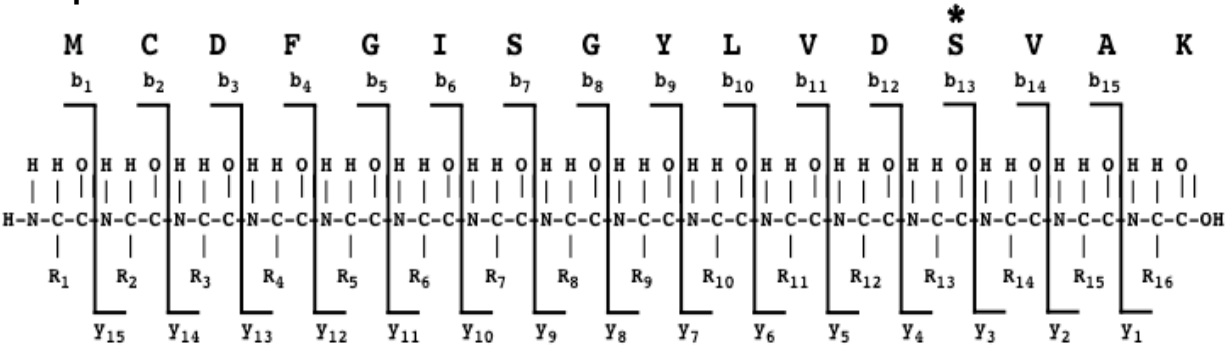


C



D

Peptide A



Peptide B

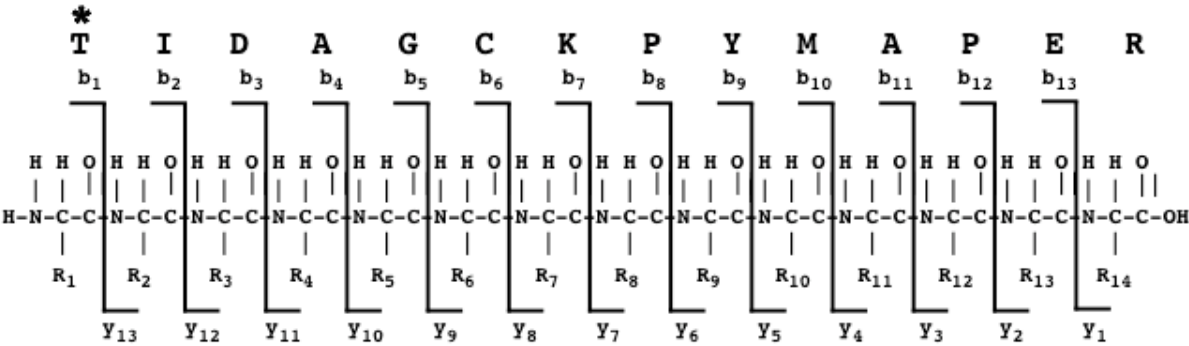


Figure 39: rMKK6-J is acetylated on Ser 207 and Thr 211 residues in its activation loop. (A) Reconstructed molecular mass profiles of rMKK6, rMKK6-J, and rMKK6-C/A. (B and C) Electrospray ionization (ESI) tandem mass spectrometry (MS/MS) spectra of modified tryptic peptide A [mass-to-charge ratio (m/z) of 902.4 ($z=2$)] and peptide B [m/z of 825.9 ($z=2$)] from rMKK6-J. The b and y ions are marked on the MS/MS spectra. The amino acid sequence for each peptide is shown below. Acetylated residues are designated with a red circle. Masses that show an increase of 42 amu are marked with an asterisk. Two ions related to acetylated peptide B were detected, m/z of 825.9 ($z=2$) and m/z of 833.9 ($z=2$). MS/MS data of both ions indicated that peptide B was modified by acetylation on Thr 211. The only difference between these two ions is that Met 220 is oxidized in m/z of 833.9. (D) The amino acid sequence for peptide A (top panel) and peptide B (lower panel) are shown with detailed mapping of the b and y ions.

YopJ acetylates rMKK6 on Ser²⁰⁷ and Thr²¹¹ residues in its activation loop

The residues on rMKK6 that are modified by acetylation in a YopJ dependent manner are Ser 208, Lys 210 and Thr 211 (Figure 39, B and C). These amino acids were then mapped onto the MKK6 sequence. Residues 195 to 224 map to the end of beta strand 9, which is the activation loop region in MKK6. This loop contains Ser 207 and Thr 211, the sites that are phosphorylated by upstream kinases to induce activation of MKK6. Although the serine and threonine residues are conserved throughout the MKK superfamily, the lysine residue is not (Figure 40). This residue is predicted to be modified in a YopJ-dependent manner because of its coincidental location in the activation loop. The observation that YopJ covalently modifies the representative MKK, MKK6, by acetylation on the same residues that are used for activation of the kinase suggests a mechanism for the inhibition of MKKs and IKK β ; namely acetylation prevents

phosphorylation.

YopJ can bind and inhibit MKKs and IKK β but not IKK α (chapter three, Figure 15A) and all of these kinases contain serine and/or threonine residues in their activation loop that must be phosphorylated to activate the kinase (Figure 40). rMKK6, co-expressed with YopJ and shown to be acetylated at Ser 207 and Thr 211 (Figure 39, B and C), was not phosphorylated by upstream signaling machinery (Figure 38). These observations support the hypothesis that YopJ functions to modify the MKKs without noticeably changing their migration pattern on SDS-PAGE (Figure 37A).

In this study, acetylation of serine/threonine residues in a protein was the first demonstration of residues other than lysine to be acetylated. Enzymes that acetylate lysines have been studied for many years, including the eukaryotic and bacterial N-acetyltransferases [70-72]. Immunoblotting and the usage of MASCOT software are some of the common ways of identifying lysine acetylation [73]. These assays, however, do not detect acetylation of serines and threonines. Thus, not only antibody production but also a careful manual analysis of MS/MS data maybe required for determining whether an amino acid other than lysine is modified by acetylation.

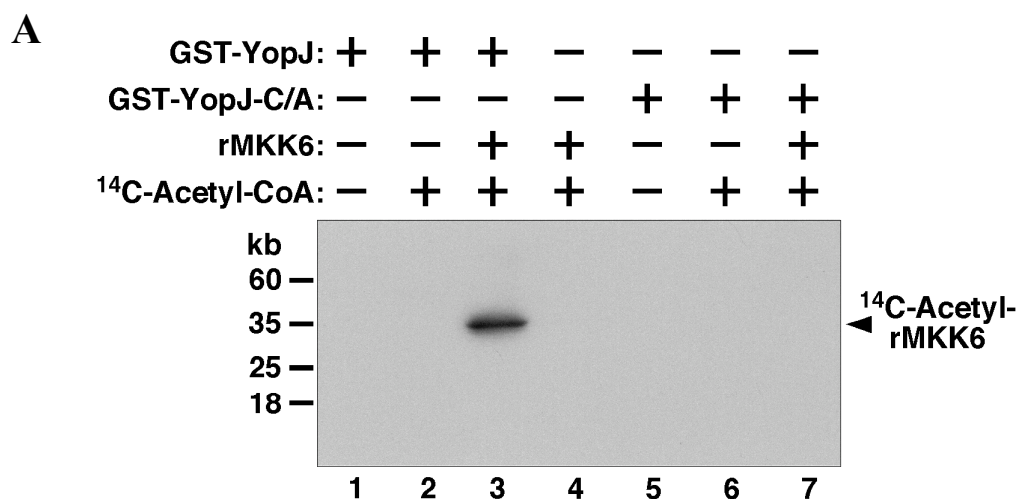
MKK-1	KLCDFGVSGQLID-SMANS-FVGTRS	YMSPERL	
MKK-2	KLCDFGVSGQLID-SMANS-FVGTRS	YMAPERL	
MKK-3	KMCDFGISGYLVD-SVAKTMDAGCKP	YMAPERI	
MKK-4	KLCDFGISGQLVD-SIAKTRDAGCRP	YMAPERI	
MKK-5	KLCDFGVSTQLVN-SIAKT-YVGTNAY	MAPERI	
MKK-6	KMCDFGISGYLVD-SVAKTIDAGCKP	YMAPERI	
Pbs2	KLCDFGVSGNLVA-SIAKT-NIGCQS	YMAPERI	
Ste7	KLCDFGVSKKLIN-SIADT-FVGTSTY	MSPERI	
IKK- α	KIIDLGYAKDVDQGS	LCTS-FVGT	LQYLAPELF
IKK- β	KIIDLGYAKELDQGS	LCTS-FVGT	LQYLAPELL
	KLCDFG.SG L. GS.A T .VGT	YMAPERI	
		*	*

Figure 40: Alignment of the members of the superfamily of MAPK kinases. Sequence alignment of the activation loop region of the MKK superfamily with conserved serine and/or threonine residues that are indicated by asterisks.

In vitro Acetyltransferase Assay

rMKK6 expressed in the presence of YopJ, but not YopJC172A, gets modified by acetylation on its critical serine and threonine residues located on the activation loop. To determine whether YopJ directly functions as an acetyltransferase, recombinant GST-YopJ and GST-YopJ-C/A were purified from *E. coli* and an acetyltransferase reaction was performed in the presence of ^{14}C -labeled acetyl CoA [69]. As shown in Figure 41A, lane 3, the ^{14}C -labeled acetyl moiety was incorporated onto MKK6 only in the presence of YopJ and the labeled acetyl donor [^{14}C] acetyl-CoA. In addition, a scintillation count experiment also gave similar results (Figure 41B). GST-YopJ or GST-YopJC/A bound to glutathione sepharose beads were incubated with ^{14}C -labeled Acetyl-

CoA, in the presence and absence of rMKK6, followed by affinity purification of GST-YopJ and GST-YopJ-C/A. Scintillation count measurements of purified proteins showed that GST-YopJ, but not GST-YopJ-C/A, was radiolabeled with ^{14}C only in the presence of rMKK6. Based on this observation and also upon analysis of the GST-YopJ protein beads, rMKK6 associated with GST-YopJ served as the source of the ^{14}C label (Figure 41C). Thus, YopJ requires both an intact catalytic site and acetyl-CoA to acetylate rMKK6. In the *in vitro* assay, no bands were observed in reactions that contained only GST-YopJ and [^{14}C] acetyl-CoA, indicating that the charging of YopJ with a [^{14}C] acetyl moiety might be transient, labile, and/or dependent on the presence of a substrate or that the reaction proceeds through direct transfer. Similarly, rMKK1 was also modified by [^{14}C] acetyl moiety in a YopJ-dependent manner (Figure 41D). Thus, these experiments show that YopJ acts as an acetyltransferase to modify MKKs.



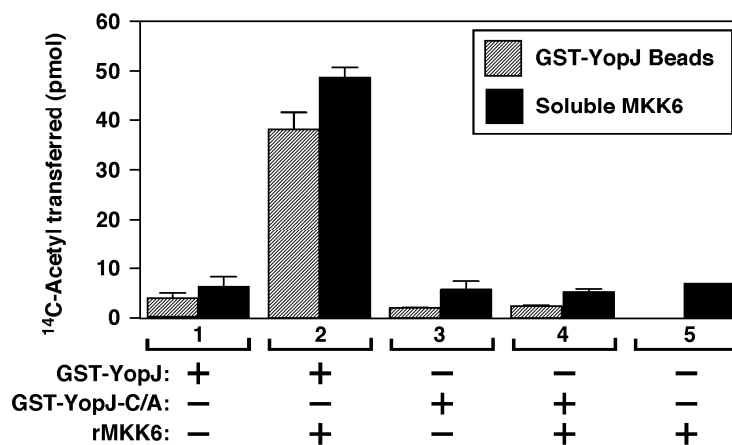
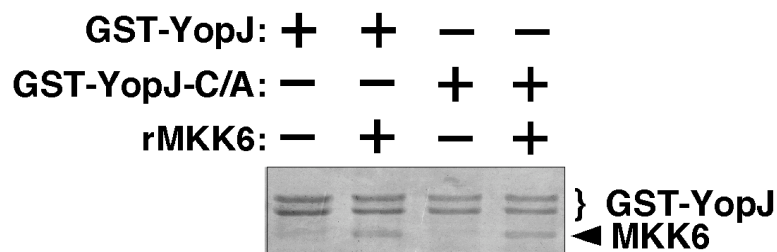
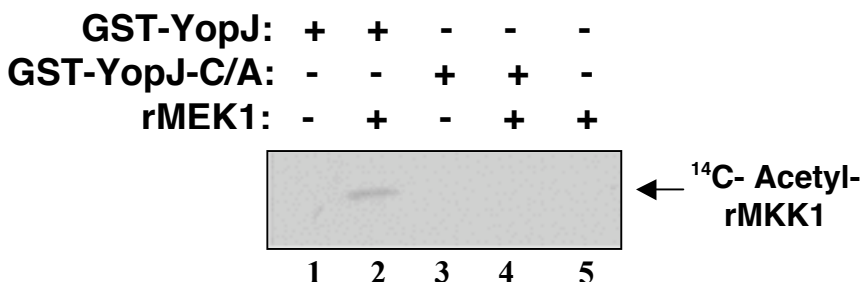
B**C****D**

Figure 41: *In vitro* acetylation of rMKK6 by YopJ. (A) Purified recombinant GST-YopJ or GST-YopJ-C/A was incubated with and without rMKK6 in the presence and absence of ¹⁴C-labeled acetyl-CoA for 1 hour at 30°C. Samples were separated by SDS-PAGE and analyzed by autoradiography. (B) Purified

recombinant GST-YopJ or GST-YopJ-C/A bound to glutathione sepharose beads was incubated with and without 200pmol of rMKK6 in the presence and absence of 35mM [^{14}C] acetyl- CoA. YopJ beads were washed, and supernatants were trichloroacetic acid (TCA)- precipitated, followed by measurement of the associated radiolabel. (C) Bead samples from (B) were separated by SDS-PAGE, followed by staining with Coomassie blue. (D) Acetylation by YopJ *in vitro*. Purified recombinant GST-YopJ or GST-YopJ-C/A was incubated with and without rMKK1 in the presence of [^{14}C] acetyl CoA for one hour at 30°C. Samples were separated by SDS-PAGE and analyzed by autoradiography.

Specificity of YopJ Acetylation

The critical serine and threonine residues in the activation loop of MKK6 that are acetylated by YopJ are highly conserved in the superfamily of MAPK kinases (Figure 40). The lysine at position 210, is however, not conserved within the different family members. Thus, in order to determine which residues on MKK6 are crucial for acetylation by YopJ, a series of MKK6 mutants were made that included MKK6-K/A, MKK6-ST/AA, MKK6-SKT/AAA and MKK6-ST/EE. All of these MKK6 mutants were expressed in bacteria and the proteins were purified by nickel affinity chromatography followed by gel filtration and then tested in *in vitro* acetyltransferase assays in the presence of GST-YopJ or GST-YopJC/A. Not only wt MKK6, but also MKK6-K/A, were acetylated in a YopJ-dependent manner (Figure 42, lanes 1 and 2). This implies that this non-conserved lysine residue is not critical for acetylation by YopJ and as explained earlier, it gets acetylated because of its coincidental location in the activation loop region of MKK6. As expected, MKK6-ST/AA and MKK6-SKT/AAA were unable to be acetylated by YopJ (Figure 42, lanes 3 and 4). This indicates the critical role played by the conserved serine and threonine residues in the activation loop. The

last mutant ST/EE corresponds to MKK6 in its constitutively active form. This mutant was used to address the question whether YopJ can inhibit MKKs in their activated state. The result, that YopJ does not acetylate and thereby inhibit constitutively active MKK6 (Figure 42, lane 5), confirms previous observation where YopJ was unable to inhibit MAPK signaling in the presence of constitutively active MKK1, MKK1-ED [8].

The fact that YopJ's mechanism of inhibition is evolutionarily conserved [33] can now be explained from the high degree of conservation of serine and threonine residues in the activation loop of the superfamily of MKKs (Figure 40). Studies with the MKK analog in yeast, Pbs2, have demonstrated that YopJ acetylates Pbs2, thereby preventing its activation [*Y-H.H and K.O., unpublished observations*]. However, IKK α , one of the members of this group that contains the essential serine and threonine residues, is not inhibited by YopJ, and does not bind YopJ [8]. It is thus hypothesized that YopJ inhibits only that molecule to which it binds. This will be discussed in detail in chapter seven.

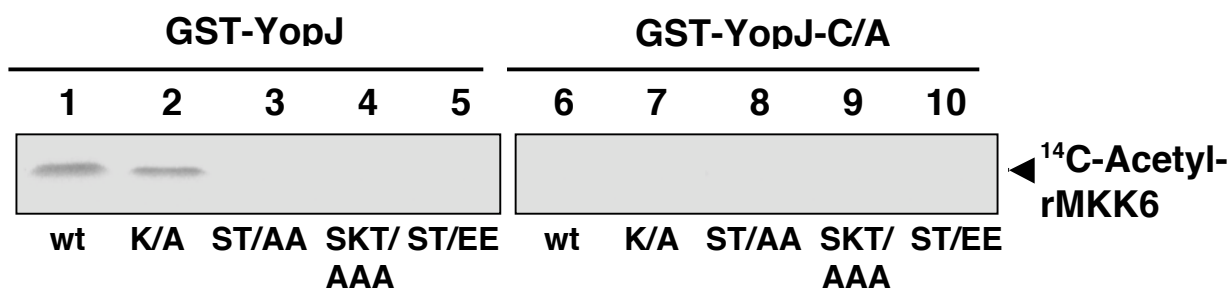


Figure 42: Ser 207 and Thr 211 are the critical residues for rMKK6 acetylation by YopJ. MKK6 mutants in the activation loop region (K/A, ST/AA, SKT/AAA and ST/EE) were constructed using site-directed mutagenesis. Each of these mutants were purified from bacteria using nickel affinity chromatography, followed by gel filtration and then incubated with GST-YopJ or GST-YopJ-C/A proteins for 1 hour at 30°C. wt MKK6 served as the positive control (lanes 1 and 6). Samples were resolved on a SDS-PAGE gel and analyzed by autoradiography.

Acetylation competes for phosphorylation

After mass spectrometric studies revealed that rMKK6 gets acetylated in the presence of YopJ, *in vitro* transferase assays confirmed that YopJ is functioning as an acetyltransferase. Since YopJ acetylates the same serine and threonine residues that are essential for activation, this offers a simple, inhibitory mechanism; acetylation by YopJ competes for phosphorylation by upstream signaling machinery. To demonstrate that the modification on rMKK6 by YopJ does indeed prevent activation via phosphorylation, the *in vitro* signaling system was utilized. Immunoblotting with anti-phospho-MKK6 antibody showed that pre-incubation of recombinant GST-YopJ or GST-YopJC/A proteins with rMKK6 for one hour at 30°C did not prevent phosphorylation of rMKK6 by upstream signaling machinery (Figure 43, lanes 1 and 3). However, pretreatment of rMKK6 with GST-YopJ protein, for the same amount of time, in the presence of acetyl-CoA diminished the ability of the upstream signaling machinery to activate rMKK6 by phosphorylation (Figure 43, lane 2). As expected, incubation of rMKK6 with GST-YopJC/A in the presence of acetyl-CoA did not show any inhibitory effect (Figure 43, lane 4). Hence, these observations are consistent with

the hypothesis that acetylation of a MKK by YopJ competes for phosphorylation and thereby activation of this kinase. YopJ acetylates the hydroxyl moiety on Ser 207 and Thr 211 and as such the resulting modified MKK6 can no longer be recognized or modified by phosphorylation by upstream MAPK kinase kinases.

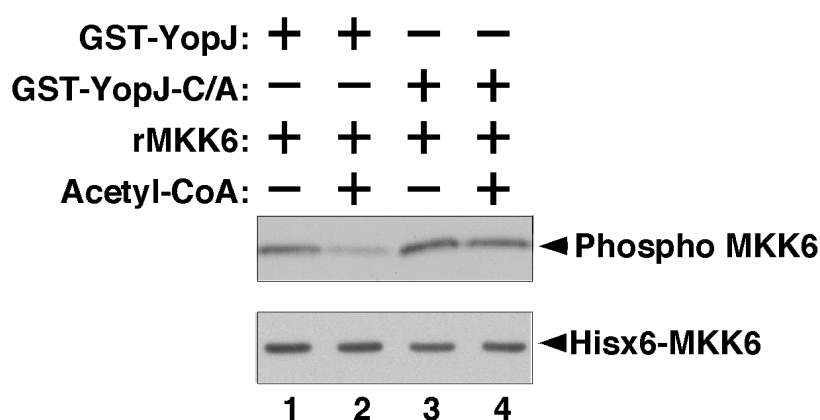


Figure 43: *In vitro* acetylation by YopJ prevents phosphorylation of rMKK6. Purified recombinant GST-YopJ and GST-YopJ-C/A were incubated with rMKK6 in the presence and absence of acetyl-CoA for 1 hour at 30°C, followed by incubation with serum-stimulated cleared lysate for 10 minutes at 37°C and immunoblot analysis with anti-phospho-MKK6.

Reconstitution of the TTSS

YopJ protein is delivered into the cytoplasm of a host cell by a type III secretion system where it inhibits the activation of the MKKs and IKK β [7].

Previously, addition of recombinant YopJ to cell-free lysates did not show an inhibitory effect on the signaling pathways. However, when GST-YopJ, but not GST-YopJC/A proteins were incubated with cleared lysate that had been supplemented with acetyl CoA, the NF κ B pathway was inhibited, as demonstrated by the lack of phosphorylation of I κ B (Figure 44). Thus, as observed during infection, when delivered to a lysate, YopJ uses acetyl-CoA to target and inactivate MKKs and IKK β .

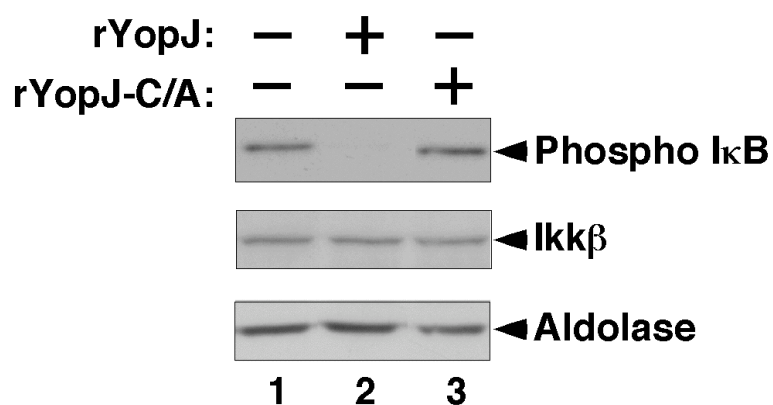


Figure 44: Inhibition of NF κ B pathway by YopJ in an acetyl-CoA-dependent manner. Acetyl-CoA (50 μ M) was added to cleared lysate (10mg/ml), followed by addition of recombinant GST-YopJ or GST-YopJ-C/A (100ng), and incubated for 1 hour at 30°C. Lysates were then incubated with purified TRAF6 protein for 10 min at 37°C, followed by immunoblotting with anti-phospho-I κ B, anti-IKK β and aldolase.

Experimental trials for IKK β purification in the presence of YopJ

Based on the above results, it has now been elucidated that YopJ inhibits the MAPK pathway by having a direct effect on the MAPK kinase. *In vitro* assay in Figure 44 demonstrates how YopJ uses acetyl-CoA to block NF κ B signaling. In view of current findings, it is understood that IKK β also gets acetylated by YopJ on the same serine and threonine residues as MKK6, and is not activated by upstream signaling machinery resulting in the inhibition of the NF κ B pathway in a YopJ-dependent manner. However, unlike MKK6, direct acetylation for IKK β has not been demonstrated as yet. Several different strategies have been utilized but demonstration of IKK β acetylation has been a very challenging task.

Purification of recombinant IKK β from bacteria has always produced a constitutively phosphorylated kinase (Figure 45, lanes 1 and 4). In addition, purification of IKK β from insect cells also produced a constitutively active kinase. Purifying out just the kinase domain of IKK β (IKK β -KD) also gave similar results. Since YopJ cannot acetylate or inhibit IKK β in its activated state, removal of the phosphate group is important to observe YopJ's effect. Unfortunately, *in vitro* phosphatase assays carried out with different phosphatases failed to remove the phosphate groups from both the full length and IKK β -KD proteins (Figure 19, lanes 2 and 3).

In order to detect IKK acetylation by YopJ under *in vivo* conditions, different experiments were designed to isolate the IKK complex from HEK293 cells in the presence of YopJ or YopJC/A. The goal of these experiments was to purify and isolate the endogenous IKK signaling machinery in the presence of

YopJ and look for changes in M.W. by mass spectrometry, similar to MKK6. The purification scheme involved large-scale harvesting and lysis of HEK293 cells transfected with either vector control or YopJ or YopJC/A plasmids, followed by anion exchange chromatography using a HiTrap MonoQ column, gel filtration on a Superdex 200 column and a second MonoQ column with linear salt gradient. Alternatively, the IKK complex was immunoprecipitated out with α -IKK γ antibody on beads after the gel filtration step. In both cases, the last step involved resolving the purified IKK protein or beads on a SDS-PAGE gel and analyzing the protein bands by silver staining. After numerous efforts, however, there were many setbacks associated with the purification of the IKK complex from cells, resulting in extremely low yield. After every transfection, the YopJ lysates would have to be checked to confirm inhibition of the NF κ B pathway. Cell lysates with poor transfection quality or high background were discarded. Bands corresponding to IKK β were observed a few times but due to low yield the peaks on the mass spectrometric data were always difficult to interpret. In addition, because of the low yield, the peaks were always masked by keratin contamination. Since purification of endogenous IKK was giving poor yields, strategies were also developed to overexpress IKK β in HEK293 cells. For example, cells were transfected with GST-tagged IKK β in the presence of YopJ or YopJC/A and the IKK complex was then isolated from these cell lysates by GST-affinity purification using glutathione sepharose beads. However, these experiments also failed to provide an optimal yield of IKK β for mass spectrometric studies. The results from these experiments remain inconclusive.

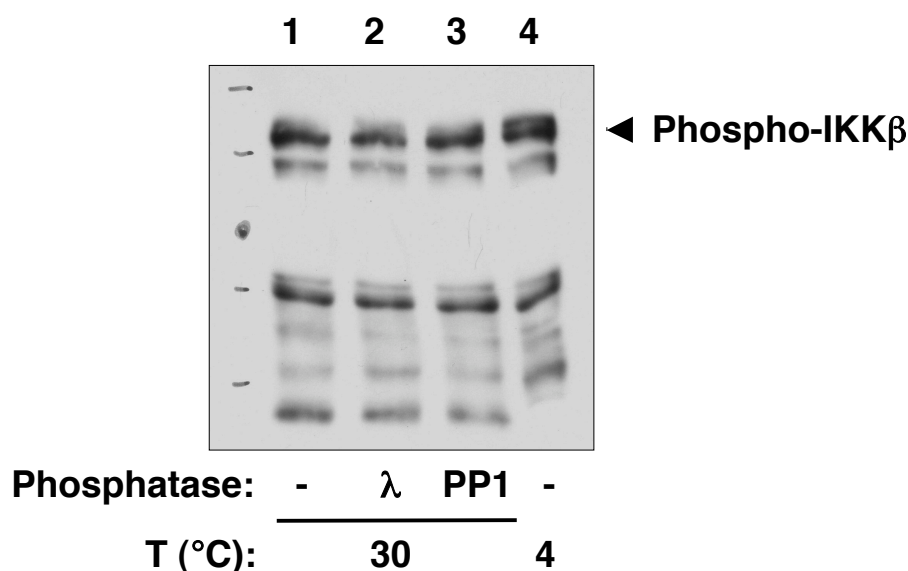


Figure 45: IKKβ purified from bacteria is constitutively phosphorylated.

Full-length Hisx6 IKKβ, purified from bacteria, was incubated with or without lambda and PP1 phosphatases for 1 hour at 30°C. Reactions were stopped by addition of sample buffer. Samples resolved by SDS gel were analyzed by immunoblotting with anti-phospho-IKKβ antibody.

Discussions

This study demonstrated YopJ's mechanism of inhibition of the MAPK and NFκB pathways. Experiments from previous studies had predicted that YopJ maybe modifying the MAPK kinases, to which it binds, such that they can no longer be activated by the upstream stimuli. Herein, it was discovered that YopJ acted as an acetyltransferase to modify critical serine and threonine residues in the activation loop of MKK6 and thereby blocking phosphorylation.

The study was initiated by taking a simple and straightforward approach

of isolating and purifying a representative member of the superfamily of MAPK kinases, MKK6, in the presence or absence of YopJ, using a bacterial expression system. MKK6 protein bands purified alone (rMKK6) or co-expressed with YopJ (rMKK6-J) or YopJC172A (rMKK6-C/A) were indistinguishable from each other and their gel filtration profiles were also very similar. This indicated that YopJ is not functioning as a protease or an isopeptidase and that it does not disrupt MKK6 dimerization. However, the most striking observation was made when these proteins were used in the *in vitro* signaling assay system. rMKK6-J, by contrast to rMKK6 and rMKK6-C/A, was not phosphorylated by the upstream signaling machinery, which implied that coexpression of YopJ with rMKK6 in bacteria is producing a modified kinase.

To determine why rMKK6-J was inactive upon stimulation, mass spectrometric methods were adopted to understand the biochemical nature of modification in rMKK6-J, if any, and showed that YopJ altered the mass of rMKK6 by adding single, double or triple post-translational modifications equal to a mass of 42 amu. Analyses of the peptides of rMKK6-J, after a trypsin digest, by LC-MS/MS further revealed that Ser 207 and Thr 211 are acetylated. Mapping of these residues corresponded to the activation loop region of MKK6, which includes the highly conserved serine and threonine residues, essential for activation by upstream kinases, in all the different members of MAPK kinase family. This indicated that YopJ blocks activation of the MAPK kinases by acetylating those same critical serine and threonine residues that are required for phosphorylation and thus offers a straightforward mechanism that acetylation prevents phosphorylation. *In vitro* acetyltransferase assays using both

radiolabeled and cold acetyl CoA further confirmed YopJ's role as an acetyltransferase.

These findings present the first-time demonstration of acetylation of residues other than lysine. Acetylation of serine or threonine residues have gone undetected in the past because assays that detect lysine acetylation such as immunoblotting and data analysis by the MASCOT software have not been developed to explore whether an amino acid other than lysine is modified by acetylation.

CHAPTER SEVEN

DISCUSSION AND CONCLUSIONS

YopJ: What is known?

The bacterial pathogen *Yersinia pestis* is the causal agent of plague, also known as the Black Death [1]. Two related pathogens, *Y. pseudotuberculosis* and *Y. enterocolitica*, cause gastroenteritis [2]. All three *Yersinia* species harbor a virulence pathogen that encodes a TTSS and secrete effector proteins, referred to as Yops [2]. Yops are delivered by this system into a eukaryotic cell to cripple the host defense system [7]. The six well-studied Yops in *Yersinia* are: YpkA, YopE, YopH, YopM, YopT and YopJ. Interestingly, each *Yersinia* effector appears to have usurped or mimicked the activities of eukaryotic proteins that are essential for maintaining normal signaling in the target cell [7]. The *Yersinia* effector protein YopJ (also called YopP in *Y. enterocolitica*) disrupts signaling essential for eukaryotic cells to elicit an immune response by inhibiting the evolutionarily conserved MAPK pathways (including p38, ERK and JNK) and the NF κ B signaling pathway [8]. YopJ inhibits these pathways by blocking the phosphorylation of the MAPK kinases, MKK and IKK β , by the upstream MAPK kinase kinases (MKKK).

YopJ contains a catalytic domain that is similar to Clan CE of cysteine proteases, which includes the AVP family and the Ulp1 family [9]. These

proteins contain a highly conserved catalytic triad of amino acids- His, Asp/Glu and Cys. Mutation of the putative catalytic cysteine residue to an alanine in YopJ (YopJ-C/A) abolished its ability to inhibit the MAPK and the NF κ B signaling pathways [9]. This indicated that YopJ requires the maintenance of its catalytic site to disrupt signaling pathways inside the target cell. Using yeast two-hybrid analysis, it was demonstrated that YopJ binds MAPK kinases including MKK1, MKK3, MKK4 and MKK5 and prevents their activation [8]. The related kinase that activates the NF κ B pathway, IKK β , was also shown to bind YopJ using GST-pull down experiments [8]. The mechanism by which the binding of YopJ leads to inactivation of these kinases is unknown.

Orth and colleagues demonstrated that YopJ decreases the level of SUMO and SUMO-conjugated proteins in cells [9] and Zhou and colleagues showed that YopJ functions as a DUB [45]. These observations were based on overexpression-based systems and both of them failed to explain how does YopJ specifically inhibit the MAPK and NF κ B pathways at the level of MKK and IKK β , respectively. Thus, the goal of this thesis project is to discover and characterize YopJ's mechanism of inhibition of the eukaryotic signaling machinery.

Discussion of Research Findings

YopJ is neither a deSUMOylating enzyme nor a DUB

Owing to YopJ's strong resemblance to AVP and Ulp1, initial experiments were set-up to test YopJ's activity as a protease; specifically as a

deSUMOylating enzyme or a DUB. Modification of MKK by SUMO was reported in *Dictyostelium* and was shown to be important for its activation [48]. To determine whether mammalian MKK also got SUMOylated, *in vitro* SUMOylation assays were developed that successfully demonstrated Ulp1-sensitive MKK SUMOylation (Figure 10C). After several experimental trials, SUMOylation of MKK, however, could not be demonstrated *in vivo*. Based on the premise that YopJ could be functioning as a deSUMOylating enzyme, addition of recombinant YopJ, purified from different sources, failed to cleave off the SUMO moiety from MKK, unlike Ulp1 (Figure 12). In addition, there was no inhibition or decrease in the levels of TRAF6-poly ubiquitin ladder in cells expressing YopJ (Figure 13B). This result was in contrast to that observed by Zhou and colleagues wherein YopJ decreased TRAF6 polyubiquitin chains [45]. This discrepancy could be due to the different experimental approaches taken. In the former case, the experiment was done in TRAF6-expressing stable cell lines and TRAF6 ubiquitination was observed by immunoblotting with anti-TRAF6 antibody. In the latter case, however, TRAF6 was co-expressed with HA-ubiquitin in the presence of YopJ and TRAF6 ubiquitination was observed by anti-HA immunoblot. The YopJ-dependent decrease in TRAF6 polyubiquitin chain, observed in the latter case, may represent global cellular effects, that can arise when a protein, usually present at low levels in the cell, is overexpressed [74].

Potential DUBs or deSUMOylating enzymes can form complexes with vinyl sulfone (VS) adducts that can then be visualized by SDS-PAGE [51]. Lysates expressing YopJ, and incubated with SUMO-VS or Ub-VS did not show

any YopJ-SUMO-VS or YopJ-Ub-VS adducts (Figure 26B). Thus, this further rules out the possibility of YopJ being a deSUMOylating enzyme or a DUB.

YopJ's inhibitory effects on the MAPK and NFκB pathways

To understand YopJ's inhibition of the signaling pathways, the signaling components and the regulatory mechanisms of each of these pathways was closely analyzed. YopJ inhibits the MAPK and NFκB pathways by blocking the phosphorylation of MKK and IKKβ respectively. Experiments were designed to explore all the possible ways that lead to the phosphorylation of MKK or IKKβ by upstream MKKKs and then test whether they are sensitive to inhibition by YopJ. Focusing first on MAPK signaling, KSR, a scaffold protein, plays a key role in the activation of the MAPK pathway. It functions as an adapter protein to bring together Raf and MKK for MKK phosphorylation [31]. Experiments with KSR and YopJ co-expressed together showed that YopJ alters the migration pattern of KSR, possibly by inhibiting KSR phosphorylation. An important observation made during the course of these studies, was that YopJ could no longer inhibit ERK phosphorylation in KSR *-/-* cells. This indicated a crucial role played by KSR in YopJ's inhibitory activity. Both KSR and MKK are known to undergo nucleocytoplasmic shuttling. In the presence of growth stimulus, the KSR-MKK complex is recruited to the membrane, whereupon it is activated by the Ras-Raf complex [32]. To determine whether YopJ affects the recruitment of this machinery to the membrane, subcellular localization cellular fractionation

techniques were employed. In all cases, YopJ never disrupted the subcellular localization of any of the components and neither did YopJ affect the stability of these protein complexes. Although the preliminary studies with KSR seemed promising, the study was discontinued because of several technical difficulties.

Based on similar grounds, all pathways that lead to IKK β activation in the NF κ B pathway were scrutinized in the presence and absence of YopJ. The NF κ B pathway is activated by different upstream stimuli that finally converge at a common point, the IKK complex. YopJ inhibited IKK β phosphorylation by all the different kinases tested- NIK, MEKK1 and TAK1 (Figure 14). HTLV-1 protein Tax, unlike the MKKKs, has been proposed to activate the IKK complex by inducing a conformational change [17]. In accordance with previous studies [18], YopJ even inhibited Tax-mediated activation of the NF κ B pathway (Figure 34). By contrast, YopJ failed to inhibit the pathway when the constitutively active form of IKK β (IKK-EE) was overexpressed, similar to that observed with MKK-ED for the MAPK pathway [8]. Techniques such as glycerol density gradients failed to reveal any inhibitory effect of YopJ on the stability of the IKK complex. Biochemical fractionation and co-immunoprecipitation techniques also showed that this massive complex of ~700kD was intact in YopJ's presence. These were some of the regulatory mechanisms that could have been sensitive to YopJ's inhibition. However, one key observation made was that YopJ specifically inhibited the IKK β -dependent canonical NF κ B pathway and had no effect on the non-canonical pathway mediated via IKK α . Based on this result and the previous observation that YopJ binds to IKK β , but not IKK α [8], it was quite clear that

YopJ only inhibits that molecule to which it binds. Thus, although these experiments did not provide enough information on YopJ's mechanism of inhibition of the MAPK and NF κ B pathways, it definitely helped rule out and eliminate different regulatory mechanisms that could have been sensitive to YopJ's inhibitory effect. Ultimately, all the experiments pointed to the common observation, that is, in the presence of YopJ, the MKKs and IKK β are in an inhibited state.

Development of an *in vitro* assay to study YopJ's inhibitory effect

Up till now, all studies demonstrating YopJ's inhibitory activity were based on *in vivo* transfection assays and there was no evidence to prove that YopJ was acting as a protease. Thus, an unbiased approach was taken to establish an *in vitro* biochemical assay to study YopJ's mechanism of inhibition [19]. The *in vitro* assays for the MAPK pathway showed that upstream activators such as EGF, Ras or Raf could not activate cell-free lysates expressing YopJ. Similarly, recombinant TRAF6, MEKK1 or NIK proteins also failed to induce IKK β activation when added to YopJ-expressing lysates. This inhibitory effect by YopJ required the maintenance of its catalytic site. Although the phosphorylated states of MKK and IKK β were decreased in YopJ lysates, the total amount of these kinases remained unchanged. SDS-PAGE revealed that MKK and IKK β from YopJ lysates looked exactly like those from control lysates or YopJC172A-expressing lysates. This indicated that YopJ did not cause any molecular weight

shifts or affect the stability of MKK and IKK β . Thus, the *in vitro* assay system successfully recapitulated YopJ's inhibition of the MAPK and NF κ B signaling pathways. The observations from these studies were consistent with previous genetic, microbial and cellular studies on the activity of YopJ and provided a method for analyzing inhibition of signaling by YopJ *in vitro*.

A similar *in vitro* cell-free signaling assay system was also developed to gain insight into Tax-mediated activation of the IKK complex (Chapter five). This assay demonstrated that addition of recombinant Tax resulted in robust activation of the NF κ B pathway (Figure 29). Assays with a panel of different Tax mutants and with the phosphatase inhibitor, okadaic acid, showed that Tax-induced IKK activation was independent of any phosphatase activity. Instead, a preformed native complex requiring active Hsp90 was essential for the activation of the IKK complex by Tax. This supported the proposed model that binding of Tax to IKK γ in the IKK complex causes a conformational change that induces autoactivation of the kinases in the complex [17]. Although the question still remains that how exactly is Tax activating the IKK complex, the development of this assay provided an important tool that could be further used to dissect the molecular mechanism of Tax-mediated IKK activation.

YopJ functions as an acetyltransferase

Results from the *in vitro* assays revealed that the MKK and the IKK signaling complexes from YopJ-expressing lysates could not be activated by

upstream kinases. In a similar manner, co-expression of YopJ with a representative MAPK kinase, MKK6, in bacteria also produced an inactive kinase that could no longer be activated by the upstream signaling machinery. To determine what are the differences between these complexes in the presence and absence of YopJ and why are these kinases inactive in YopJ's presence, mass spectrometric methods were adopted. LC-MS/MS revealed that YopJ altered the mass of MKK6 by adding single, double or triple post-translational modifications equal to a mass of 42 daltons (Figure 39). Detailed manual analyses of the individual peaks further revealed that YopJ added acetyl groups onto Ser 207 and Thr 211 residues in the activation loop of MKK6. These residues are highly conserved in all the members of the MAPK kinases and are essential for activation by upstream kinases (Figure 40). Thus, acetylation of the critical serine and threonine residues by YopJ blocked the ability of the upstream kinases to phosphorylate and thereby activate the MKKs (Figure 46). These observations supported the hypothesis that YopJ functions to modify the MKKs without noticeably changing their migration pattern on SDS-PAGE (Figures 21D, 23D and 37A) and also offers the straightforward mechanism that acetylation prevents phosphorylation.

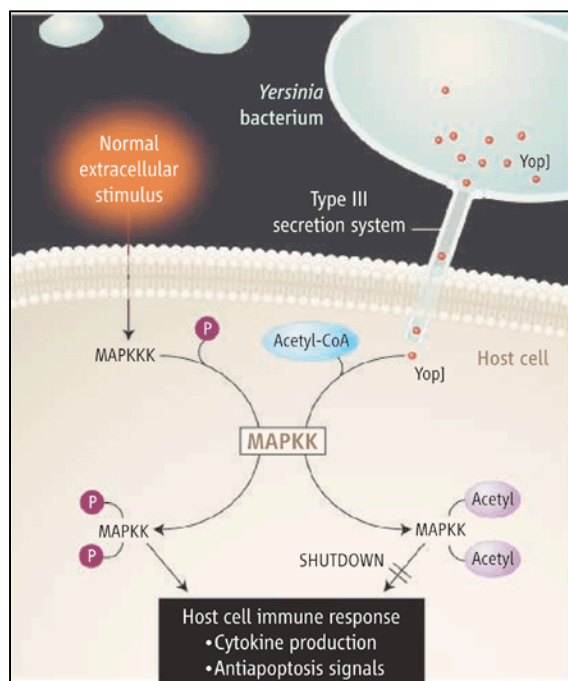


Figure 46: *Yersinia* YopJ acetylates and inhibits kinase activation by blocking phosphorylation. During infection by *Yersinia*, YopJ is translocated inside the host cell via the TTSS whereupon it blocks signaling pathways by acetylating the MAPK kinases. Acetylation of the critical serine and threonine residues by YopJ blocks the ability of the upstream kinases to phosphorylate and thereby activate the MKKs. [Taken from: *Science* 2006, 312:1150]

In vitro assays with [^{14}C]acetyl-CoA further confirmed that YopJ is functioning as an acetyltransferase. Previously, adding recombinant YopJ to lysates did not show an inhibitory effect on signaling pathways (Figure 27C). However, by using an acetyl-CoA-supplemented lysate, recombinant YopJ was able to inhibit the MAPK and NF κ B signaling pathways (Figures 43 and 44). Thus, as observed during infection, when delivered to a lysate, YopJ uses acetyl-

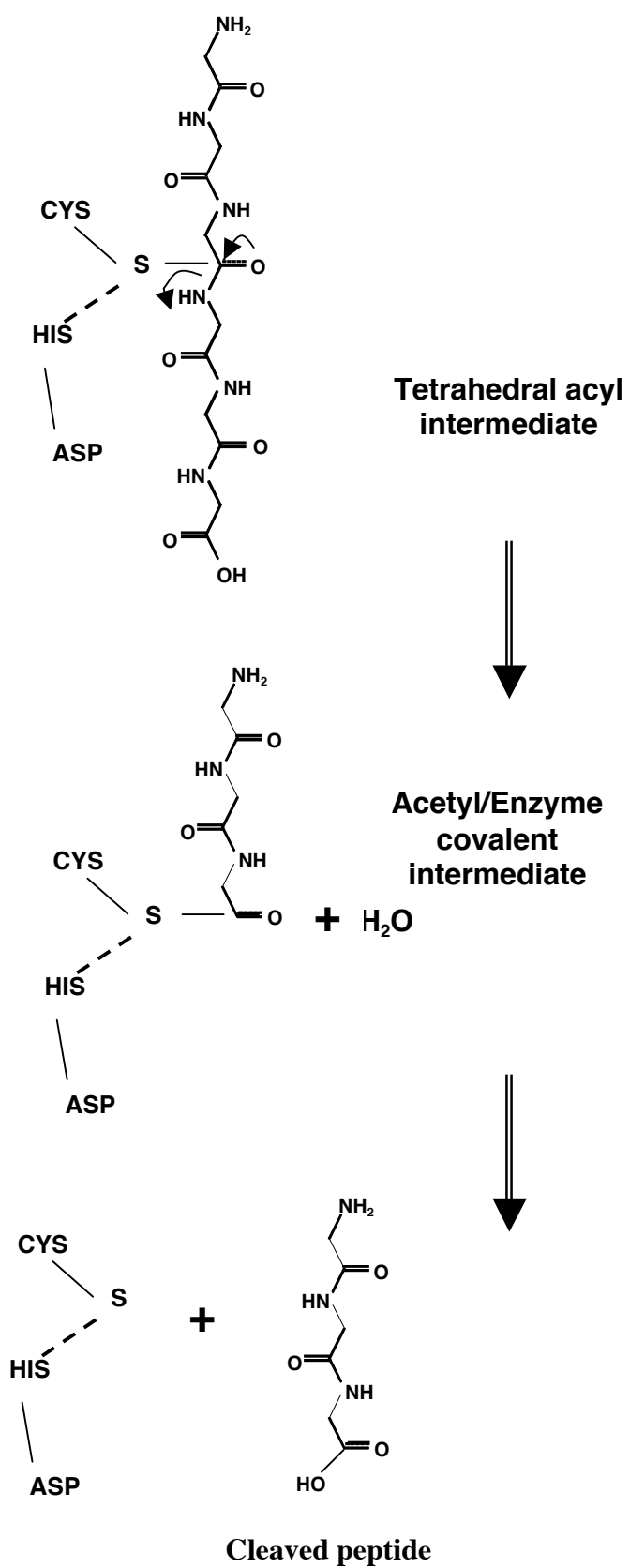
CoA to target and inactivate MKKs and IKK β (Figure 46). These findings present the first-time demonstration of acetylation of residues other than lysine and leads to the appealing hypothesis that the modification of phosphorylatable residues by acetylation might be commonly used to regulate eukaryotic cellular machineries. Thus, the characterization of a bacterial effector as a serine or threonine acetyltransferase presents a previously unknown paradigm to be considered for other biological signaling pathways. A very recent study by Mittal and colleagues demonstrated acetylation of MKK2 and IKK β isolated from mammalian cells expressing YopJ [75]. This reflected YopJ-dependent MKK2 and IKK β acetylation under *in vivo* conditions and directly proved that not only MKK6 but other MKKs and IKK β also undergo similar modification by YopJ.

Summary of Main Contributions: YopJ's Mechanism

The mechanism of YopJ inhibition is both surprising and beautiful in its simplicity. On the basis of current studies on a representative kinase, MKK6, YopJ blocks signaling of the MAPK and NF κ B pathways by binding and acetylating critical residues in the activation loop of MKKs and IKK β , respectively, thereby preventing these residues from being phosphorylated. Initial studies with YopJ were based on the analysis of the predicted secondary structure of YopJ that demonstrated similarities with the protease AVP [76]. Because of the similarities between AVP and its distant relative, Ulp1, it was proposed that YopJ

might act as an Ulp1-like protease or a general hydrolase [9]. Inconsistent with this earlier hypothesis is the observation that YopJ selectively targets MKKs and IKK β without any obvious changes in their migration on SDS-PAGE [2, 7, 8]. However, because YopJ shares similarities with a family of cysteine proteases, this provides mechanistic insight into the chemistry of YopJ catalysis [9]. A likely first step in the acetyltransferase reaction is that YopJ is acetylated on Cys 172 by formation of a thioester bond, and in the second step of the reaction this bond is attacked by a hydroxyl moiety on a serine or threonine residue of MKK, resulting in the formation of an acetylated amino acid. For both YopJ and a cysteine protease, the catalytic mechanisms are similar using the same catalytic triad of Cys-His-Asp (Figure 47).

Cysteine Protease



YopJ (Acetyltransferase)

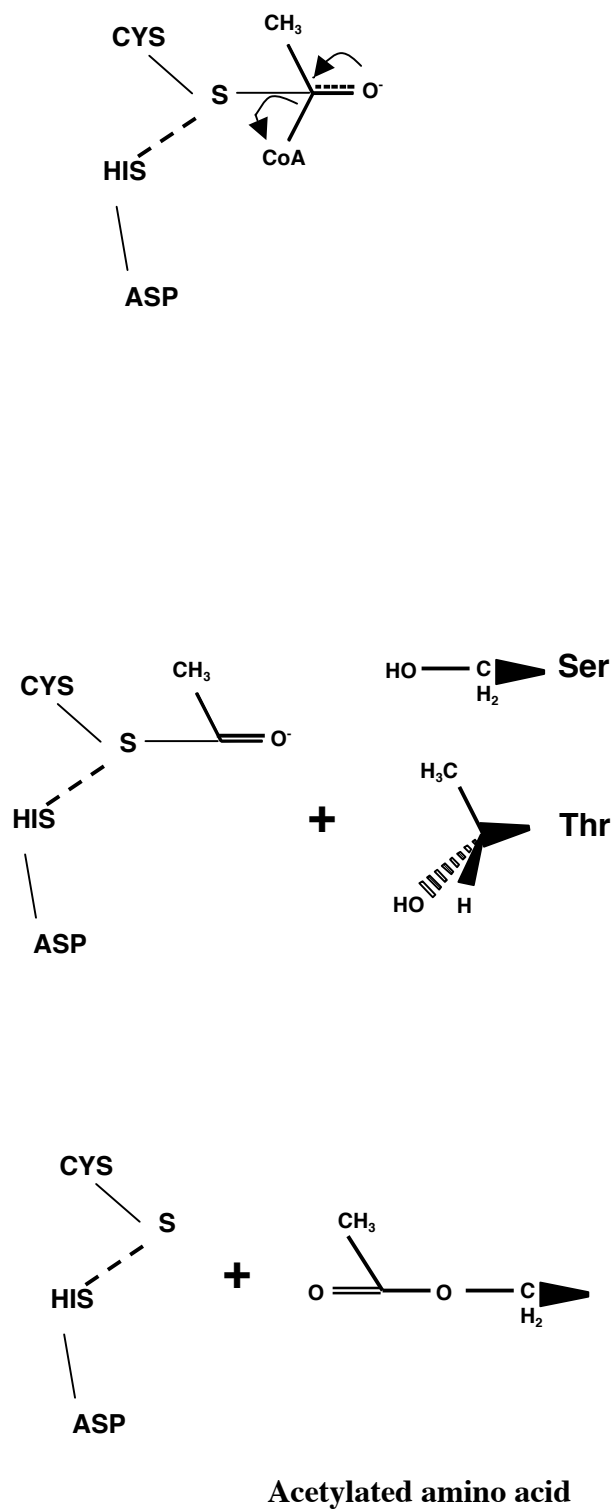


Figure 47: Comparison of the catalytic mechanism of a cysteine protease and YopJ. Cysteine proteases and YopJ use the same catalytic triad (Cys-His-Asp) to target a peptide and acetyl-CoA, respectively, to form tetrahedral acyl intermediates. A water molecule serves as the second substrate for cysteine proteases and leads to the cleavage of the peptide whereas a serine or threonine residue serves as the second substrate for YopJ that results in an acetylated amino acid.

Both form acetyl/enzyme covalent intermediates, however, differences lie in the substrates involved; YopJ targets acetyl-CoA whereas a cysteine protease targets a peptide. Water acts as the second substrate for cysteine proteases to result in the formation of a cleaved peptide whereas a serine or a threonine (or lysine) residues serves as the second substrate for YopJ that results in an acetylated amino acid (Figure 47). The substrate specificity determined by a bacterial effector protein, YopJ, and its interaction with target host proteins, MKKs and IKK β , illustrates a common mechanism used by many bacterial effectors to ensure that their potent activity does not harm the bacterial host [7].

Future Directions

YopJ-dependent acetylation occurs on the critical serine or threonine residues, thereby directly competing with the posttranslational modification, phosphorylation. Although the possibility exists that this is a unique modification developed by pathogenic bacteria to affect signaling in eukaryotic cells, a major characteristic of bacterial effector proteins is that they usurp or mimic a

eukaryotic activity and refine this activity to produce an extremely efficient mechanism to combat eukaryotic signaling. Therefore, the modification of phosphorylatable residues by acetylation could be a commonly used eukaryotic mechanism that simply has not been detected previously. Lysine acetylation, initially discovered with histone proteins, and amino-terminal acetylation play important regulatory roles in the functioning of eukaryotic, bacterial and viral proteins and enzymes that mediate these acetylation events have been studied for many years. For example, the bacterial N-acetyltransferases (NATs) are known to utilize in its active site a triad that is similar to papain-like cysteine proteases (His-Glu-Cys) [70-72]. Immunoblotting and the interpretation of tandem mass spectrometry data by MASCOT are commonly used for the identification of lysine acetylation [73]. However, these assays do not detect acetylation of serines and threonines. In view of the current finding, a more careful manual analysis of liquid chromatography followed by tandem mass spectrometry data may be required to determine whether an amino acid other than lysine is modified by acetylation. In addition, the availability of an antibody that recognizes acetylated serine and/or threonine would greatly facilitate proteomic analysis for this modification.

Posttranslational modifications of proteins occur to bring about changes in their function or activity. These modifications can function synergistically or antagonistically with other posttranslational modifications, like for example phosphorylation of I κ B leads to its ubiquitination [77] and SUMOylation of I κ B competes with ubiquitination on the same lysine residue [49]. This raises the intriguing possibility that acetylation of serine and threonine amino acids may

also compete with various other types of posttranslational modifications, such as ubiquitination, SUMOylation and glycosylation and result in critical changes in the cellular signaling machinery. Each of the aforementioned modifications is reversible and thus one of the most important questions that need to be addressed is whether the acetylation of serine/threonine residues is reversible or not. If not, is this modification used for tagging non-reversible cellular events such as cell death or differentiation? What are the eukaryotic proteins that add and remove this type of posttranslational modification? How do bacterial effectors use this activity?

Acetyltransferases utilize two different catalytic mechanisms. With a ping-pong mechanism, the enzyme first binds acetyl CoA and forms an acetylated enzyme intermediate. The protein substrate then binds to the enzyme intermediate resulting in the final acetylated protein product. For the ternary complex mechanism, both acetyl CoA and the protein substrate together bind to the enzyme and form a ternary complex. Studies involving kinetic data, to determine the molecular mechanism of different acetyltransferases, are well established [78]. Detailed enzymatic assays and steady-state kinetic parameters will provide evidence whether the serine/threonine acetyltransferase, YopJ, the first of its kind, follows a ping-pong mechanism or a ternary complex mechanism to catalyze the formation of serine or threonine acetylated proteins.

APPENDIX **TABLES OF PRIMERS**

GST-YopJ

Construct Name	5' Primer	3' Primer
GST-YopJ C172A	5'CAGCGAAGCTCATCTGAAGCC GGCATTTTTAGTTTTGCACTGGC	5'GCCAGTGCAAAACTAAAAATG CCGGCTTCAGATGAGCTTCGCTG

MKK1-myc

Construct Name	5' Primer	3' Primer
K1 (MKK1-K36R-myc)	5'CCAACTTGGAGGCCTTGCA GAAGAGGCTGGAGGAGCTAG AGCTTG	5'CAAGCTCTAGCTCCTCCAG CCTCTTCTGCAAGGCCTCCA AGTTGG
K2 (MKK1-K64R-myc)	5'GCAGAAGGTGGGAGAACTG AGGGATGACGACTTTGAGAA GATCAG	5'CTGATCTTCTCAAAGTCGT CATCCCTCAGTTCTCCCACC TTCTGC
K3 (MKK1-K183R-myc)	5'GGCCTGACATATCTGAGGG AGAGGCACAAGATCATGCAC AGAGAT	5'ATCTCTGTGCATGATCTTG TGCCTCTCCCTCAGATATGT CAGGCC

His₆-Tax

Construct Name	5' Primer	3' Primer
M22 (His ₆ -Tax-xxx)	5'ACCCTTGGGCAGCACCTCCC AAGCGCGTCTTTTCCAGACCCC GGACTC	5'GAGTCCGGGGTCTGGAAAAG ACGCGCTTGGGAGGTGCTGCCC AAGGGT
His ₆ -Tax H41Q	5'GGACTATGTTTCGGCCCGCCT ACAGCGTCACGCCCTACTGGC CACC	5'GGTGGCCAGTAGGGCGTGAC GCTGTAGGCGGGCCGAACATA GTCC

His ₆ -Tax H43Q	5'GGACTATGTTTCGGCCCCGCCT ACATCGTCAGGCCCTACTGGC CACC	5'GGTGGCCAGTAGGGCCTGAC GATGTAGGCGGGCCGAACATA GTCC
His ₆ -Tax K85N	5'TTCCCCACCCAGAGAACCTC TAATACCCTCAAGGTCCTTACC CCG	5'CGGGGTAAGGACCTTGAGGG TATTAGAGGTTCTCTGGGTGGG GAA

His₆-MKK6

Construct Name	5' Primer	3' Primer
His ₆ -MKK6 K210A	5'AGTGGCTACTTGGTGGACTC TGTTGCTGCAACAATTGATGCA GGTTGC	5'GCAACCTGCATCAATTGTTG CAGCAACAGAGTCCACCAAG TAGCCACT
His ₆ -MKK6 S207A,T211A	5'AGTGGCTACTTGGTGGACGC TGTTGCTAAAGCAATTGATGC AGGTTGC	5'GCAACCTGCATCAATTGCTT TAGCAACAGCGTCCACCAAGT AGCCACT
His ₆ -MKK6 S207A, K210A, T211A	5'AGTGGCTACTTGGTGGACGC TGTTGCTGCAGCAATTGATGCA GGTTGC	5'GCAACCTGCATCAATTGCTG CAGCAACAGCGTCCACCAAG TAGCCACT
His ₆ -MKK6 S207E, T207E	5'GGCTACTTGGTGGACGAAGT TGCTAAAGAAATTGATGCAGG TTGC	5'GCAACCTGCATCAATTTCTT TAGCAACTTCGTCCACCAAGT AGCC

Table of primers used for site-directed mutagenesis of specified constructs

BIBLIOGRAPHY

1. Hinnebusch, B.J., *The evolution of flea-borne transmission in Yersinia pestis*. Curr Issues Mol Biol, 2005. **7**(2): p. 197-212.
2. Viboud, G.I. and J.B. Bliska, *Yersinia outer proteins: role in modulation of host cell signaling responses and pathogenesis*. Annu Rev Microbiol, 2005. **59**: p. 69-89.
3. Ghosh, P., *Process of protein transport by the type III secretion system*. Microbiol Mol Biol Rev, 2004. **68**(4): p. 771-95.
4. Juris, S.J., et al., *A distinctive role for the Yersinia protein kinase: actin binding, kinase activation, and cytoskeleton disruption*. Proc Natl Acad Sci U S A, 2000. **97**(17): p. 9431-6.
5. Von Pawel-Rammingen, U., et al., *GAP activity of the Yersinia YopE cytotoxin specifically targets the Rho pathway: a mechanism for disruption of actin microfilament structure*. Mol Microbiol, 2000. **36**(3): p. 737-48.
6. Persson, C., et al., *The PTPase YopH inhibits uptake of Yersinia, tyrosine phosphorylation of p130Cas and FAK, and the associated accumulation of these proteins in peripheral focal adhesions*. Embo J, 1997. **16**(9): p. 2307-18.
7. Orth, K., *Function of the Yersinia effector YopJ*. Curr Opin Microbiol, 2002. **5**(1): p. 38-43.
8. Orth, K., et al., *Inhibition of the mitogen-activated protein kinase kinase superfamily by a Yersinia effector*. Science, 1999. **285**(5435): p. 1920-3.
9. Orth, K., et al., *Disruption of signaling by Yersinia effector YopJ, a ubiquitin-like protein protease*. Science, 2000. **290**(5496): p. 1594-7.
10. Fehr, D., et al., *AopP, a type III effector protein of Aeromonas salmonicida, inhibits the NF-kappaB signalling pathway*. Microbiology, 2006. **152**(Pt 9): p. 2809-18.
11. Collier-Hyams, L.S., et al., *Cutting edge: Salmonella AvrA effector inhibits the key proinflammatory, anti-apoptotic NF-kappa B pathway*. J Immunol, 2002. **169**(6): p. 2846-50.
12. Trosky, J.E., et al., *Inhibition of MAPK signaling pathways by VopA from Vibrio parahaemolyticus*. J Biol Chem, 2004. **279**(50): p. 51953-7.
13. Yoshida, M., *Multiple viral strategies of HTLV-I for dysregulation of cell growth control*. Annu Rev Immunol, 2001. **19**: p. 475-96.
14. Chu, Z.L., et al., *IKKgamma mediates the interaction of cellular IkappaB kinases with the tax transforming protein of human T cell leukemia virus type I*. J Biol Chem, 1999. **274**(22): p. 15297-300.
15. Fu, D.X., et al., *Human T-lymphotropic virus type I tax activates I-kappa B kinase by inhibiting I-kappa B kinase-associated serine/threonine protein phosphatase 2A*. J Biol Chem, 2003. **278**(3): p. 1487-93.
16. Kray, A.E., et al., *Positive regulation of IkappaB kinase signaling by protein serine/threonine phosphatase 2A*. J Biol Chem, 2005. **280**(43): p. 35974-82.
17. Harhaj, E.W. and N.S. Harhaj, *Mechanisms of persistent NF-kappaB activation by HTLV-I tax*. IUBMB Life, 2005. **57**(2): p. 83-91

18. Carter, R.S., et al., *Persistent activation of NF-kappa B by the tax transforming protein involves chronic phosphorylation of IkappaB kinase subunits IKKbeta and IKKgamma*. J Biol Chem, 2001. **276**(27): p. 24445-8.
19. Mukherjee, S., et al., *Yersinia YopJ acetylates and inhibits kinase activation by blocking phosphorylation*. Science, 2006. **312**(5777): p. 1211-4.
20. Thanassi, D.G. and S.J. Hultgren, *Multiple pathways allow protein secretion across the bacterial outer membrane*. Curr Opin Cell Biol, 2000. **12**(4): p. 420-30.
21. Straley, S.C. and W.S. Bowmer, *Virulence genes regulated at the transcriptional level by Ca²⁺ in Yersinia pestis include structural genes for outer membrane proteins*. Infect Immun, 1986. **51**(2): p. 445-54.
22. Cornelis, G.R., et al., *The virulence plasmid of Yersinia, an antihost genome*. Microbiol Mol Biol Rev, 1998. **62**(4): p. 1315-52.
23. Mills, S.D., et al., *Yersinia enterocolitica induces apoptosis in macrophages by a process requiring functional type III secretion and translocation mechanisms and involving YopP, presumably acting as an effector protein*. Proc Natl Acad Sci U S A, 1997. **94**(23): p. 12638-43.
24. Monack, D.M., et al., *Yersinia signals macrophages to undergo apoptosis and YopJ is necessary for this cell death*. Proc Natl Acad Sci U S A, 1997. **94**(19): p. 10385-90.
25. Ruckdeschel, K., et al., *Yersinia enterocolitica promotes deactivation of macrophage mitogen-activated protein kinases extracellular signal-regulated kinase-1/2, p38, and c-Jun NH2-terminal kinase. Correlation with its inhibitory effect on tumor necrosis factor-alpha production*. J Biol Chem, 1997. **272**(25): p. 15920-7.
26. Boland, A. and G.R. Cornelis, *Role of YopP in suppression of tumor necrosis factor alpha release by macrophages during Yersinia infection*. Infect Immun, 1998. **66**(5): p. 1878-84.
27. Palmer, L.E., et al., *YopJ of Yersinia spp. is sufficient to cause downregulation of multiple mitogen-activated protein kinases in eukaryotic cells*. Infect Immun, 1999. **67**(2): p. 708-16.
28. Hardt, W.D. and J.E. Galan, *A secreted Salmonella protein with homology to an avirulence determinant of plant pathogenic bacteria*. Proc Natl Acad Sci U S A, 1997. **94**(18): p. 9887-92.
29. Qi, M. and E.A. Elion, *MAP kinase pathways*. J Cell Sci, 2005. **118**(Pt 16): p. 3569-72.
30. Cobb, M.H. and E.J. Goldsmith, *How MAP kinases are regulated*. J Biol Chem, 1995. **270**(25): p. 14843-6.
31. Morrison, D.K., *KSR: a MAPK scaffold of the Ras pathway?* J Cell Sci, 2001. **114**(Pt 9): p. 1609-12.
32. Brennan, J.A., et al., *Phosphorylation regulates the nucleocytoplasmic distribution of kinase suppressor of Ras*. J Biol Chem, 2002. **277**(7): p. 5369-77.
33. Yoon, S., et al., *Yersinia effector YopJ inhibits yeast MAPK signaling pathways by an evolutionarily conserved mechanism*. J Biol Chem, 2003.

- 278**(4): p. 2131-5.
34. Israel, A., *The IKK complex: an integrator of all signals that activate NF-kappaB?* Trends Cell Biol, 2000. **10**(4): p. 129-33.
 35. Chen, G., P. Cao, and D.V. Goeddel, *TNF-induced recruitment and activation of the IKK complex require Cdc37 and Hsp90.* Mol Cell, 2002. **9**(2): p. 401-10.
 36. Ghosh, S. and M. Karin, *Missing pieces in the NF-kappaB puzzle.* Cell, 2002. **109 Suppl**: p. S81-96.
 37. Deng, L., et al., *Activation of the IkappaB kinase complex by TRAF6 requires a dimeric ubiquitin-conjugating enzyme complex and a unique polyubiquitin chain.* Cell, 2000. **103**(2): p. 351-61.
 38. Li, S.J. and M. Hochstrasser, *A new protease required for cell-cycle progression in yeast.* Nature, 1999. **398**(6724): p. 246-51.
 39. Yeh, E.T., L. Gong, and T. Kamitani, *Ubiquitin-like proteins: new wines in new bottles.* Gene, 2000. **248**(1-2): p. 1-14.
 40. Melchior, F., *SUMO--nonclassical ubiquitin.* Annu Rev Cell Dev Biol, 2000. **16**: p. 591-626.
 41. Kolch, W., *Meaningful relationships: the regulation of the Ras/Raf/MEK/ERK pathway by protein interactions.* Biochem J, 2000. **351 Pt 2**: p. 289-305.
 42. Mahajan, R., et al., *A small ubiquitin-related polypeptide involved in targeting RanGAP1 to nuclear pore complex protein RanBP2.* Cell, 1997. **88**(1): p. 97-107.
 43. Jentsch, S. and G. Pyrowolakis, *Ubiquitin and its kin: how close are the family ties?* Trends Cell Biol, 2000. **10**(8): p. 335-42.
 44. Carter, R.S., et al., *Signal-induced ubiquitination of I kappaB Kinase-beta.* J Biol Chem, 2003. **278**(49): p. 48903-6.
 45. Zhou, H., et al., *Yersinia virulence factor YopJ acts as a deubiquitinase to inhibit NF-kappa B activation.* J Exp Med, 2005. **202**(10): p. 1327-32.
 46. Hotson, A., et al., *Xanthomonas type III effector XopD targets SUMO-conjugated proteins in planta.* Mol Microbiol, 2003. **50**(2): p. 377-89.
 47. Rickwood, J.M.G.a.D., *Subcellular Fractionation. A Practical Approach.* 1997, New York: Oxford University Press Inc.
 48. Sobko, A., H. Ma, and R.A. Firtel, *Regulated SUMOylation and ubiquitination of DdMEK1 is required for proper chemotaxis.* Dev Cell, 2002. **2**(6): p. 745-56.
 49. Desterro, J.M., M.S. Rodriguez, and R.T. Hay, *SUMO-1 modification of IkappaBalpha inhibits NF-kappaB activation.* Mol Cell, 1998. **2**(2): p. 233-9.
 50. Gan-Erdene, T., et al., *Identification and characterization of DEN1, a deneddylase of the ULP family.* J Biol Chem, 2003. **278**(31): p. 28892-900.
 51. Borodovsky, A., et al., *A novel active site-directed probe specific for deubiquitylating enzymes reveals proteasome association of USP14.* Embo J, 2001. **20**(18): p. 5187-96.
 52. Roy, F., et al., *KSR is a scaffold required for activation of the ERK/MAPK module.* Genes Dev, 2002. **16**(4): p. 427-38.
 53. Gottlieb, R.A. and S. Adachi, *Nitrogen cavitation for cell disruption to*

- obtain mitochondria from cultured cells. Methods Enzymol*, 2000. **322**: p. 213-21.
54. Zhou, G., Z.Q. Bao, and J.E. Dixon, *Components of a new human protein kinase signal transduction pathway. J Biol Chem*, 1995. **270**(21): p. 12665-9.
55. Bailey, J.L., *Techniques in Protein Chemistry*. 1967: Elsevier, New York.
56. Russell, J.S.a.D., *Calcium-phosphatse-mediated Transfection of Eukaryotic Cells with Plasmid DNAs*. 3rd. ed. CSH Protocols. 2006, Cold Spring Harbor, NY: Cold Spring Harbor Laboratory Press.
57. Dent, P., et al., *Activation of the mitogen-activated protein kinase pathway in Triton X-100 disrupted NIH-3T3 cells by p21 ras and in vitro by plasma membranes from NIH 3T3 cells. Mol Biol Cell*, 1993. **4**(5): p. 483-93.
58. Verma, R., Y. Chi, and R.J. Deshaies, *Cell-free ubiquitination of cell cycle regulators in budding yeast extracts. Methods Enzymol*, 1997. **283**: p. 366-76.
59. Lee, F.S., et al., *Activation of the IkappaB alpha kinase complex by MEKK1, a kinase of the JNK pathway. Cell*, 1997. **88**(2): p. 213-22.
60. Kanayama, A., et al., *TAB2 and TAB3 activate the NF-kappaB pathway through binding to polyubiquitin chains. Mol Cell*, 2004. **15**(4): p. 535-48.
61. Jin, D.Y., et al., *Role of adapter function in oncoprotein-mediated activation of NF-kappaB. Human T-cell leukemia virus type I Tax interacts directly with IkappaB kinase gamma. J Biol Chem*, 1999. **274**(25): p. 17402-5.
62. Xiao, G., E.W. Harhaj, and S.C. Sun, *Domain-specific interaction with the I kappa B kinase (IKK)regulatory subunit IKK gamma is an essential step in tax-mediated activation of IKK. J Biol Chem*, 2000. **275**(44): p. 34060-7.
63. Yin, M.J., et al., *HTLV-I Tax protein binds to MEKK1 to stimulate IkappaB kinase activity and NF-kappaB activation. Cell*, 1998. **93**(5): p. 875-84.
64. DiDonato, J.A., et al., *A cytokine-responsive IkappaB kinase that activates the transcription factor NF-kappaB. Nature*, 1997. **388**(6642): p. 548-54.
65. Semmes, O.J. and K.T. Jeang, *Mutational analysis of human T-cell leukemia virus type I Tax: regions necessary for function determined with 47 mutant proteins. J Virol*, 1992. **66**(12): p. 7183-92.
66. Smith, M.R. and W.C. Greene, *Identification of HTLV-I tax trans-activator mutants exhibiting novel transcriptional phenotypes. Genes Dev*, 1990. **4**(11): p. 1875-85.
67. Pratt, W.B. and D.O. Toft, *Regulation of signaling protein function and trafficking by the hsp90/hsp70-based chaperone machinery. Exp Biol Med (Maywood)*, 2003. **228**(2): p. 111-33.
68. Broemer, M., D. Krappmann, and C. Scheidereit, *Requirement of Hsp90 activity for IkappaB kinase (IKK) biosynthesis and for constitutive and inducible IKK and NF-kappaB activation. Oncogene*, 2004. **23**(31): p. 5378-86.
69. Gu, W. and R.G. Roeder, *Activation of p53 sequence-specific DNA binding by acetylation of the p53 C-terminal domain. Cell*, 1997. **90**(4): p. 595-606.

70. Bode, A.M. and Z. Dong, *Inducible covalent posttranslational modification of histone H3*. Sci STKE, 2005. **2005**(281): p. re4.
71. Brooke, E.W., et al., *An approach to identifying novel substrates of bacterial arylamine N-acetyltransferases*. Bioorg Med Chem, 2003. **11**(7): p. 1227-34.
72. Sim, E., et al., *An update on genetic, structural and functional studies of arylamine N-acetyltransferases in eucaryotes and procaryotes*. Hum Mol Genet, 2000. **9**(16): p. 2435-41.
73. Roth, S.Y., J.M. Denu, and C.D. Allis, *Histone acetyltransferases*. Annu Rev Biochem, 2001. **70**: p. 81-120.
74. Worby, C.A. and J.E. Dixon, *Microbiology. Bacteria seize control by acetylating host proteins*. Science, 2006. **312**(5777): p. 1150-1.
75. Mittal, R., S.Y. Peak-Chew, and H.T. McMahon, *Acetylation of MEK2 and $\{kappa\}$ B kinase (IKK) activation loop residues by YopJ inhibits signaling*. Proc Natl Acad Sci U S A, 2006. **103**(49): p. 18574-9.
76. Ding, J., et al., *Crystal structure of the human adenovirus proteinase with its 11 amino acid cofactor*. Embo J, 1996. **15**(8): p. 1778-83.
77. Chen, Z.J., L. Parent, and T. Maniatis, *Site-specific phosphorylation of IkappaBalpha by a novel ubiquitination-dependent protein kinase activity*. Cell, 1996. **84**(6): p. 853-62.
78. Berndsen, C.E. and J.M. Denu, *Assays for mechanistic investigations of protein/histone acetyltransferases*. Methods, 2005. **36**(4): p. 321-31.

VITAE

Sohini Mukherjee was born in Kolkata, West Bengal, India on July 16, 1978, the daughter of Dola Mukherjee and Tapan Kumar Mukherjee. After graduating from D.A.V. Jawahar Vidya Mandir, Ranchi, India, she entered the All India Institute of Medical Sciences, New Delhi in 1996. She earned the degree of Bachelor of Science in Human Biology with major in Biophysics in 1999. In August 1999, she entered the Masters in Biophysics Program at the All India Institute of Medical Sciences, New Delhi. During the following two years, she completed her thesis entitled “Design, Syntheses and Structure Analyses of Dehydro-Residue Containing Peptides” in the laboratory of the chair of the department of Biophysics, Dr. Tej Pal Singh. She received the degree of Master of Science in Biophysics in 2001. In August 2001, she entered the Division of Basic Sciences at the University of Texas Southwestern Medical Center at Dallas. In 2002 she joined the program of Biological Chemistry and began her doctoral research in the laboratory of Dr. Kim Orth. She has been married to Hemanta Kumar Sen since February of 2004. Sohini will continue research as a post-doctoral fellow at University of Texas Southwestern Medical Center, Dallas, Texas with Dr. Lora Hooper in the department of Immunology.

Permanent Address: C-5, MECON Towers
357, Prince Anwar Shah Rd.
Kolkata- 700068
West Bengal, India